Saving lives through early cancer detection: Breaking the current PET efficiency barrier with the 3D-CBS

Dario B. Crosetto
900 Hideaway Pl, DeSoto, Texas 75115
Crosetto@att.net, Dario.Crosetto@cern.ch

Abstract

An innovative, low-radiation 3-D Complete-Body-Scan (3D-CBS) medical imaging device is presented, combining the benefits of the functional imaging capability of the Positron Emission Tomography (PET) with those of the anatomical imaging capability of the Computed Tomography (CT). Until now, the greatest impediment to extending the axial field of view (FOV, the length of the detector) has been the electronics of current PET, which could not efficiently capture the photons. The unique architecture of the 3D-CBS electronics allows for the extension, in a cost-effective manner, of the FOV to over one meter in length. The 3D-CBS captures about 1,000 out of 10,000 photons in time coincidence, compared with only 2 out of 10,000 captured by current PET. In addition, the overall architecture of the 3D-CBS permits the use of a single detection apparatus acquiring PET and CT data concurrently without moving the patient or the detector. This uniquely provides functional and anatomical whole-body three-dimensional dynamic imaging and also allows real-time tracking of moving tumors during radiation therapy. The 3D-CBS features significant improvements in the scanning speed by providing PET and CT exams combined in two to four minutes. It achieves increased resolution and accuracy, providing better imaging with a reduction in "false positives" and "false negatives," and allows for the radiation dosage to the patient be reduced to 1/30th of the dose required by existing PETs. The faster scanning time allows for at least six times as many PET examinations per day with a five-fold increase in net revenues or an examination cost floor as low as $300; currently the price of a PET scan is $2,000-$4,000. The lower examination cost and higher imaging quality of the 3D-CBS will compete with the cost and quality of current diagnostic workups of CT and PET. The low radiation dosage requirements will open the door to new applications by permitting annual whole-body screening for early detection of cancer and other systemic anomalies (heart functions, blood flow, brain activity, metabolic activity). This will replace most other current procedures for partial cancer screening (prostate, lung, breast, uterus, colon, etc.) because it is faster, less expensive, more accurate, and less invasive. The proposed 3D-CBS device makes it possible to achieve improved performance now, while using cheaper, slower BGO, CsI crystals, currently available in abundance, unlike the nearly ideal fast LSO crystals, which have limited production capabilities. Comparisons are made of the superior cost effectiveness of the 3D-CBS versus both the current PETs that use the ideal crystal (LSO) and those with the highest spatial resolution (300 μm). The need for the 3D-CBS is apparent after analyzing the number of people in a high-death-rate group (i.e., from 45-64 years old, which is still below general life expectancy) who are lost, not because the drugs to cure the disease do not exist, but because low radiation, and high sensitivity instrumentation for early detection of the disease does not exist. Cancer and heart disease are responsible for 60% of the deaths in the 45-64 age range. Clearly, a great proportion of these deaths could be avoided through early detection and treatment. Current expenditures for prescription drugs in the U.S. (excluding those used in hospitals, nursing homes, and by health care practitioners) are $116.9 billion per year and are projected by the Health Care Financing Administration (HCFA) to increase to over $360 billion per year by 2010, whereas expenditures for electromedical, diagnostic and irradiation equipment total only $13 billion per year. It is obvious that the impact of early detection with improved diagnostic imaging, in terms of both reduced mortality and increased global heath care savings, would be immense. Global health care costs will be reduced by helping hospitals and physicians select the most effective drugs and monitor their effects and by reducing costs related to morbidity. The 3D-CBS will also facilitate the development and testing of new drugs. Comparisons of the U.S. national health care expenditures (NHE) as a share of the gross domestic product (GDP) and the NHE/GDP of other countries are provided. Currently, PET imaging efficiency improves 2- to 3-fold every 5 years; a careful analysis of the 3D-CBS project, which increases efficiency over 400-fold compared to current technology, will show that all parties (investors, hospitals, physicians, drug researchers, insurance companies, the government, and patients) will benefit from the implementation of this technology as soon as possible.

TABLE I. COMPARISON OF THE OPERATING COSTS[10] PER SCANNER PER YEAR WHEN USED FOR THE SAME NUMBER OF HOURS PER DAY, AT THEIR HIGH THROUGHPUT AT A PRICE OF $400/EXAM. (SOURCE: RADIOISOTOPE MANUFACTURERS, HOSPITALS ADMINISTRATION FOR USA AND TABLE 5-1 OF [29] FOR EUROPEAN COSTS).

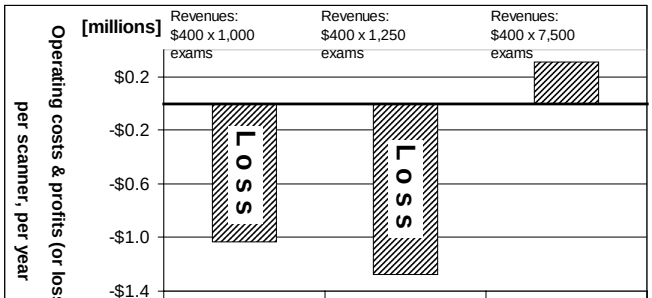

	Current PET <14 cm FOV [millions $]	Current PET ~25 cm FOV [millions $]	3D-CBS ~150 cm FOV [millions $]
Capital amortiz. (8yr)	-$0.125	-$0.275	-$0.750
Capital cost (5%)	-$0.050	-$0.110	-$0.300
Service contract	-$0.060	-$0.100	-$0.200
Upgrading	-$0.060	-$0.100	-$0.150
Building	-$0.090	-$0.090	-$0.090
Personnel	-$0.200	-$0.250	-$0.350
Radioisotope FDG	-$0.850	-$0.850	-$0.850
Revenues	$0.400	$0.500	$3.000
⊠ Profit (or loss)	-$1.035	-$1.275	$0.310

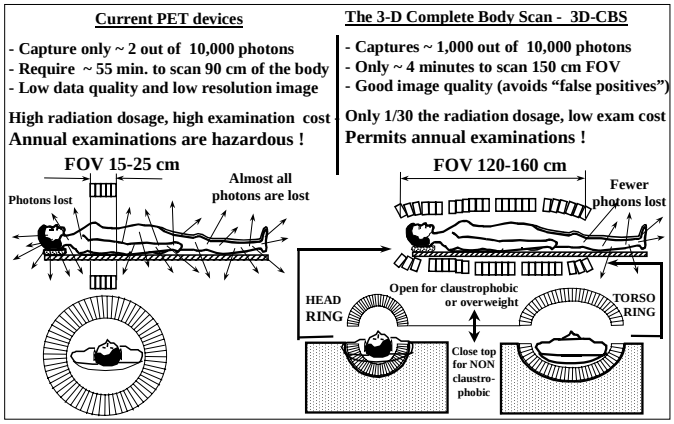

Figure 1. Differences between the current PETs and 3D-CBS.

If you are interested in this proposal but don't have time to review it in depth, please see summary of advantages of the 3D-CBS on Table XV on page 34. Also see Section 17.2, for a request for comment and collaboration, and an opportunity for you to contribute and hasten the benefits of the 3D-CBS.

Presented on May 16, 2001 at the University of Geneva, Switzerland, http://dpnc.unige.ch/seminaire/annonce.html. Revised on July 30, 2001.

TABLE OF CONTENTS

FIGURES

TABLES

1 INTRODUCTION

Figure 1 and Table I show general characteristics and cost comparisons of the current PET and the 3D-CBS [1], [2], [3].

The aim of the author is to provide a tool with a safe, low radiation requirement that uses materials available in abundance for providing a life-saving medical procedure at a low, affordable cost to a large population.

This article presents the technological advances of the 3D-CBS diagnostic imaging machine, which allows earlier diagnosis of various diseases in patients with symptoms of illness as well as in the asymptomatic people, and shows how it compares to currently available technology. It explains how the use of the 3D-CBS will help improve life expectancy and the quality of life, and will do so in a cost-effective manner.

PET Technology

Positron Emission Tomography (PET) is a medical imaging technique that involves injecting a natural compound, such as sugar or water, labeled with a radioactive isotope into a patient's body to reveal internal biological processes. As the isotope circulates within the patient's body, it emits pairs of photons in diametrically opposed directions (back-to-back). A PET device is made of a set of detectors coupled to thousands of sensors that surround the human body. These detectors (crystals) capture the photons emitted by the isotope from within the patient's body at a total rate of up to hundreds of millions per second, while the sensors (transducers such as PMTs) convert them to electrical signals, and send the signals to the electronics. (see Figure 6, Figure 31, and Section 3).

Current PET limitations

The electronics of the current PET limits its performance; it is not fully capable of extracting the complete characteristics of the interaction between the photon and the detector from signals arriving at high data input rates from thousands of sensors. The electronics have been the main impediment to extending the axial FOV; the increases in efficiency that would justify extending the axial FOV are not possible with the electronics of the current PET.

Figure 13 and the left side of Figure 31 show the inefficiencies of the electronics of current PET in detecting photons, which occurs because there is no independent digital signal processing (DSP) at each electronic channel and there is no communication between adjacent electronic channels. This limitation affects sensitivity and spatial resolution. Sensitivity is lowered when photons striking a crystal coupled to the border of two sensors, causing them to release half (or less) of their energy in two (or more) adjacent electronic channels, are not recognized as photons because each channel receives less than the nominal energy to be considered as a 511 keV photon of a PET emission event.

Spatial resolution suffers at the edge of each 2x2 photomultiplier (PMT) block because the centroid algorithm (see left side of Figure 31) cannot weigh the PMT signals from both sides of the PMT closest to the point at which the photon struck the crystal. This causes a reduction of the overall sensitivity, which translates into greater patient exposure to radiation, poorer image quality, and longer scanning time.

Overcoming PET limitations and lowering radiation

The revolutionary approach of the electronics and the unique 3D-CBS design result in great improvements in the efficiency of the current PET devices. Section 4 describes the key innovations that enable the 3D-CBS to capture more photons by making use of a set of specially designed DSPs (3D-Flow processors) on each electronic channel, extending the processing time on each data packet received from each sensor and exchanging information between adjacent electronic channels. In addition to these innovations that increase sensitivity, the 3x3 (or 5x5) centroid calculation (as shown in the right side of Figure 31) make it possible to improve the 4-mm spatial resolution of the current PET that makes use of large crystals and allow the improvement of the 1.3 mm resolution of the current PET that makes use of the 2.1 mm x 2.1 mm crystals [49]. (See also Section 8.6)

Because the inefficiency of the electronics has been solved with the 3D-Flow sequentially implemented parallel-processing architecture [1], [2], [3], [4], the FOV can now be expanded (see Figure 3), providing a PET efficiency improved at least 400-fold in one giant step. This breaks the historical barrier of only two- to three-fold[31] [5] improvement every five years and opens the door to new uses to which scanners can be put. The 400-fold increase in efficiency approaches as close as possible the theoretical limit. (See Figure 2, Figure 16, and Figure 17. See also Section 4 and Appendix C.2 for the description of the technology, Section 8.5 for the calculation of the 400 fold improvement in efficiency, and Appendix C.6 and Figure 34 for an example of a 3D-Flow real-time algorithm that can fully extract the characteristics of the interaction between the photons and the detector.).

Phase II of Section 4 describes the inefficient approach to finding photons in time coincidence used by current PETs, which use a circuit that compares information from all detector elements, even though most of these detectors did not receive a hit. Conversely, the approach used in the 3D-CBS greatly simplifies the circuit and increases the efficiency by checking and comparing for time coincidence only the detector elements that received a hit. The circuit of the 3D-CBS, sensitive to the radiation activity rather than to the number of detector elements, allows an increase in the length of the detector (FOV) without increasing the complexity of the circuit.

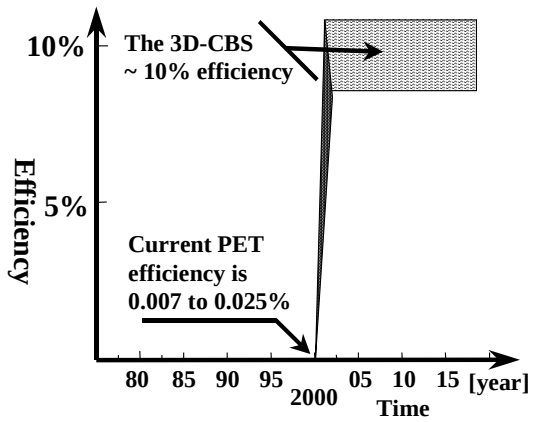

Figure 2. The innovations of the 3D-CBS break the barrier of 2- to 3-fold improvement in efficiency of PET every 5 years to 400-fold improvement in one breakthrough step.

Although the use of the proposed electronics will also improve the efficiency of the current PET, the best performance and cost effectiveness of the 3D-CBS will be achieved only if it is not implemented as an upgrade of a current PET but as an entirely new device.

Adapting a Boeing 747 for supersonic flight by adding heavier, more powerful engines and reinforcing the structure of the airplane with special expensive material, would not be very cost effective, if feasible at all. Similarly, using more expensive, faster crystals and faster processors will not offer much improvement unless the overall design is changed from several small 2x2 PMT cameras, as shown in the left side of Figure 31, or large modules with a few analog signals as shown in Figure 32, used in current PET, to a large array of sensors, each coupled to a set of DSPs which communicate with their neighbors as is used in the 3D-CBS. An ultra-fast general purpose Pentium will never be able to compete with a special design parallel 3D-Flow DSP network, even with slow processors.

A simple, low-speed 3D-Flow processor architecture, say 80 MHz, is more cost efficient in executing real-time pattern-recognition algorithms for photon identification than a Pentium at 1.7 GHz.

Instead of trying to adapt the electronics of this proposal to current PET, one should understand how the pipeline technique and the parallel-processing technique have been uniquely fused (see Figure 9, Figure 10, Table III of this article and Figure 5 and 6 of [2]) in a practical and cost-effective implementation of the 3D-Flow architecture that provides a breakthrough in simplicity of construction (see Figure 5 of [2]) and improvement of efficiency using a relatively low-speed processor.

The longer the FOV of the detector, the more efficient will be the 3D-Flow parallel architecture. The 3D-CBS is particularly effective because of the large number of crystals/detectors.

The 3D-Flow sequentially implemented parallel-processing architecture matches particularly well with the requirements of extracting the characteristics from the signals generated by the sensors coupled to different crystals for the identification of the back-to-back photon emission technique of PET, and the single-photon transmission technique of CT. The apparent complexity becomes simple. For instance, there is no need to have detectors with slits of variable length of reflecting material. (See Appendix C.4). As is described in more detail in this document and in the references, the construction of the 3D-CBS (see Figure 11 and Figure 12) is not difficult, because most of the components have been already built, tested, and verified and these results have been made available in several articles by several parties. (See references in the book [1]).

Application advantages

Examples of how the 3D-CBS can be used are: a) whole-body screening even as frequent as yearly; b) monitoring of the effectiveness of prescribed drugs during diagnostic workups; c) verification of treatment for cancer during and after radiation, surgery, or chemotheraphy; d) a research tool for the development of new drugs and the study of their effects; and e) use in emergency rooms (see also Section 10).

The combination of the improved electronics and the extension of the FOV[1] (see Figure 17) makes it possible to reduce the scanning time required for a thorough image and reduces the amount of radiation[2] given to the patient to 25-45 mrem, or about one month's worth of the background radiation one would receive from living in Dallas, Texas, instead of the 700-1,600 mrem, or three to six years' worth[2] [11], [6], [7] required by current PET.

The faster whole-body[3] scan with the 3D-CBS allows for the examination of over six times the number of patients per day than the current PET allows.

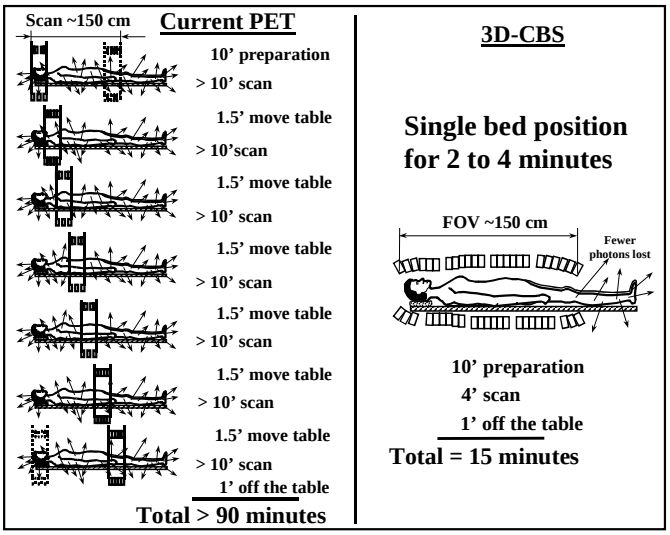

Figure 3. The current PET (figure at left) with short (< 25 cm) axial FOV (the length of the detector) requires ≥ 7 scanning table positions,[3] each longer than ten minutes, to cover about 150 cm of the body. The 3D-CBS (figure at right) with a longer axial FOV (~150 cm) and with more efficient electronics, requires only one position of the table to capture in < four minutes the number of photons which provide a sufficient statistic to yield a good image (see also Figure 16).

PET/CT technology

There is a substantial difference between the 3D-CBS and the PET/CT units recently manufactured by General Electric and CTI/Siemens. The current PET/CT machines, consisting of two units placed side by side, still have most of the

---

[1] If the length of the FOV of a PET scanner is extended, the machine could capture more data of the photons emitted from inside the patient's body (e.g., sensitivity of one organ in the center of the FOV increases four times when doubling a short axial FOV. See Figure 14).

[2] The recommended limits to exposure of radiation workers (whole-body dose) are stricter in Europe (e.g., maximum 1,500 mrem per year at CERN and U.K., and 2,000 mrem per year in France and Switzerland) than in the U.S. (5,000 mrem per year) [11]. The recommended limits to exposure of radiation for asymptomatic patients is even lower (e.g, 100 mrem per year in Switzerland, see Article 37 of [6]). However, it is recommended that everyone monitor his/her radiation exposure to keep it to the minimum level. For example it was estimated in [7] that when mammography screening saves 20 women (age 40 to 50) within a large group, the amount of radiation given to the same group may induce one lethal cancer.

[3] Although someone might claim that one could scan a shorter axial FOV, it is not in the patient's best interest to do so, because once he has received a radiation dose (which spreads over the entire body), it is best for him to get the maximum coverage of disease searches on the entire body.

problems of the older PET machines. These two separate scanners do not eliminate the motion of the patient's table which generates motion artifacts in the image, require high radiation, and provide limited quality of the images. They further diminish cost effectiveness, because the fast CT scanner (which requires one to four minutes) is limited by the slow PET scanner (requiring 50-90 minutes). This limits the number of patients who can be examined in a given time and increases the examination cost. Conversely, the new 3D-CBS combines both units (CT and PET) intrinsically in a single detector, which captures photons from both sources (CT x-rays and PET γ-rays). The 3D-CBS requires a combined examination time of only two to four minutes, eliminates the image motion artifacts with its stationary bed, increases the number of examinations possible per day, and reduces the radiation administered to the patient. In summary, the 3D-CBS device synergizes the efficiencies of the two machines.

While CT measures morphological changes and must be capable of the best spatial resolution to provide the clearest possible image of these changes, PET measures biological processes, which show up with varying amounts of photon emission activity, thus requiring the best sensitivity in photon detection (See Section 3, Figure 5, and Figure 7).

Breakthrough in sensitivity

The high sensitivity[5] of the 3D-CBS yields better information concerning cancer size and growth activity at very early stages, before morphological changes take place, and can show the body's reactions to a drug by measuring the activity of the biological processes and displaying the information (with slow or fast motion) on the monitor (see Section 3, Section 4 and Section 8).

Lower radiation and lower cost CT

The CT section of the 3D-CBS can work at very low radiation[4], [8] for the purpose of providing only the attenuation correction coefficients necessary during PET examination (e.g., used during cancer screening), or can be used during clinical workup with higher dosage as a current fast CT fluoroscopy (display of constantly updated images produced by continuous rotation of CT source(s)). The 3D-Flow digital signal processing on each electronic channel of the 3D-CBS with a sampling rate of 50 ns functions in counting mode, detecting single photons, or in integration mode, similar to the commercially available CT, to provide a higher resolution picture at lower radiation.

The CT examination in the 3D-CBS scanner is combined with the 2- to 4-minute PET, and its cost is included in the costs reported in Table I, Table X, Table XII, and Table XIII.

Functional and anatomical whole-body three-dimensional dynamic imaging

The unique functionality of the 3D-CBS, is its capability of showing combined functional and anatomical dynamic three-dimension images of most (~ 130 cm in length) of the body of the patient. Current scanners cannot provide such functionality; because of their small detector, they cannot acquire data concurrently from a large portion of the body but can, at best, acquire data sequentially from a 15 cm PET FOV and in slices of 32 mm of the body from a CT. (See the latest multi-slice CT scanners from GE (8-slice), Marconi and Siemens (16-slice), and Toshiba with more slices in the near future. See also Figure 7, Figure 11 and Sec. 8.7). Because the slices represent conditions at different times, the collage of images does not give a clear, true picture.

Breakthrough in cost-efficiency

A detailed analysis of the cost of the entire project and its improvements in efficiency[5], compared to current PETs with best sensitivity or highest resolution, and compared to historical data, should answer any questions about its cost effectiveness. (See Section 7 and Figure 25 for the cost of the entire project, Section 8.6, Table IV, and references [1], [2] for best sensitivity, highest resolution and historical data).

Focus on electronics rather than on fast crystals

During the past 20 years, designers of PET devices have focused on improvement of the crystal detectors. For about 15 years, the fast lutetium orthosilicate (LSO) crystals, which are nearly ideal[6], have been available; however, the world-wide production capability[7] of LSO is still far from what would be necessary for a development plan such as the one proposed in this article. (See also Section 8.6 and Section 14.)

If LSO or other similar fast crystals become more readily available[7] or less expensive in the future, the design of the 3D-CBS can accommodate these fast crystal detectors as well simply by loading a different program (a real-time pattern recognition algorithm) into the 3D-Flow processors' program memory. However, slow crystals such as BGO and CsI(TI),

---

[4] One example of an application of CT with very low radiation is described in Section V of [8] where the author estimates radiation dose to the skin of less than 0.1 mGy (or about 10 days worth of background radiation).

[5] The breakthrough in efficiency of the 3D-CBS in capturing photons, even if slow crystals are used, is achieved through the 3D-Flow architecture of the electronics, which can perform, with zero dead-time, pulse shape analysis with Digital Signal Processing (DSP) on each channel, with correlation with signals from neighboring channels as well as from channels far apart and with improvement of the signal-to-noise ratio (S/N) before adding them during reconstruction of the total photon's energy. In addition, the unique architecture of the electronics can accurately determine the photon's arrival time, resolve pile-up, perform several measurements requiring complex calculations (depth of interaction, clustering, signal interpolation to increase spatial resolution, etc.), and limit the detector dead time to the very small area where the incident photons hit the crystal, rather than a large area of the detector as now occurs with current PET electronics (see Appendix C.3, C.4, C.5, C.6, Figure 31 and Figure 34).

[6] An ideal scintillating crystal should not be hygroscopic and would have the speed of the Barium Fluoride (BaF_2), the density of Bismuth Germanium (BGO) and the light of thallium-activated Sodium Iodide (NaI(TI)), yttrium orthosilicate (YSO), or Cesium Iodide activated by Thalium (CsI(TI)). Lutetium orthosilicate (LSO) is nearly ideal and has been incorporated in the most recent PETs. However, the search for an economical new material that is dense and has a short decay time (or narrow light pulse) is still underway.

[7] In order to achieve the very conservative projection of about 3,000 3D-CBS scanners by 2010, approximately 150 m^3 of scintillating crystals (see calculation in Section 14) will be needed during the next 9 years just for the U.S. market, and over 500 m^3 would be needed if the world wide market was considered. Because during the past fifteen years the overall worldwide production of fast LSO crystals was less than 5 m^3, it is difficult to imagine that the production capability for LSO crystals could increase to 500 m^3 during the next nine years.

which are available in abundance now, can be used in the 3D-CBS (see App. C.2, item 5, Appendix C.6 and Figure 34).

The 3D-CBS unit cost

A common question arising from a description of the 3D-CBS is "How much does the machine cost?" Often the person asking the question is discouraged to hear that it costs more than the current PET. However, the focus should be on the cost per examination rather than on the cost per machine. When a person needs to go from France to England (or *vice versa*), he or she does not ask how much the tunnel under the Channel costs, but rather he asks how much a ticket to cross the Channel costs. (A row boat would cost less than a tunnel project costing billions of dollars; however, the tunnel has obvious advantages that made it worth building). In the case of medical imaging, it is hoped that the 3D-CBS will, as did the CT[8] [9], [10] some twenty years ago, surmount the initial resistance against it and come to be recognized as an effective tool in the fight against cancer and heart disease.

The higher cost of the larger 3D-CBS detector (by a factor of two or three) compared to the current PET can be recovered twice as fast because of the significant reduction in radioisotope and personnel costs; six times the number of patients examined per day with 1/30 the radiation dose[2] [11].. See Table XIII.

Projected market of the 3D-CBS

The example described in this article considers only the U.S. market, which is presently less than 1/3 the world market for medical imaging. This market is expected to reach the level of only one quarter of the scans for diagnostic workups currently done by CT in the U.S by the year 2010 and to screen only 15% of the U.S. population over 50 (see Table XIV and Table VII). This estimate is very conservative compared to the 60% market of fused[9] images projected by Dr. Wagner, one of the founders of nuclear medicine. However, even this limited market would require about 3,000 3D-CBS scanners in the U.S. by 2010. (See Table IV and Table VII).

A very conservative estimate of the 3D-CBS diagnostic workup and cancer screening market is about $5 billion per year by the year 2010 in the U.S. (See Table V and Table VI) If Dr. Wagner's projection[9] is considered, the market will more than double; and if we consider the world-wide market (using Dr. Wagner's projection), the market could be over $50 billion per year by 2010. (See Sections 12 and 14).

Although these figures seem high, they are low when one considers (a) overall health care expenditures, (b) the benefits of the new technology in lives saved, and (c) the savings in the cost of other procedures avoided because of the superior imaging of the 3D-CBS diagnostic device (see Table XI). To illustrate, the projected annual $2.46 billion expense by the year 2010 for diagnostic workups using the 3D-CBS is only 0.093% of annual health care expenditures; even if the 3D-CBS' markets for diagnostic workups and cancer screening are considered, it would be only 0.189% of U.S. health care expenditures. See Figure 25.

The 3D-CBS operating costs

The operating costs[10] of the 3D-CBS shown in Table I include the capital cost of the machine amortized over 8 years; the capital cost of the building where the machine is located (estimated at $1 million) amortized over 40 years; and the operating cost, including the expenses of the radioisotope[11], the personnel[12], the maintenance[13], and the upgrades.[14]

For purposes of comparison, let us use an examination price of $400. At this price, the revenues per year for the current PET with about 25 cm axial FOV (see left side of Figure 3) are based on a quantity slightly above the average[15] [12] (about 5 per day or 1,250 per year) as 1,250 x $400 =$500,000 per year. Because of the expenses of $1.775 million per year (see center column of Table I), the current PET would show a loss of about $1.275 million per year.

---

8 Several experts in the field, such as the president of RSNA, Dr. Robert Parker, have facts [9] showing that a more expensive machine (such as the CT scanner) compared to several smaller, organ-specific, medical imaging machines, reduced health care costs and improved the patient's care. Statistics show that imaging equipment is not driving the cost of health care. AK Dixon et al. showed as early as in 1987 that the cost of treatment and diagnosis can be reduced considerably using whole-body CT (see reference [10]). The number of CT units per million inhabitants is the highest in Japan with 68 machines compared to 29 in USA; however health care costs per capita are lower in Japan compared to USA. (See Table XVII). Perhaps we should consider whether increasing our investment in imaging technology would reduce the cost of health care.

9 Dr. Henry Wagner, one of the founders of nuclear medicine, made the following prediction at the 2000 meeting of the Society of Nuclear Medicine: "Within five to 10 years, 60% of all imaging studies will be fused images." (The term "fused" refers to multimodality, such as PET combined with CT, or functional and anatomical imaging).

10 The last line of the table is the profit or loss calculated as the total revenues (price of the exam times the number of exams) less all the operating costs (see details of the operating costs from line 1 to line 7 of the table).

11 Radiopharmaceutical costs, as well as building costs, may vary substantially depending on the location; figures in this article are conservative, using the figures toward the highest costs (Radiopharmaceuticals for PET are more expensive in the U.S. than in Europe, while the buildings are more expensive in Europe.) Although the 3D-CBS will be scanning more patients per day and it will use a lower daily quantity of radioisotope, the daily cost for ^{18}F-FDG radioisotope has been kept the same for the three scanners ($3,400/day). The cost of the ^{18}F-FDG is higher in the U.S. compared to Europe. This estimate is based on the higher U.S. cost for the amount of radioisotope needed by a ~25 cm axial FOV PET, which is ~$3,100 per day for scanning 4 patients/day, ~$3,400 per day for scanning 5 patients/day, ~$3,600 for scanning 6 patients/day, and ~$3,800 per day for scanning 7 patients/day.

12 Personnel costs have been based on Table 5-2 on page 37 of [29]: ½ MD, 2 technologists/administrators for the >14 cm FOV; ½ MD, 2 ½ technologists/administrators for the ~25 cm FOV; 1 MD, 2 ½ technologists/administrators for the 3D-CBS.

13 Annual maintenance cost has been assumed to be $60,000 for the < 14 cm FOV PET, $100,000 for the ~25 cm FOV PET, and $200,000 for the 3D-CBS.

14 Annual costs for the upgrade of the scanners have been assumed to be $60,000 for the < 14 cm FOV PET, $100,000 for the ~25 cm FOV PET, and $150,000 for the 3D-CBS. Because the 3D-CBS has included all possible improvements, the costs for upgrades is relatively low and is mainly due to software upgrade, while for the short FOV PETs there is room for more improvements.

15 See the article in reference [12] reporting that in the year 2000, 250 PET units in the U.S. made over 250,000 examinations.

(This explains why the current PET exams cost between $2,000 and $4,000. See Section 9).

The current PET with a shorter axial FOV (< 14 cm) would entail a lower expense than the PET with about 25 cm axial FOV; however, because it is also slower than the 3D-CBS, it can perform even fewer examinations (about 4 per day or 1,000 per year). The loss, therefore, will still be about $1 million per year (see left column of Table I).

Conversely, the 3D-CBS with about 150 cm axial FOV (see right side of Figure 3) can perform more diagnostic workup examinations (about 30 per day or 7,500/year), providing a net revenue of about $310,000 per year per scanner. This is calculated as $400 x 7,500 exams = $3 million, less costs of $2.69 million (see right column of Table I).

The 3D-CBS will still be advantageous when used for a lower volume of patients per unit because it will perform the examinations in fewer days per week, saving radioisotope and personnel costs. (See Table X). Table XII reports a detailed study of the lowest price possible for an examination using 3D-CBS vs. other PET devices. It shows that the 3D-CBS could sustain a $300/examination price (compared to the current average price of $3,000/exam). A major beneficiary of the entire process will be the patient who will receive, thanks to the competition, a better examination with a better quality image and lower radiation requirement[2] at about 1/10 of its current cost.

Overview of this article

This article provides (a) a study of the social impact of the introduction of this new 3D-CBS device (see Sections 1, 2, 8, 9, 11, 12, 13, and 14), (b) an analysis of its economic impact in health care (see Sections 1, 6, 8, 9, 10, 11, 12, 13, 14, and Appendix A), and (c) the basic concepts of the technological advances of the 3D-CBS[2]. (See Sections 2, 3, 4, 5, 7, 13, 14, Appendix B, and C).

The technological issues which are addressed in this document are: (a) the deficiencies of current PET, described in Appendix C.1; (b) how these deficiencies are remedied by the 3D-CBS, described in Appendix C.3, C.4, C.5, and C.6; and (c) the distinctive innovative features of the 3D-CBS, described in Section 4 and Appendix C.2

Section 10 shows the main reasons for the need for technological advancement in non-invasive pre-clinical diagnosis.

2 THE IMPACT OF THE 3D-CBS IN HEALTH CARE

2.1 The need for imaging devices and drugs

Effective treatments are available and a considerable budget for research on new drugs is also in place; however, without a diagnosis of the disease at a treatable stage, existing drugs and other treatments cannot be optimally effective (see Appendix A.2).

Section 10.2 provides statistical data of the major causes of death among people under 67 (the lowest general statistical life expectancy figure) and indicates what is necessary to help to defeat cancer and heart diseases. (See Table VIII. See also Figure 20, showing the areas which need more improvement.)

The historical and projected costs of global health care in the U.S. are shown in Table II, while Figure 4 shows the annual expenditures on prescription drugs at retail outlets[16] [13], [14] for the years 1980-2010 (historical statistics and HCFA's underestimated[17] projected growth for the next decade) and the expenditure on electromedical imaging[18] [15] devices in the U.S.

Table II details health care expenditures in the U.S. It shows that from 1980 expenditures by health insurance plans increased more than "out-of-pocket" expenditures and are projected to more than double by 2010. In 1995 about half of health care costs were paid with public funds, while in 2000, private expenditures increased more than public. The projection by HCFA for 2010 is that private expenditures will be about 25% higher than public expenditures.

TABLE II. HISTORICAL AND PROJECTED DATA OF U.S. HEALTH EXPENDITURES DURING 1980-2010 (SOURCE: HCFA[19] [13], [14]). SEE ALSO THE U.S. HEALTH CARE EXPENDITURES AS A SHARE OF THE GDP IN TABLE XVI.

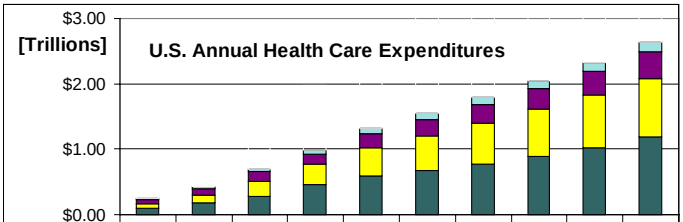

	1980	1985	1990	1995	2000	2002	2004	2006	2008	2010
Total exp.	$0.25	$0.43	$0.70	$0.99	$1.31	$1.54	$1.79	$2.05	$2.33	$2.64
other priv.	$0.01	$0.03	$0.04	$0.06	$0.08	$0.10	$0.11	$0.12	$0.14	$0.15
Out of pocket	$0.06	$0.10	$0.14	$0.15	$0.20	$0.24	$0.28	$0.32	$0.36	$0.40
Insurance	$0.07	$0.13	$0.23	$0.32	$0.44	$0.53	$0.63	$0.72	$0.81	$0.90
Public	$0.10	$0.17	$0.28	$0.46	$0.59	$0.68	$0.78	$0.89	$1.02	$1.18

16 Drug class of expenditure reported by HCFA is limited to spending for products purchased from retail outlets. The value of drugs and other products provided to patients by hospitals (on an inpatient or outpatient basis) and nursing homes, and by health care practitioners as part of a provider contact, are implicit in estimates listed in [13] of spending for the service of those providers.

17 The growth of prescription drug expenditures in the U.S. of 16.9% in 1999 reported by HCFA in Exhibit 2 of [16] is underestimated because it accounts for only some of the drugs. A more complete analysis by IMS Health in [14] where all prescription drugs in the U.S. in 1999 are considered, shows a growth of 19%. This will further increase the difference in percentage of expenditures in 2010 between drugs and medical imaging with respect to the projected growth shown in Figure 4.

18 Sales of electromedical and irradiation equipment in the U.S., (manufactured in the U.S., export and import) are available from [15]). Total U.S. electromedical and irradiation equipment manufacturing sales were $6.7 billion in 1990, $9.8 billion in 1995, $13.1 billion in 1998 and $13.9 billion in 1999. During 1998 scanners were sold in the U.S. in the following categories: $560.5 million CT scanners ($542.6 million worth produced in the U.S., of which $114.2 million worth were exported, plus $132.2 million worth imported); $884.7 million ultrasound scanning devices ($1,300.6 million produced minus $497.2 million exported plus $81.3 million imported); and $882.6 million MRI devices ($842.9 million produced minus $251.6 million exported plus 291.2 million imported).

19 Source: U.S. Health Care Financing Administration (HCFA), Office of the Actuary, National Health Statistic Group.

Although the total cost of health care in the U.S. is increasing every year (however, with a lower increase compared to the increase in the Gross Domestic Product (GDP) during the last three years[20] [16]), advances in technology such as the 3D-CBS can help to keep health care costs lower and improve efficiency[8].

On the other hand, while the percentages expended for health care in most of the categories, such as hospitals and electromedical equipment, were lower or the same (see Table XVIII), spending on drugs during the past decade has increased out of proportion, and there has not been a commensurate positive impact on the death rate or quality of life[21]. It is worth mentioning here that most cancer cases are still detected in stage II or later, requiring painful procedures of radiation and, chemotherapy, instead of being detected in the first stage, when cancer can be completely eliminated with surgery before it enters the blood stream.

To the degree that we can assume a direct correlation, the increased expenditure was not cost-effective. If the increased drug use shown in Figure 4 had an impact on quality of life and death rate, one would expect to see a decrease in the death rate shown in Table IX; however, that slope does not show a variation for that period different from that of the previous years. The combination of the new, improved drugs and the 3D-CBS diagnostic imaging system capable of giving the physician a means of measuring the effects of new drugs will optimize the use of drugs and reduce their cost.

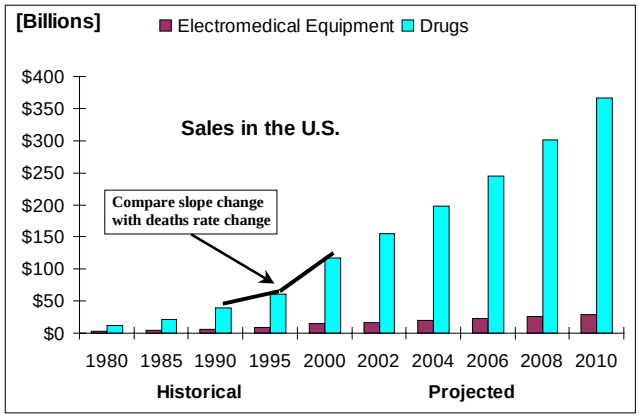

Figure 4. Annual sales of prescription drugs (historical and HCFA underestimated[17] projected growth) in U.S. from 1980 to 2010, excluding the cost of drugs used in hospitals, nursing homes, and by health care practitioners. If all prescription drugs were considered, 20% would be added to the reported cost (source[16] [16]). The expenditures for electromedical equipment were obtained from the U.S. Census Bureau (source[18] [15]). See also the percentage of personal health care expenditures for service in categories such as hospitals, dental, etc. in Figure 24 and Table XVIII. The positive change in slope in 1995 shown in this figure should generate a negative change in slope in Table IX.

Drug expenditures have increased more than other health care expenditures[22] []. We should evaluate whether health benefits are maximized by the apparent current emphasis placed upon an increasing drug expenditure, or whether increasing health care expenditures in other areas would be more beneficial or cost effective.

In 1992 HCFA projected that total U.S. health care expenditures would reach $1.7 trillion by the year 2000, an amount equal to 18.1% of the GDP. (See Table 7 of [17].) However, the actual figure reported for 2000 by HCFA in 2001 [16] was $1.3 trillion, or 13.1% of the GDP, considerably better than expected. Instead of registering a growth in health care expenditures as a percentage of the GDP, a reduction was registered during the years 1996-1999. (See exhibit 3 of [16], and Table XVI of this document.)

In the same article (see Table 8 of [17]) HCFA projected a decline in expenditures for drugs (and medical non-durables[16]). Starting at 9.4% in 1991, HCFA (in 1992) expected this figure to be 9.1% in 1992, 8.9% in 1995, 8.3% in 2000, 7.4% by the year 2010, and as low as 7.2% in 2030. (See also Table XVIII and [18], [19], [20], [21], [22], [23]). Conversely, and unfortunately, HCFA grossly underestimated spending on pharmaceutical; the actual expenditures for drugs and medical non-durables went in the opposite direction to 10.8% in 1997 and 12.7% in 2000. HCFA now expects[17] expenses for drugs and medical non-durables to be 17% by the year 2010. (These projections can be calculated from exhibit 1 of [16]).

Improved medical imaging equipment (such as the 3D-CBS, with reduced radiation[2] to the patient) will not only save more lives with early detection of diseases, but will also reduce the cost of prescription drugs by monitoring the efficacy of drugs and providing a tool to utilize them more efficiently. They will also promote the development of new drugs by more accurately monitoring their effect at the anatomical and molecular levels.

2.2 Early detection and diagnostic workup

There are two distinct applications for the 3D-CBS imaging device: the current application in diagnostic workups on patients with symptoms of cancer or other illnesses, and the proposed application for preventive screening for cancer, heart disease, and monitoring of asymptomatic patients (people who appear to be healthy). See Section 10.

Regarding diagnostic workups, about 30 million Americans[23] received a CT scan during the year 2000 at a

[20] The title of the article [16] refers to health care expenditures in absolute dollars; however, a careful reading of the data in the article reveals that during 1999 (as well as during 1994 and 1996-1998) Americans spent less money for health care compared to the previous years expressed as a percentage of the GDP.

[21] During 1999, drug expenditures increased by 19% over 1998 [14]; however, measurements of additional lives saved did not show a great reduction in the death rate compared to the previous years.

[22] The entire electromedical[18] [22] imaging budget in the U.S. of about $13 billion in 1998, or 1.1% of the total health care expenditures (see Figure 25) are responsible for the increase in the entire health care expenditures. On the other hand, an increase in drug expenditures [16] from 4.9% of the total U.S. health care expenditures (or $12 billion) in 1980, to 8.9% (or $116.9 billion) in 2000, with a projection of 13.8% (or $366 billion) in 2010, should be analyzed to see if drugs are optimally utilized. (See Figure 4 and Figure 24).

[23] The number of CT examinations in the U.S. is calculated as 2,600 exams per scanner per year. (In past years, each scanner performed more exams. See also Table IV for the CT scanners and Table XIV for the projected number of exams in the U.S.). Fewer exams per scanner are performed in Japan.[8]

price of about $400 to $800 (depending on whether the exam was with or without a contrast agent, or if both exams were required). Using the 3D-CBS, only one exam at a price of about $400 would be necessary: a PET exam with the 3D-CBS using a radioisotope will provide better information than current CT with a contrast agent, and a CT exam within the 3D-CBS will provide an image without a contrast agent because its data can be filtered electronically from PET exam.

Regarding preventive care screening, the $300 cost minimum (see Table XII) for the non-invasive 3D-CBS exam offers, in a single exam of two to four minutes' duration, a more thorough search for disease in the whole body at lower risk than some current procedures, and it is competitive with the summation of the costs of several current screening procedures regularly reimbursed by health insurance, such as mammograms, pap smears, digital rectal examinations (DRE), prostate specific antigen (PSA) tests, etc. In addition, the 3D-CBS would take the place of some other procedures not always covered by health insurance, such as colonoscopy, CT scan, etc. (see Table XI).

Sixty percent of deaths in the 45-64 age group are due to cancer and heart disease. Because of the limited screening of people over 50 years of age and the limited scope of organs screened by current procedures, this figure is much higher than it might be with an annual preventive, whole-body health care screening program. In other words, many of these untimely deaths could be avoided with whole-body preventive screening. A study conducted by the National Cancer Institute determined that cancer alone costs the U.S. $107 billion per year. An annual screening of about 15 million Americans (about 15% of the population over 50) by the year 2010 as shown in Table XIV would cost only about $4.5 billion ($300 x 15 million exams), would offer greater coverage in terms of the percentage of the population examined and in terms of the comprehensiveness of the individual examination, and would reduce the death rate from cancer and heart disease and reduce health care costs[8].

3 HOW DO IMAGING SCANNERS AND THE 3D-CBS WORK?

The Computed Tomograph (CT) measures the density of body tissue by sending low-energy x-rays (60 to 120 keV) through the patient's body and computing their attenuation on the other side (see left side of Figure 5).

Positron Emission Tomography (PET) uses radioactive substances injected into the patient's body that emit photons at higher energy (511 keV) and shows biological processes by tracking, at the molecular level, the path of the radioactive compound (see right side of Figure 5).

A PET examination detects cancer by using the body's consumption habits (metabolism) allowing it to monitor blood flow and brain activity.

The patient is injected with a radioactive isotope (e.g., fluorine ^{18}F) attached to a tracer (i.e., Fluorodeoxyglucose - FDG - or ^{15}O-water) that is a normal compound used in the biological process of the human body.

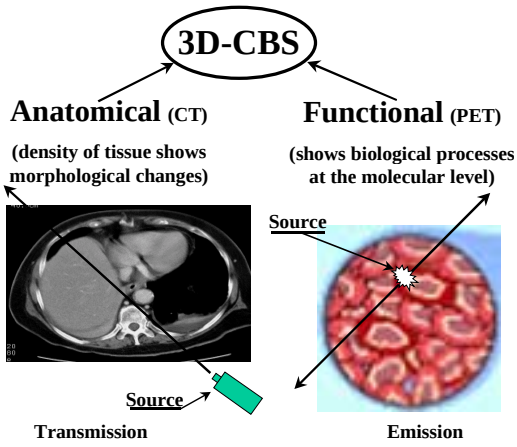

Figure 5. Differences between CT (left in the figure) and PET technologies (right in the figure).

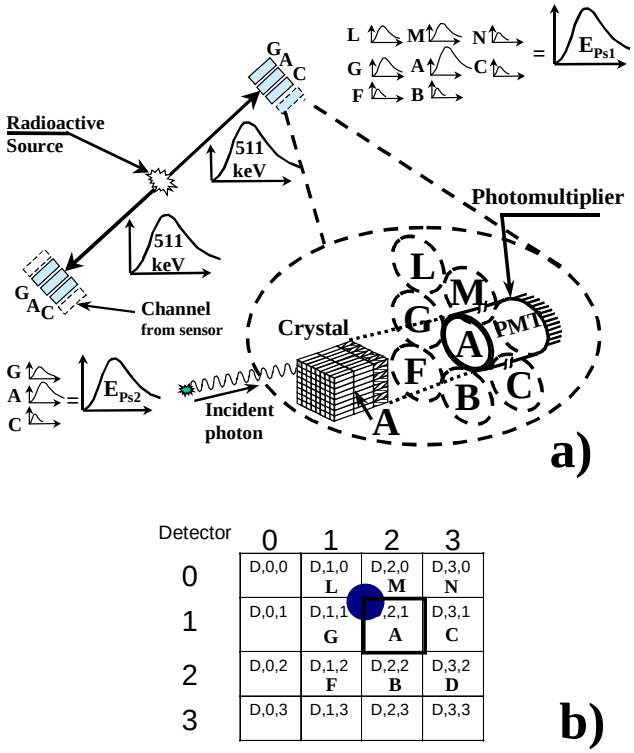

Figure 6. Detail of photon's detection (CT at 60-120 keV, or PET 511 keV) in the new 3D-CBS device design. When a photon hits the detector, it is absorbed by the crystal, which then emits light. The crystals are coupled with sensors (photomultipliers –PMT- or Avalanche PhotoDiode –APD-) which convert light into electrical signals, and these signals are in turn sent to an array of 3D-Flow processors. (See Section (a) in the figure and see also Figure 8 and Figure 10) An incident photon may induce signals in several adjacent PMTs or APDs. (See Section (b) in the figure and see also Figure 31.) The area under the curve of the electrical signal and its shape contains the information of the interaction between the photon and the crystal, such as, energy, amplitude, narrow or large light pulse, etc. Acquiring all the information requires adding and comparing the information from adjacent detector elements. The array of processors, which are interconnected in the same geometrical arrangement of the detector elements, exchange signals in order to rebuild the total energy of the incident photon. (See in Appendix C.6 and Figure 34 an example of the 3D-Flow programmable real-time algorithm which extracts the information of the interaction between the photons and the detector).

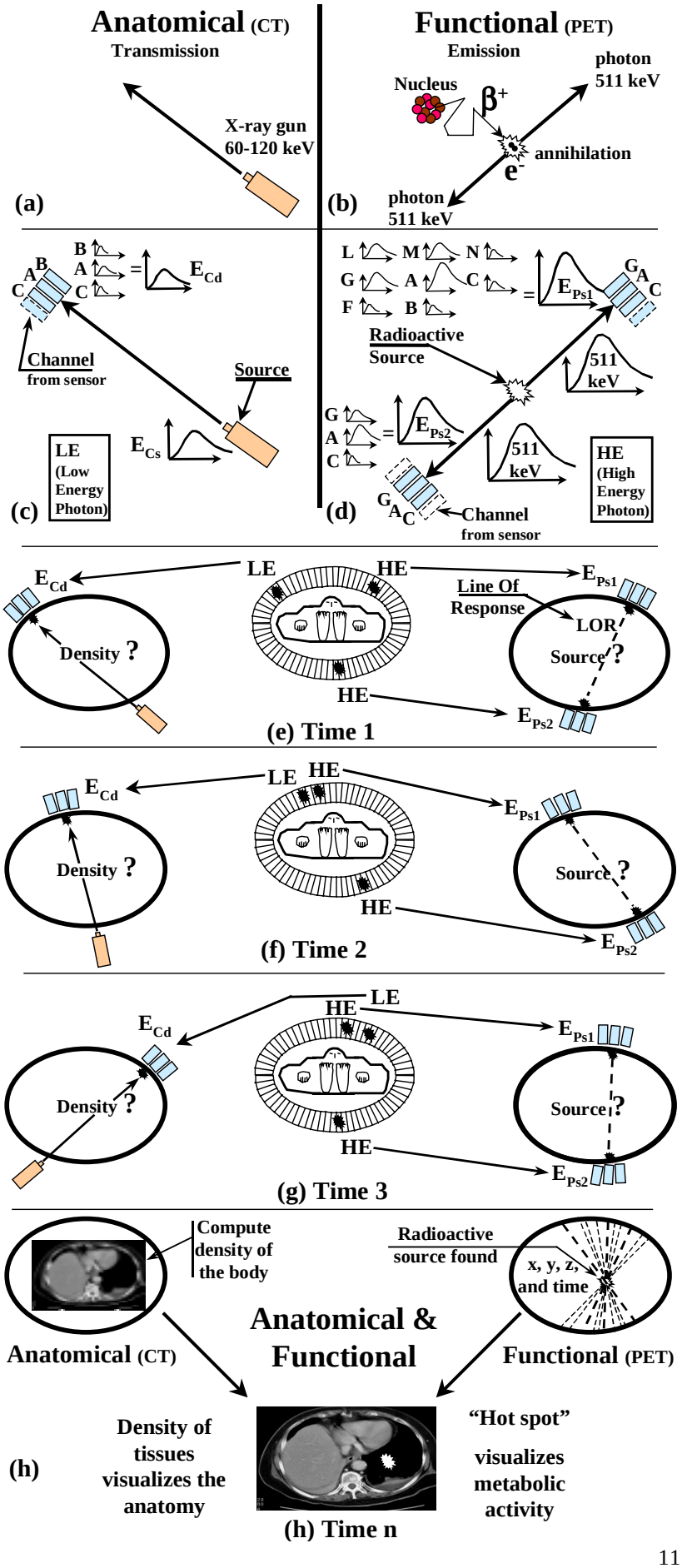

Figure 7. Details of the paths of the x-ray (CT) and γ-ray (PET) photons and the techniques used to compute the anatomical and functional images. Photons arrive at the detector at random time intervals. When a short time interval of 2 to 3 ns is considered (e.g., as shown in section e, f, and g of the figure) there is a high probability of capturing not more than two high-energy photons (HE) in time coincidence from the same PET event and eventually one low-energy photon (LE) in the target area of the x-ray gun. The task of the detector and of the electronics is to recognize most of these PET and/or CT events and to provide accurate information to the workstation that computes the anatomical and functional images. Each photon is recognized only if thorough[5] measurements are performed on the signals as they are received from the sensors through the electronic channels. Statistically, with a dose of 10 mCi of ^{15}O-water, equivalent to 42 mrem radiation to the patient, about 100 million photons per second (see Figure 17) will hit the 3D-CBS detector (~ 150 cm FOV), which is coupled to 1,792 PMTs. On average, each PMT will receive one photon every 18,000 nanoseconds. The 3D-Flow system of the 3D-CBS samples and independently processes all 1,792 electronic channels every 50 ns with the capability of measuring the photon arrival times with a resolution of 500 ps by making use of a Time-to-Digital converter (TDC). Among the most important of several measurements performed is that of rebuilding the total energy of the incident photon. Because a photon may strike the detector crystal in a location where it can produce signals in neighboring sensors, the sum of signals from neighboring sensors must be computed. Thus, the energy of a CT event measured at the detector is the sum E_{Cd} = A + B + C (see section c in the figure). The programmability of the 3D-Flow front-end electronics (see Figure 34) makes it possible to acquire the CT photons in counting mode (detecting the arrival of single photons), or in integrating mode for obtaining faster acquisition and higher resolution images. (See also Section 8.7). An example showing the process in PET, found in section d of the figure, shows the energy of one 511-keV photon that has been measured as E_{ps1} = (A + B + C + F + G + L + M + N); note that the matching 511-keV photon has been measured as E_{ps2} = A + C + G. When the detector receives more than one hit within 2 to 3 ns (e.g., during Time 1 in section e of the figure), the elctronics separates the HE events from the LE events. It finds the location of the HE event and the LOR passing through the two detectors that received the hits. The intersection of millions of LOR per second locates the emitting source, as shown in the right side of section h of the figure, while the computation of the attenuation of the x-rays (LE) determines the density of the body and displays its anatomical image on the monitor.

It is possible to reveal the molecular pathways of the tracer, because the radioactive fluorine isotope emits a positron β^+ that annihilates with a nearby electron e^- after a path of about 1.4 mm to over 13 mm depending on the radioisotope used. (See Figure 7b in this document and Table 7-1 at page 26 of [1].) This produces two annihilation photons, emitted in diametrically opposed directions (back-to-back). This phenomenon, the annihilation of a positron β^+ and an electron e^- simultaneously producing two photons is called "an event."

In PET technology, the two photons travel through and out of the body and are absorbed by the crystals in the detector rings of the detector apparatus. (See Figure 6, Figure 31 and central column of Figure 7e, f, g). The crystals are coupled with photomultipliers which in turn send the electrical signals to an array of 3D-Flow processors [4], [24], [25], [26], [27]. See the shaded rectangles labeled with the letters A, B, C, etc., in Figure 6, which are magnified at the bottom of the same figure and see also Figure 7d. See also top of Figure 8 and Figure 9.)

The processor array analyzes and correlates the received signals with the nearest neighbors, measuring the amount of energy absorbed by the crystals, the light-pulse duration, the arrival time and the location of the photon. This information regarding the total energy of each incident photon and its arrival time will be used during phase II of the processing, when the correlation between two distant photons will be made. This will make it possible to identify the matching pair of photons originating from the same event.

The photons are emitted by the radioisotope inside the patient's body at a rate of up to hundreds of millions per second. When the 511-keV photon pair is simultaneously recorded by opposing detectors, an annihilation event is known to have taken place on a line connecting the two detectors. This line is called the "Line of Response" (LOR). (See right column of Figure 7e).

First, while processing[5] during phase I, based upon when and where the photons' energies were absorbed by the crystal detector, the electronics identifies the "good photons[24] [28]." (See right column of Figure 7d). Second, each photon needs to find its companion emitted at the same time (or in time coincidence). Third, the pairs of photons are identified and LOR is described. Fourth, the intersection of millions of LOR per second indicates the location of the source (x, y, z, and time), and its activity is translated into graphics on a computer screen. (See right column of Figure 7h).

The same electronics of the 3D-CBS also detects photons at low energy (LE) occurring concurrently with the high-energy (HE) photons but being received at the expected locations, according to where the x-ray gun is directed (see Figure 7a, c). The electronics then calculates the attenuation of the signal, which is proportional to the type of body tissue it traversed, and computes the anatomical image of the patient's body from this data (see left columns of Figure 7e, f, g, and h).

The main characteristic, and value of the PET technology compared to other technologies is its exploitation of the unique back-to-back emission of the two 511 keV. This quality coupled with the high sensitivity of the 3D-CBS to uniformly detect the emission source, regardless of its location, makes for a powerful tool in medical imaging.

Biochemical processes of the body's tissues, such as metabolism of glucose, are altered in virtually all diseases, and PET detects these changes by identifying areas of abnormal metabolism, which are indicated by high photon emission. Diagnostic imaging with the 3D-CBS will detect, at early stages, cancer and practically all diseases in which abnormal metabolism is signaled by increased or decreased radioactivity.

Cancer cells, for instance, typically have a much higher metabolic rate, because they are growing faster than normal cells, thus they absorb 60 to 70 times more sugar than normal cells and consequently emit more photons. Inflammatory diseases also absorb more sugar than normal cells.

Detecting these changes in metabolic rates with the PET enables physicians to find diseases at their very early stages, because in many diseases the metabolism of the cells changes before the cells are physically altered. Similarly, a PET machine can use different radioactive substances to monitor brain or heart metabolism activity.

There are areas, such as brain, kidney, and bladder wall, with normally higher metabolism activity than other areas of the body. The computer can subtract from each area the quantity of photons attributed to normal activity and show only the abnormal metabolism, by assigning different colors to levels of activity (e.g. yellow for low abnormal activity and red for high). This is a standard technique in image processing. The physician then looks for abnormal metabolism "hot spots," in the body. The recorded timing information of the data (or their recorded sequential order) allows the physician to display dynamically, for example, four minutes of recorded data in ten seconds, or to expand one second of recorded data to one minute of dynamic display (e.g., slow motion to better appreciate the speed of the metabolism, or the activity of cancer).

In general, PET technology has already replaced multiple medical testing procedures with a single examination[25] [29], [30]. In many cases, it diagnoses diseases before morphological changes have occurred, when other tests or other devices are incapable of detecting any anomaly.

Combining different technologies in one device further assists physicians in clinical examinations. Viewing PET functional imaging data in conjunction with CT morphologic cross-sectional data is sometimes mandatory if lesions are found.

[24] Good photons are those that originate from the same event and that arrive at the detector straight from the source without bouncing off other matter (Compton scatter). Efficient electronics at the front end can identify some Compton scatter events by accurately measuring the energy and the time of arrival of the photons; however, other Compton scatter events can only be identified after acquisition during the image reconstruction phase [28]. Missing good photons fail to provide a clear image to help the physician recognize subtle differences in normal health conditions.

[25] Two recent works on PET imaging in oncology are the book [29] and the article [30] with over 300 references

4 WHAT ARE THE KEY INNOVATIONS IN THE 3D-CBS ENABLING IT TO CAPTURE MORE PHOTONS?

The most significant improvements the 3D-CBS offers over the current PET are: (a) capturing more data from the emitting source and (b) processing the acquired data with a real-time algorithm which best extracts[5] the information from the interaction between the photons and the crystal detector. (See Appendix C.4, C.5, C.6 and Figure 34).

If more data from a radioactive source at the level of radiation currently used (or from a source with lower radiation activity) is captured by the detector, sent to the PET electronics, and processed correctly, then the examination time, radiation dosage, and consequently also the cost per examination can be significantly reduced.

In order to obtain more data, the axial field of view (FOV, the total length of the rings of crystals in the scanning detector) must be lengthened to cover most of the body. In order to process these data, the electronics must be designed to handle a high data input rate from multiple detector channels. The 3D-CBS can handle up to 35 billion events per second with zero dead time in the electronics (when a system with 1,792 channels as described in [2] is used), versus the 10 million events per second with dead time that the current PET can handle [31], [32], [33], [34]. High input bandwidth of the system is necessary because the photons arrive at random time intervals. (See Section 13 and 14 of [1]).

The references [2], [4] describe (a) a novel architectural arrangement of connecting processors on a chip, on a Printed Circuit Board (PCB), and on a system, and (b) a new method of thoroughly processing data arriving at a high rate from a PET detector using the 3D-Flow sequentially-implemented parallel architecture [1], [3] (See Table III and Figure 10.)

In layman's terms, the processing of the electronics on the data arriving from the detector can be compared to the task of reuniting families that have been separated by a catastrophic natural event. The following analogy in human terms is made: the two groups of signals (see Figure 6) generated by the sensors, that are coupled to the detectors hit by the two back-to-back photons of a single event are similar to the two halves of a families split apart, the mother with some of her children being separated far from her husband with the other children. The task of the detector is to find the back-to-back photons that came from the same annihilation event, or to reunite the two half families. The sequence of events in the family reunion example is one billion times slower than the sequence of annihilation events in the PET:

- A catastrophic event separates on average 17 families every 50 seconds. During the attempt to reunite the families, unfortunately, only about 12% of the husbands and wives can arrive at a reunion center. The reduction of families is analogous to the reduction of photons that are absorbed by the patient's body, or not captured by the detector because of the limited FOV and solid angle of the detector. See Figure 16.
- When a family was split, the husband and wife went in opposite directions, each with some of their children (similar to the back-to-back photons of the PET as described in Section 3 and shown in Figure 7b). In the analogy, the children in neighboring paths and the parent represent signals on neighboring sensors (or electronic channels) that have been generated by a photon striking the detector. The analogy illustrates the fact that the total energy of the incident photon that was split among several neighboring electronic channels must be reconstituted, just as the children must be first reunited with the parent. (See Figure 8 for an example showing channels A, B, C, and D of Figure 7c and d, the top of Figure 8 and the top of Figure 9)

The family reunion takes place in two phases. During the first phase, the father and the children who went with him but followed a neighboring path are reunited. The same process is followed independently, in a separate venue, by the mother with their other children; however, that takes place far from where the father is. During the second phase the two half-families are reunited.

Figure 8 shows an example of information split over several channels (or wires). A photon striking in such a way that its information is divided among several electronic channels is analogous to one parent with some children going down several paths. (See on the second row of the figure in the dotted lines, the split of a family among four paths, or wires, and on the third row the split of a family between two wires).

Because there are on average about four groups of fathers with their children (or mothers with their children) arriving[26] at random time intervals every 50 seconds at any place in the 1,792 channels at the reunion center, it is necessary to clearly identify family members and reunite the half-family (or to rebuild the energy of the incident photon) at their arrival site, before the children are mixed with millions of unrelated people.

4.1 Phase I: Reunite the half-family (rebuild the energy of each incident photon, determine its exact arrival time, measure the exact position of its center of gravity, measure the DOI, and resolve pile-up).

The solution to the problem of phase I, which is illustrated in a cartoon of the "family reunion" of Figure 9, is mainly provided by the "bypass switch" (or multiplexer) of the 3D-Flow architecture (see Table III and Figure 10). Information concerning the father and children, that is, the signals generated by the photon, arrives at the top of the channel (wire) and moves down one step each time new data arrive at the input. The numbers in Figure 9 correspond to the positions of the objects (data set or smiling face) at time 14t of Table III. Objects outlined in dotted lines correspond to the status one instant before time "14t."

The 3D-Flow architecture allows a high throughput at the input because (a) each data packet relative to the information about the photon (or about the family member) has to move

only a short distance at each step, from one station to the next, and (b) complex operations of identification and measurement can be performed at each station for a time longer than the time interval between two consecutive input data.

Every time a new data packet arrives at the top of the channel, all other data packets along the vertical wire move down one step, but the wire is broken (equivalent to a bypass switch in input/output mode) in one position where the station is free to accept a new input data packet and is ready to provide at the same time the results of the calculations of the previous data packet.

At any time, four switches in "bypass mode" and one switch in "input/output mode" (or the wire broken at a different place) are always set on the vertical wire. This synchronous mechanism will prevent losing any data at input and will fully process all of them.

When a data packet relative to a photon enters a measuring station (that is, a 3D-Flow processor, or the station represented on the right side of Figure 9), it remains in that station for its complete identification, measurements, and correlation with its neighbors. Several operations are performed at each station:

1. A "picture" is taken and sent along with the time of arrival to the neighbors, while "pictures" from the neighbors, along with their time of arrival are also received and checks are performed to see if there were any family members in the neighboring channels: similarly, the energy and arrival time of photons are exchanged between neighboring elements to check if the energy of the incident photon was fragmented between several channels. See Figure 34.
2. Local maxima (checking to see if the signal is greater than the neighbors) are calculated to determine if the parent arrived at that channel; this is equivalent to comparing the photon's energy and arrival time to similar information in the neighboring channels. If the parent did not arrive at that channel, the process at that channel is aborted to avoid duplication. The neighboring channel that finds the father will carry on the process.
3. Center of gravity is calculated (that is the point at which the weight of an object is equally distributed). This calculation will provide an accurate location where the half-family was found; this is equivalent to the spatial resolution of the incident photon. See Figure 31.
4. Pile-ups, which occur when two half-families belonging to two different families arrive within a very short time interval, or when two events occur in a nearby detector area within a time interval shorter than the decay time of the crystal. When this happens, the apparent integral of the second signal will show it riding on the tail of the previous signal. Digital Signal Processing (DSP) techniques of the 3D-Flow processor can detect the change of slope of the tail of the signal and separate the two signals.
5. The accurate arrival time of the half-family group is calculated and assigned to be carried for the rest of the trip; similarly, the accurate arrival time of the photon is calculated.
6. Other measurements are performed on the input data (half-family or photon), such as the depth-of-interaction (DOI) on the incident photon. DOI measurements solve the problem of identifying the affected crystal when the incident photon arrives at an oblique angle instead of perpendicularly to the face of the crystal. The 3D-Flow processor can utilize several DOI measurement techniques [35], [36], [37] that allow for correcting the effect commonly referred to as "parallax error."
7. Finally, the half-family is reunited (the total energy of the photon is calculated), all measurements are performed, and results are sent to the channel for its trip to the exit (See in Figure 9 the object r4 in the fourth station from the top, which is the result of the input data No. 4).

Only some of the above processing is carried on in the current PET. The most important task of rebuilding the energy of the incident photon (equivalent to reuniting a half-family) is not performed. On the contrary, current PET technique add analog signals before checking whether the signals belong to the same incident photon; this is equivalent to grouping father and children before checking if they belongs to the same half-family.

Figure 8. "Family reunion." A solution, that identifies family members and checks in detail for their characteristics, is needed for the reunion of the families. The figure shows an example of the arrival of information about the particles from several electronic channels at one time. As an analogy, several members of a family arriving at the same time on different channels (e.g. see four members of a family in the second row from top) are compared to a photon that has its energy split among several electronic channels. (The size of a family member is proportional to the area of the signal of Figure 6).

TABLE III. SEQUENCE OF THE DATA PACKET AT DIFFERENT TIMES IN THE PIPELINE STAGE (SEE FIGURE 10). ONE DATA PACKET IN THIS APPLICATION CONTAINS 64-BIT INFORMATION FROM ONE CHANNEL OF THE PET DETECTOR. THE CLOCK TIME AT EACH ROW IN THE FIRST COLUMN OF THE TABLE IS EQUAL TO $t = (t_1 + t_2 + t_3)$ OF FIGURE 10. THE NUMBER IN THE LOWER POSITION IN A CELL OF THE TABLE IS THE NUMBER OF THE INPUT DATA PACKET THAT IS PROCESSED BY THE 3D-FLOW PROCESSOR AT A GIVEN STAGE. THE VALUES IN THE RAISED POSITION, INDICATED AS ix AND rx, ARE THE INPUT DATA AND THE RESULT DATA, RESPECTIVELY, WHICH FLOW FROM REGISTER TO REGISTER IN THE PIPELINE TO THE EXIT POINT OF THE SYSTEM. NOTE THAT INPUT DATA 1 REMAINS IN THE PROCESSOR AT STAGE 1d FOR FIVE CYCLES, WHILE THE NEXT FOUR DATA PACKETS ARRIVING (i2, i3, i4, AND i5) ARE PASSED ALONG (BYPASS SWITCH) TO THE NEXT STAGE. NOTE THAT AT CLOCK 14t, WHILE STAGE 4d IS FETCHING 9, IT IS AT THE SAME TIME, OUTPUTTING r4. THIS r4 VALUE IS THEN TRANSFERRED TO THE EXIT OF THE 3D-FLOW SYSTEM WITHOUT BEING PROCESSED BY ANY OTHER d STAGES. NOTE THAT CLOCK 14t SHOWS THE STATUS REPRESENTED IN FIGURE 10 AND THAT INPUT DATA AND OUTPUT RESULTS ARE INTERCALATED IN THE REGISTERS OF THE 3D-FLOW PIPELINED SYSTEM.

Time	Proc (1d)	Reg (1d)	Proc (2d)	Reg (2d)	Proc (3d)	Reg (3d)	Proc (4d)	Reg (4d)	Proc (5d)	Reg (5d)
3t	1									
4t	1	i2								
5t	1	i3	2							
6t	1	i4	2	i3						
7t	1	i5	2	i4	3					
8t	6	r1	2	i5	3	i4				
9t	6	i7	2	r1	3	i5	4			
10t	6	i8	7	r2	3	r1	4	i5		
11t	6	i9	7	i8	3	r2	4	r1	5	
12t	6	i10	7	i9	8	r3	4	r2	5	r1
13t	11	r6	7	i10	8	i9	4	r3	5	r2
14t	11	i12	7	r6	8	i10	9	r4	5	r3

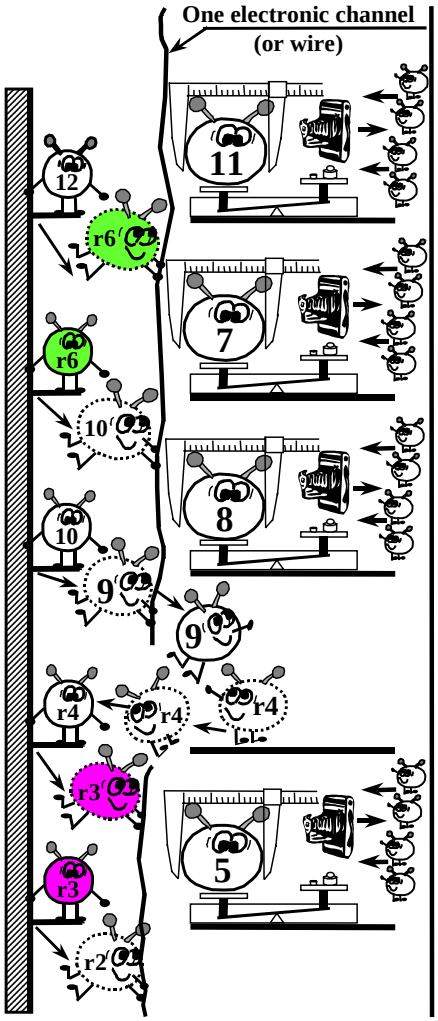

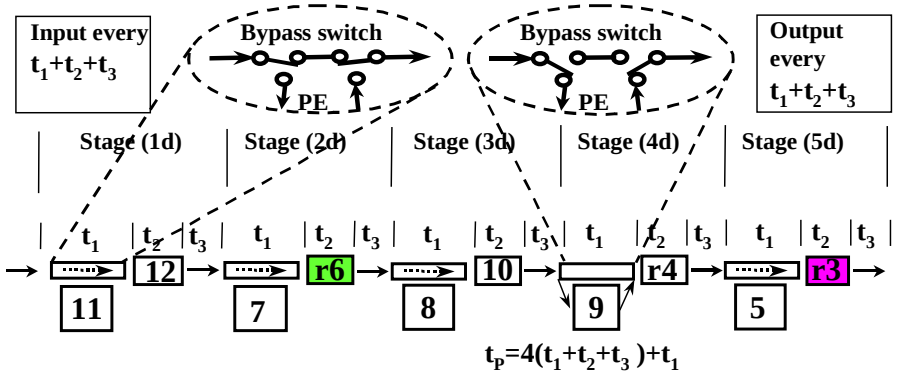

Figure 9. A "family reunion" cartoon for time 14t of Table III and Figure 10. Each photon remains in the measuring station (processor) for a duration five times longer than the time interval between two consecutive input data. The result from any measuring station will not be an input to the next station (as it is in a typical pipeline system) but will be passed on with no further processing in the 3D-Flow sequentially implemented, parallel-architecture until it exits (see additional description on next page).

Figure 10. The example shows how the 3D-Flow system extends the execution time in a pipeline stage beyond the time interval between two consecutive input data (sequentially-implemented, parallel architecture). An identical circuit (a 3D-Flow processor) is copied 5 times at stage d (the number of times the circuit is copied corresponds to the ratio between the algorithm execution time and the time interval between two consecutive input data). A bypass switch (or multiplexer) coupled to each processor in each 3D-Flow stage 1d, 2d, 3d, 4d, and 5d sends one data packet to its processor and passes four data packets along to the next stage ("bypass switch"). Thus, the execution time at each substation d will be $t_P = 4(t_1 + t_2 + t_3) + t_1$. The numbers in the rectangles below the switches identify the input data packets to the CPU of the 3D-Flow processor. (See also Table III for the sequence of operations during the previous clock cycles). A 3D-Flow processor is shown in the figure with the three functions of (a) a bypass switch (dotted right arrow in the rectangle), (b) an output register (rectangle to the right), and (c) a CPU (rectangle below). See the practical implementation of the 3D-Flow architecture on Figure 27, Figure 28, Figure 29.

Adding several analog signals before checking whether the signals belong to the same incident photon, as is done in current PET (see Figure 32), turns out to be very counterproductive at the next electronic stage because the analog signal (which is the sum of several signals) cannot be separated into its original components and the information on the single photons that is needed for several subsequent calculations is lost forever.

In the most advanced current PET, the electronics cannot complete the processing before the arrival of another data set, and consequently dead-time is introduced and photons are lost.

The conclusion is that the limitation of the electronics of the current PET (front-end and coincidence detection, described later) prevents it from detecting many photons, and the overall performance of the best current PET detects about two photons in time coincidence out of 10,000 emitted by the radioactive source. This should be compared to 1,000 photons out of 10,000 captured by the 3D-CBS, with its improved electronics and extended axial FOV. In addition, of the two out of 10,000 photons in coincidence captured by current PET, many will be discarded by subsequent processing, or will not carry accurate information. (See Section "Current PET limitations" in the introduction).

Conversely, the advantage of the 3D-Flow architecture of the 3D-CBS is a result of the use of several layers of stations (processors) with the data flow controlled by "bypass switches," (or multiplexer) allowing more than 50 nanoseconds to weigh the subject, to take the picture, to exchange them with the neighbors, to calculate the local maxima, the center of gravity, etc. Five layers of stations (or processors at the same level) allow 250 nanoseconds in each station to perform all the above calculation. In the event this processing time is not sufficient more layers are added.

The bypass switches will provide good synchronization of input data and output results at each station (or processor) by simply taking one data packet for its station and passing four of them along.

Using the scheme of Figure 9 we can follow the path of a data packet of photon (i3) through the entire system. At time 5t shown in Table III, the data packet of photon i3 enters the channel at the top of Figure 9. If it finds a busy station (processor) on the right, it rests for one cycle on the platform (or register, shown in Figure 10 as a rectangle next to the bypass switch).

During the next cycle, 6t of Table III, this data packet of photon (i3) advances to the next station. If this station is also busy, then it will rest on the next platform, and so on until it finds a free station.

When the data packet of photon (i3) finds a free station (at time 7t in Table III), it enters the station and stays there for five cycles for processing. After the data packet of photon r3 (which contains the results of the processing performed on i3) leaves the station and goes to the platform on the left, adjacent to the station (at time 12t), another data packet of photon (i8) enters the station from the upper left platform. The result from photon (r3) cannot go straight to the exit but can only advance one platform at a time until it reaches the exit.

In summary, the 3D-Flow sequentially implemented parallel-processing system is synchronous; it has a fixed number of steps and a fixed sampling rate, the data flows in an orderly fashion from input to output according to the time clock, and there is no congestion in the flow. The sequence is as follows:

- synchronously receive a data packet from the input of the system
- synchronously send out a data packet from the output of the system with a fixed time latency from when it was received by the system and with a tag identifying the result as either a non-data, a good CT photon, a good PET photon, or a Compton scatter photon, etc.
- process each data packet fully, with information exchange with neighbors, by a 3D-Flow processor in one layer of the system, regardless of whether or not it contains relevant data; no data packet is skipped or lost. The 3D-Flow system is dimensioned with the correct number of layers needed to fulfill the requirements of executing the real-time algorithm in full (a fixed maximum number of steps) on each data packet and of sustaining the maximum input data rate. There is always a free processor waiting to receive a data packet. If a processor finds no meaningful results and terminates its process in fewer steps, it waits its turn (because it is a synchronous system) before it sends out the result and fetches a new data packet at the input. If either the input data rate increases or the complexity of the algorithm increases, one or more layers are added to satisfy the requirement of zero dead-time. (See Figure 9 and the example of a real-time algorithm for identifying photons in Appendix C.6 and Figure 34. Its hardware implementation with the detailed layout of the components on an IBM PC board is described in Section V-C of [2]).

4.2 Phase II: Reunite husbands and wives (the two half-families reunited in phase I) from distant locations, or find the back-to-back photons in time coincidence

The measurements performed during phase I have reunited the half-families (each parent with some children), creating good candidates for the final entire family reunion. The result of the previous process is that, at most, four[26] new fathers (or mothers) are found every 50 seconds over the 1,792 channels.

[26] The assumption made at the beginning of this analogy of the need to reunite at the reunion center only 12% of 17 families (17 fathers + 17 mothers) separated every 50 seconds is equivalent to about four photons (two photons back-to-back per event) arriving on average at the coincidence circuit every 50 ns (which corresponds to a radiation activity of about 9 mCi administered to the patient). Six comparisons every 50 ns are necessary in order to find all possible matches among the four photons. A coincidence circuit with the capabilities of performing six comparisons every 50 ns (or 120 million comparisons per second) can handle a radioactivity of about 9 mCi of FDG which is far more the expected 0.3 mCi of FDG estimated to be required by the 3D-CBS for cancer screening. The implementation of a coincidence circuit that will perform more comparisons per second will not be a challenge even if higher doses of radioisotopes with shorter half-life, such as ^{15}O-water or ^{82}R rubidium are used. The calculation of the rate of the photons that hit the detector is as follows: 9 mCi x 3.7 x 10^7 = 333 x 10^6 disintegrations per second (or about 17 families separated every 50 seconds

The approach used in current PET in the final reunion is that the fathers and mothers do not move from the location where they are and each location interrogates about half of all the other locations[27] [32], [34] in order to find out whether there is a companion in that location.

Because, as we have mentioned, there are about 2,000 locations (electronic channels) in the system, the total number of comparisons that must be performed in order to find the companion will be enormous. For instance, for a PET with 1,792 channels, the number of comparisons[28] necessary would be: (1,792 * 1,791)/4 = 802,368 comparisons every 50 ns; that is equivalent to sixteen trillion comparisons/second. Although in our human analogy, family events are one billion times slower, it would still require sixteen thousand checks of matching families per second.

In order to avoid making that many comparisons per second, manufacturers of current PET have reduced the number of locations (electronic channels). This has several drawbacks, such as increasing dead-time, reducing resolution, etc. For example, with a reduction to 56 channels, the number of comparisons in current PETs is still (56 * 55)/4 = 770 comparisons every 250 ns, or equivalent to about 3 billion comparisons/second, which are performed in seven ASICs in the current GE PET [34].

The approach used in the proposed 3D-CBS (described in more detail in Section 13.4.14 and shown in detail in Figure 13-22 of [1]) greatly simplifies the circuit and requires only 120 million comparisons per second. This efficiency is equivalent to that of the PET with 1,792 channels, which, as noted above, would require instead sixteen trillion comparisons per second.

In layman's terms, the approach can be explained as follows: the husbands and wives should move from their location to the reunion center. At that location an average of four groups of parents with their children arrive every 50 seconds (when an original family separation rate of 17 every 50 seconds is assumed); thus, in order to make all possible combinations among four elements and avoid accumulation in the room, six comparisons every 50 seconds are necessary. (See Appendix C.2, item 6.) This would still be manageable in the world of the family reunion, only 7.2 comparisons per minute being required instead of sixteen thousand comparisons per second with the current PET approach, and with the 3D-CBS it would also be manageable in the world of photons requiring only 120 million comparisons per second.

5 HOW IS THE TECHNOLOGY VERIFIED?

The 3D-Flow architecture can be verified conceptually down to the silicon level, as described in several documents. (See [27], [4], [24], [2]. See additional information in Appendix B.)

First, the verification that the unique architecture can be implemented with processors running at normal speed on the order of 100 MHz (to avoid prohibitively costly silicon technologies, e.g., GaAs) is done by testing each 3D-Flow operation using specifications of a technology provided by the manufacturers.

Verification of the advantages at the conceptual level can be performed by comparing the old approach with the bottleneck described in [31] [38], [34], and the new 3D-Flow approach eliminating bottlenecks, as described in the previous section, in Section V of [2]. (See also Section 13 and 14 of [1]).

Second, verification at the behavioral level is performed in C++ by the 3D-Flow design real-time tools [4], [27], where the model of each electronic component has been defined at the register level. The user can advance step by step in the simulation and verify that each predefined section of the electronics processes the data correctly and that the expected results are generated.

Third, verification at the silicon gate level has already been accomplished with the synthesis of the 3D-Flow chip with four processors per chip in CMOS 0.35 micron technology, (and for FPGA technology with one processor per chip). See Section C and D of [27].

The 3D-Flow chip design is in a technology-independent, IP (Intellectual Property) form suitable to be implemented in the latest and most cost-effective technology. Tools and procedures are available [4], [27] for:

- Verification by comparison (see Figure 26)
  - Timing produces compatible results (e.g., same steps for division, multiplication, 32 comparisons)
  - Functions (or instructions) produce the same results (e.g., a "fixed-point multiply unit" produces the same result, and resolution)
  - Entire real-time algorithms produce the same result (e.g., by comparing results of application programs)
- Verification on behavioral and gate-level netlist
  - Gate-level netlist verified pre- and post-route.

Verification at the system level for a PET with a 3D-Flow system providing an input bandwidth of 35 billion events per second distributed over 1,792 input channels (well beyond the inefficient electronics of current PET) is described in [2].

The entire system (see Figure 12) can be verified and monitored by a separate workstation (System Monitor) connected to the Virtual Processing system (or real hardware) through Ethernet (which is further connected to each 3D-Flow chip of the system implemented on 28 IBM PC boards through RS232 interfaces. See references [4], [27]).

in the family reunion analogy, which, we recall, has an event rate one billion times slower).

[27] See the details on [32], [34] explaining that it is not necessary to test Lines of Response – LOR - which do not pass through the patient's body

[28] The division by 4 in the formula is required because as described in [34] approximately half the LORs do not pass through the patient's body.

6 THE CT SECTION OF THE 3D-CBS MULTIMODAL IMAGING DEVICE

Several types of CT scanners can be integrated into the 3D-CBS device such as the traditional moving, low-power x-ray generator (often referred to as fourth-generation CT system). This article describes the integration of the fastest CT scanner (often referred to as a fifth-generation CT system) with a design to enhance its features by eliminating the patient's bed motion.

The principle of operation of the electron-beam fast CT scanner was first described in [39]. It is now a proven technology (see also [40, 41, 42, 43]).

Current designs of the Electron Beam Computed Tomograph scanner (EBT) consist of an electron gun that generates a 130 keV electron beam. The beam is accelerated, focused, and deflected by the electromagnetic coils to hit one of the four stationary tungsten target rings, which emit x-ray photons. The x-ray beam is shaped by collimators into a fan beam that passes through the patient's body to strike a curved stationary array of detectors located opposite the target tungsten rings. A few rings of detectors covering an arc of about 210°, made of crystals coupled to sensors which convert light into current, detect the signal of the incident photon and sends it to the data acquisition system. The patient's bed moves through the x-ray fan beam for a whole-body scan.

The proposed design of Figure 11 eliminates the patient's bed motion by increasing the number of tungsten target rings above and below the patient. One (or more) electron beam(s) is accelerated, focused, and deflected by the electromagnetic coils at a desired angle to strike one of the tungsten rings. The collision of the electron beam with the target tungsten ring generates the x-ray fan beam (shaped by collimators), which passes through the patient's body to strike the opposite detectors (lower or upper half). One or more electron beam(s), sweeping at different deflections and hitting different target tungsten rings, will scan the patient's entire body in the axial FOV, with high resolution. The patient's body is surrounded by crystal detectors with apertures for the x-ray beam going from the tungsten rings to the detectors beyond the patient's body, and having only the patient's body as an obstacle, as shown in Figure 11. (The PMT and crystals close to the apertures are shielded from receiving the x-ray fan beam from the back of the detector).

When specific studies for high resolution using the CT alone are needed, the technique of using one, four, or more positions of the patient's bed will increase the resolution. This technique is used so as not to exceed the distance between two apertures in the detector for the passage of the x-ray beam. If four scans are performed at one fourth the distance between two apertures in the detector, the entire body will receive the x-rays from both sides and from several angles (see Figure 11, see also Section 8.7).

7 COST OF THE 3D-CBS DEVICE

Although the cost floor price of an examination using the 3D-CBS can be as low as $300/exam, due to the higher scanning speed, lower cost of the radioisotope, and lower personnel costs, the cost of the machine itself is two to three times the cost of the current PET, or about $6 million.

This estimate has been derived from the cost of the main components of the current PET in the following manner:

For comparison, the largest commercially available PET has been considered: The volume of the crystals of a CTI/Siemens 966/EXACT3D is about 13,602 cm^3. Assuming the cost of BGO crystal detectors to be $10/$cm^3$, the cost of the crystals is $136,020. Assuming the cost of 3/4" PMT to be $160 each, 1,728 PMTs cost $276,480. By estimating the cost of the electronics to be $100,000, the total cost of the main materials of a 966/EXACT3D is about $512,500. When all other components such as assembly, software, marketing, etc, are included, the price must be multiplied by five[29] times to arrive at about $2.5 million for the retail price.

Similarly, the cost of the main components of a 3D-CBS, assuming the cost of the crystals being about $10/$cm^3$, is: about $500,000 for the crystals (calculated for a 25-mm thick, small ring for the head, and elliptical form for the torso); about $350,000 for the phototubes (assuming the cost of the 1,792, 1 1/2" PMTs to be $200 each); and the electronics is estimated to cost about $200,000 (calculated as 700 processor chips assembled on 28 3D-Flow DAQ-DSP boards with 64 channels each, costing $5,000 per board, plus $60,000 for two IBM PC CPU, two IBM PC chassis, one 3D-Flow pyramidal board, hard drives, ancillary logic, and cables) for a toatl of about $1 million. (See Figure 12 of this article, Section XIII of [2] and Section 17.2 on page 181 of [1] for details.) An equivalent pricing of the main components applied to the current PET available on the market requires one to multiply this number by five to include assembly and other parts in order to obtain the estimated retail price of $5 million.

The additional cost of the CT section includes only the cost of the x-ray generator, because this is a proven technology and can be built using a traditional moving low-power x-ray generator, a more advanced electron beam technique such as the one shown in Figure 11, or a high-intensity radionuclide encapsulated in a source holder with collimator and a shutter to control the transmission.) The other components such as the detectors, photomultipliers, and the electronics are the same as those used for PET. For the additional components for the CT scanner, the cost has been generously estimated at $1 million all included. The CT + PET will make a 3D-CBS device with a cost of about $6 million.

[29] Although this multiplication factor seems high when compared to the manufacturing of products in other fields, it is low when compared to the cost of manufacturing of products related to the medical field. For example the manufacturing cost of drugs is only about 8% of the retail price as it is clearly explain in Exhibit 2 of the article by Richard G. Frank by the title "Prescription Drugs Prices: Why Do Some Pay More Than Others Do?" which was published on Health Affairs, on March/April 2001, pp. 115-128.

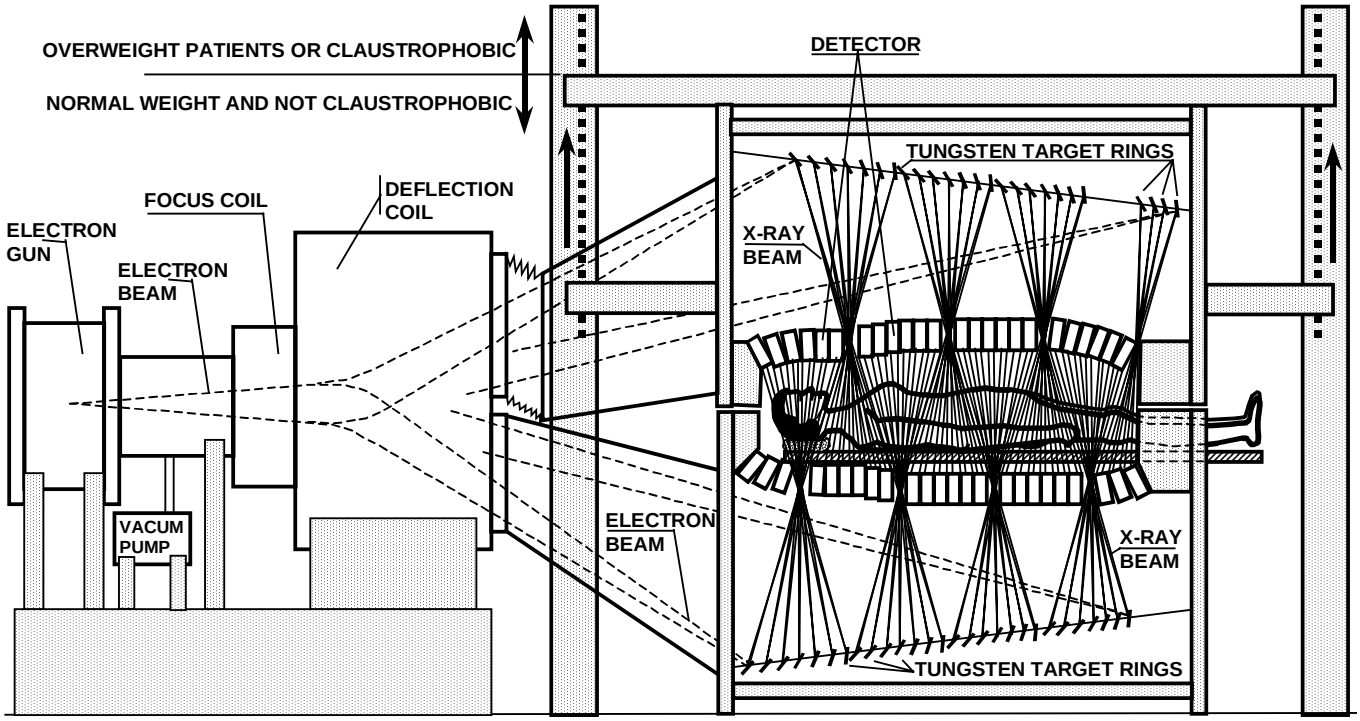

Figure 11. Design of the 3-D Complete Body Scan - 3D-CBS (CT section). The lower half detector is fixed below the patient table, while the upper half of the detector can be adjusted for patient access from the side and it can be left open for claustrophobic or overweight patients. (The closed position provides the highest efficiency) The space required for the installation of the 3D-CBS will be similar to that required by a current PET or CT when traditional moving X-ray generators will be used, and will require a slightly longer space if an electron beam technique for CT will be used, similar to the current EBCT devices. Because the radiation used during the examination will be lower, the radioprotection at the facility will be easier to handle.

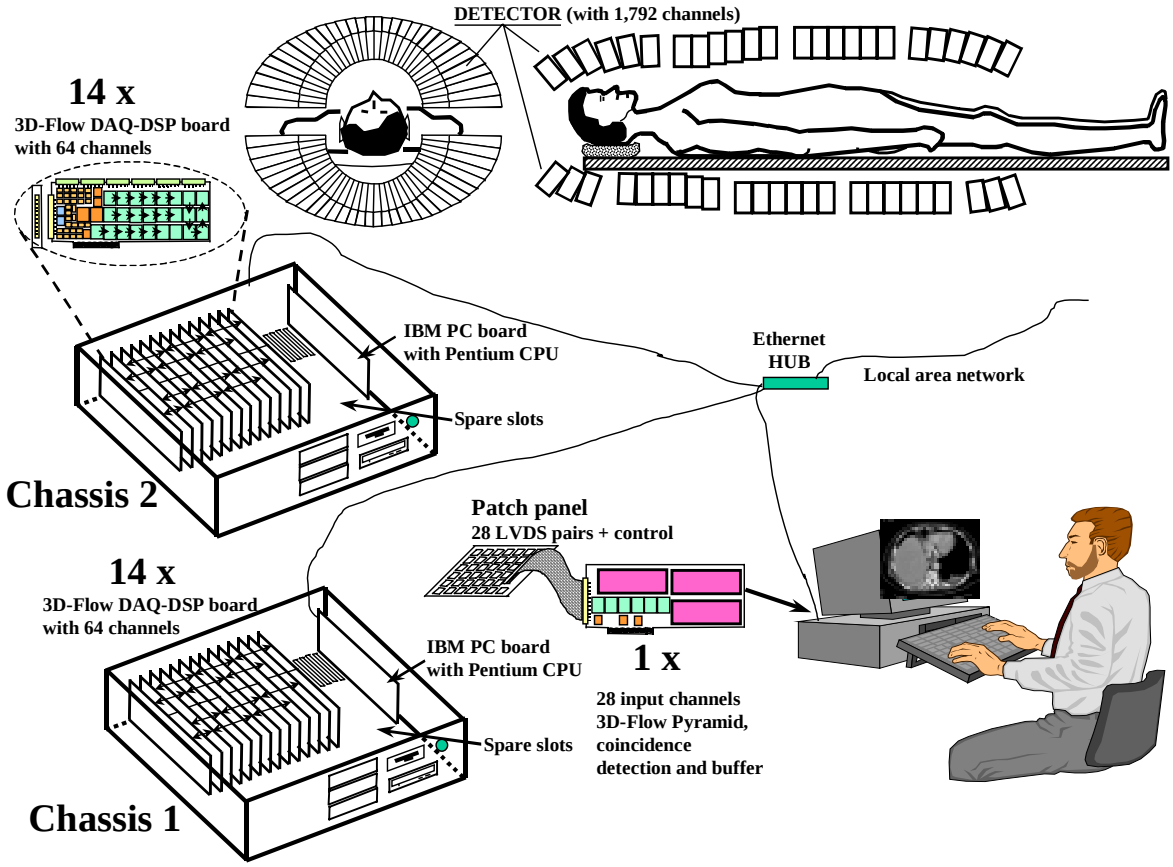

Figure 12. Layout for the hardware assembly of the 3D-CBS. (See details on Figure 30.)

8 TECHNOLOGY HIGHLIGHTS OF THE 3D-CBS THAT PERMIT ANNUAL CANCER SCREENING

A more detailed analysis of the deficiencies of current PETs can be found in Appendix C, along with how these limitations are remedied by the 3D-CBS, with precise references to the distinctive innovative features of the 3D-CBS to which the improvements are attributed.

The breakthroughs of the 3D-CBS allow for improvements in six areas: (a) quality and quantity of detection; (b) uniformity of image across the FOV; (c) improved examination time; (d) lower radiation dosage requirements; (e) unique three-dimensional dynamic imaging; and (f) lower costs.

8.1 Image quality (accuracy in detecting photons)

In the 3D-CBS system, there is a one-to-one correspondence between a processor cell and a detector channel (or sensor, or electronic channel). (See details in [4], [2].) If a photon lands across the borders of a detector channel (see Figure 13, Figure 6, and Figure 31), the signals sent by each sensor to its corresponding processor need to exchange their information with the neighbors in order to be able to reconstruct the total energy of the photon. This operation increases the sensitivity[5] by capturing more good[24] photons which are essential to reduce the "false positives" and "false negatives."

An increase in sensitivity that also increases noise, providing poor images, is undesirable. The DSP on each electronic channel in the 3D-Flow allows improvement of the signal-to-noise (S/N) ratio on signals before adding them.

The exchange of signals between neighboring channels with no detector boundary allows signal interpolation which also improves spatial resolution. (Both affect the image quality).

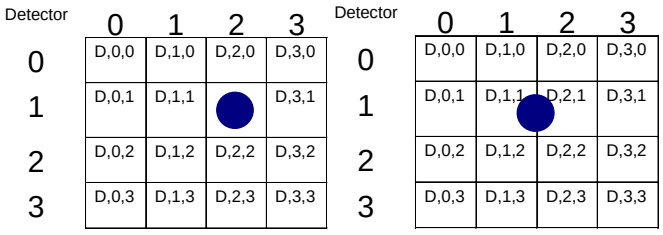

Figure 13. Inefficiency of current PET in detecting photons when they strike the crystal in a location that can produce signals in neighboring sensors. The left side of the figure represents the case when a photon is detected because it strikes a detector that is coupled to a sensor, or group of sensors (such as PMTs, or APDs), that can measure most of the photon's energy. Most current PET devices have sensors organized in groups of 2 x 2 elements. At right is the case when a photon is undetected in current PET because it strikes a detector that produces signals in neighboring sensors (or groups of sensors) and no individual signal has sufficient energy to be recognized as a photon. The 3D-Flow approach remedies this limitation by exchanging information between processors that received signals. (See also Figure 6).

More photons emitted by a single organ can be captured if the FOV is increased. Figure 14a shows that by doubling a short field of view the number of photons that can be captured is actually increased by a factor of four instead of two. Figure 14b shows also that the image resolution is increased by increasing the axial FOV.

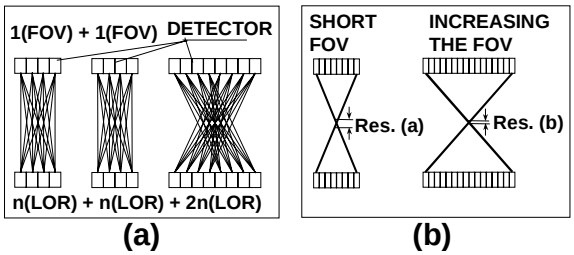

Figure 14. A PET with an axial FOV that is twice as long as the short FOV of the current PET can detect four times the number of photons in time coincidence from an organ emitting photons from the center of FOV. Section (a): Doubling the axial FOV increases the Lines of Response (LOR); thus the sensitivity increases four times when a short FOV is doubled, the electronics does not saturate and DOI measurements are performed. Section (b): Increasing the axial FOV increases the resolution.

8.2 Uniformity of image across the FOV

The sensitivity of current PET varies considerably depending on whether the organ scanned is at the center of the field of view or at one side. Figure 6 of [44] shows that the sensitivity in 3D mode of current PET devices is very low for organs at the edges of the PET detector. The graph of the number of counts (pairs of photons in coincidence) measured across the FOV has the shape of a triangle, with very poor counting rate; placing seven of these shapes (Figure 6 of [44]), one adjacent to another, for the seven positions of the current PET detector during a ~150 cm scan, results in very poor uniformity of detection of photons over the entire patient's body (see left in Figure 15).

An entire-body detector, such as the one used in the 3D-CBS, eliminates the above defects, increases the count rate, and improves uniformity (see right in Figure 15) in detecting pairs of photons in time coincidence in different sections of the patient's body, regardless of its location in the FOV.

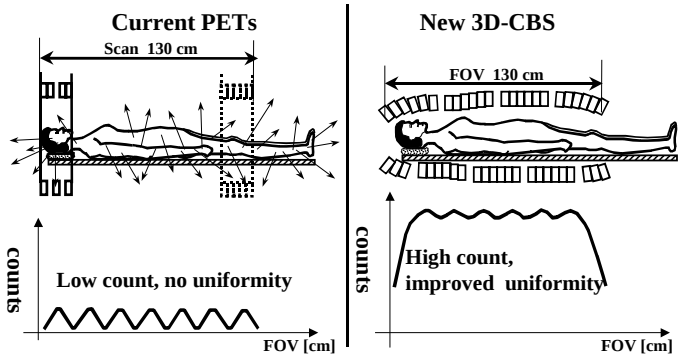

Figure 15. Higher counts and improved uniformity of the 3D-CBS in detecting back-to-back pairs of photons in time coincidence from different areas of the body. Each small triangle at the bottom left of the figure is the sensitivity of the scanner without septa for a different position as measured by Karp et al. in figure 6 of [44].

In the event the electron beam CT is implemented in the 3D-CBS, the gaps between crystals, which allow the electron beam to perform a CT scan, will introduce a slight ripple in the uniformity; this, however, is negligible compared to the non-uniformity of current PET devices. A 3D-CBS implemented with a traditional CT scanner with an x-ray gun rotating inside the detector will completely eliminate the ripple in uniformity of sensitivity. This construction will improve the uniformity of the spatial resolution because of the capability to calculate the 3x3, 4x4, or 5x5 centroid over the entire detector with no boundaries.

8.3 Less radiation to the patient

Figure 16 shows the factors contributing to an increase in radiation dose to the patients when current PETs are used. Although the text cannot be easily read in the figure, the symbols in the picture show clearly the difference between the old approach used in current PET (at left in the figure) and the new 3D-CBS approach (at right in the figure) and where the great areas of inefficiency are. See more details in Section 14 and Figure 14-1 of [1]).

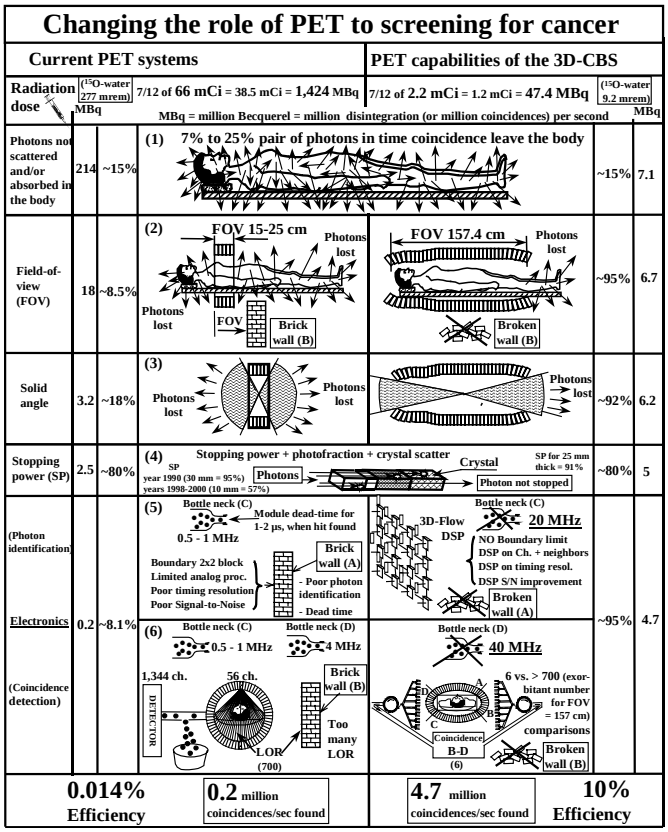

Figure 16. Comparison of the efficiency of the new 3D-CBS (right side) to that of the current PET system (left side). The subdivision of the loss of efficiency into different areas of the PET components aims to identify the areas that most need improvement. Although the estimates of the efficiency of each individual area may present slight variations from what is indicated in the figure, the overall total should be 0.014%, as measured by the PET manufacturer (see Section 8.5). The analysis in the left column of the figure shows that the lowest efficiency is due to the short FOV, the limited solid angle, and poor electronics. The first two areas cannot be improved without an improvement in the efficiency of the electronics (see Appendix C.4, C.5, C.6 and Figure 34). This proposal is a blueprint for improving the electronics, which makes possible an increase in efficiency by also increasing the FOV and the solid angle (see right column in the figure). This analysis also shows that the concentration of effort over the past 25 years on improving the efficiency of the crystals, already at over 80% with 25 mm slow BGO crystals, has not significantly changed the overall efficiency of the PET device. An increase in efficiency of the overall PET system resulting from the use of faster crystal detectors is less significant if the architecture of the electronics handles each electronic channel separately, as is done in the 3D-CBS design, limiting the detector dead-time of the slower crystals to a very small area of the detector.

Figure 17 shows the area of improvement needed in current PET devices in order to reach the theoretical limit of efficiency. The example shows, for an activity of 10 mCi, e.g., ^{15}O-water, equivalent to 42 mrem radiation to the patient, the approximate calculation of the number of single photons and pairs of photons in time coincidence that hit detectors with different FOVs, assuming a patient of about 170 pounds. Fewer photons will hit the detector for heavier patients, while more photons will reach the detector for a smaller patient. The "coincidences" include "true" (image forming events), "scatter" (non-image forming events that Compton scattered, most of which are later rejected during image reconstruction), and "randoms" (non-image-forming events which are emitted within the required time difference but belong to two different positron-electron annihilations.) Randoms can be rejected by the front-end 3D-Flow electronics by comparing the length of the LOR and the difference of the photons' arrival times; See Sect. 13.4.7 of [1].

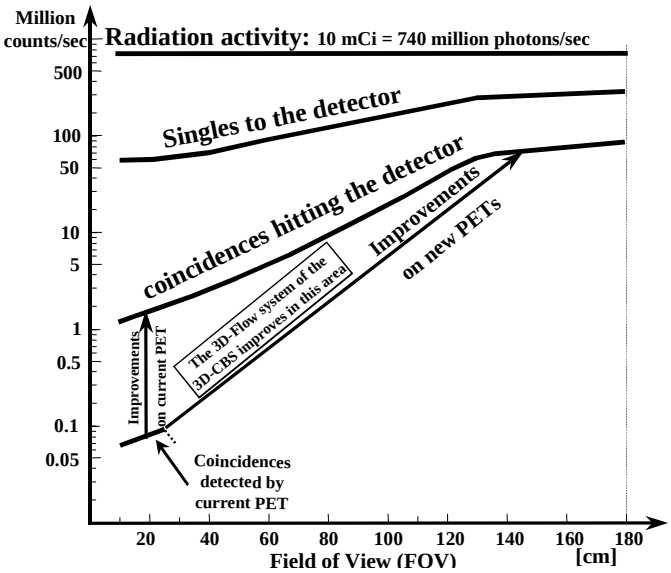

Figure 17. Graphic view of the actual coincidence detection capability of current PET vs. the theoretical limit that new PET/CT detectors should attempt to achieve. The 3D-CBS aims to approach the theoretical limits in one giant step instead of providing small incremental improvements every few years[31], as has occurred during the past quarter century. The areas of improvements are the electronics (see vertical arrow, left on figure) and the combination of the improvement of the electronics and the increased FOV (see inclined arrow to the right).

8.4 Short examination time

The short examination time of the 3D-CBS is attainable because of the long axial FOV of its detector and the highly efficient electronics. The high-photon detection efficiency (1,000 out of 10,000 compared to 2 out of 10,000) reduces the time needed for acquisition of the number of photons required to yield a good image. This allows the examinations to be performed in 15 to 20 minutes with only two to four minutes scanning time, facilitating the capture of a specific biological process one desires to observe without making the patient uncomfortable and at a greatly reduced cost. (See Figure 3).

8.5 Measurements of the inefficiency of current PETs

The measurements of the limited efficiency of the current PET devices have been reported in articles published by manufacturers. (See references [45], [46] and Sections 11.2.2.6.3.2 and 11.2.2.6.4.2 of [1].) **The calculation of the efficiency improved over 400 times using the new 3D-CBS compared to the current PET is reported in [1] and is calculated as** the ratio between 10% and 0.014% = 714. (See lower part of Figure 16.)

The 0.014% efficiency of the "GE Advance" PET is calculated by dividing 0.2 million coincidences/sec detected by 1,424 million coincidences/sec emitted by the radioisotope. Both values are taken from Figure 8 on page 1405 of the article by DeGrado et al. [46].

The 0.0193% efficiency of the CTI/Siemens ECAT EXACT HR PET is calculated from the measurements reported in [45] on page 115. The article reports that 30 minutes after the injection of 10 mCi of ^{18}FDG into a human, a total of 6 x 10^6 counts per center slice were acquired for 60 minutes. Given that there are 47 slices and that lateral slices accumulate fewer counts than the center slices (see Figure 6 of reference [44] on page 2346), then the approximate total count of coincidences of 193 x 10^6 accumulated on 47 planes during the entire examination period of 60 minutes gives the average count rate of 53.6 x 10^3 coincidence counts per second. This count rate at an approximate activity of the source after 60 minutes of 277.5 x 10^6 disintegration per second (3/4 of (10 mCi x 37 MBq) = 277.5 MBq) yields a total system efficiency of 0.0193% (53.6 x 10^3 coincidence counts/sec divided by 277.5 x 10^6 disintegration/sec).

8.6 The 3D-CBS vs. current PETs with best sensitivity (using ideal crystals, i.e. LSO) and highest resolution (300 μm)

The 3D-CBS offers the best combination of sensitivity, resolution and economy.

Current PET with high resolution (300-μm) [47] cannot have both a high sensitivity and an affordable construction cost in applications for human subjects.

For example, if a traditional PET with the best 300-μm resolution [47] were built for human scanning, with a FOV of about 150 cm, it would have less than 50% of the efficiency of the 3D-CBS. It would require two detectors (versus one detector of the 3D-CBS with only 1,792 electronic channels): One detector, consisting of a silicon Compton camera of about 22.4 million electronic channels[30], would provide the 300-μm spatial resolution; a second detector with about 450 electronic channels of electrical signals from sensors coupled to crystals would provide the timing information. In addition to being very costly and complex to build, this 300-μm resolution detector would require a high radiation dose to the patient, which would not be acceptable for annual screening.

Considering that the positron (β^+) of the FDG tracer statistically travels about 1.4 mm before encountering a free electron (see Figure 7d) and that the cells of the patient's body move due to respiration and heart beat, the high-resolution PET detector is not fully utilized in human PET applications. Such high resolution Compton cameras are best used for small-animal PETs or for quality control in testing mechanical parts, such as the fused block of an engine with inaccessible paths where high radiation is not an issue.

Because of the high cost of LSO crystals, current PET using them are subject to size limitations, having a small diameter of 35 cm with a FOV of 25.2 cm [48], [49] or a larger diameter of 82.4 cm with a FOV of 16.2 cm [50], thus requiring radiation to the patient that would be unacceptably high for annual screening.

CTI/Siemens, the manufacturer of the highest resolution PET HRRT with a FOV of 25.2 cm and the nearly ideal LSO crystals [49], shows in their performance[31] evaluation for this machine only a twofold increase in Noise Equivalent Count rate (NEC) with respect to their PET ECAT EXACT HR [45], which was built five years earlier and uses the standard BGO crystals.

The newest PET [50] by the same manufacturer announced in spring of 2001, uses the nearly ideal LSO crystals; however, it can capture fewer photons and has a worse spatial resolution than the previous HRRT PET detector, because it has a shorter FOV (16.2 cm instead of 25.2 cm) and the size of the crystals is 6.45 mm x 6.45 mm, yielding a transaxial resolution of 6 mm and an axial resolution of 4.6 mm, instead of a crystal size of 2.1 mm x 2.1 mm of the HRRT, which yields a resolution of 1.3 mm.

---

[30] The number 22.4 million channels has been calculated as follows: for an efficiency of the silicon Compton camera of about 45%, the silicon detector requires a thickness of about 15 mm. This would require fifteen silicon detectors of 1 mm in thickness. Each silicon detector with an area of 6 cm^2 and 1 mm thick has 256 electronic channels. One cm^2 of a Compton camera will have 640 electronic channels. The entire PET detector with a FOV of about 150 cm and measuring 75 cm in diameter would require about 35,000 cm^2 of silicon detector, which totals about 22.4 million electronic channels.

[31] Performance measurements comparing the HRRT PET with the PET model ECAT EXACT HR from the same company delivered five years earlier are reported in [49], and Section II.A states "A comparison with the ECAT EXACT HR [45] shows that twofold gain in maximum Noise Equivalent Count rate (NEC) with the new tomograph in spite of the largely increased random rate is mainly due to improved dead time characteristics of the fast scintillator LSO." The performance measurements of the ECAT EXACT HR PET are described in Section 8.5. See also reference [5] for the calculation of 2- to 3-fold improvement in efficiency every 5 years.

With the PET exam, the activity of the biological processes, which is related to the growth of a tumor or the effect of a drug, is more important than spatial resolution. The activity of a tumor in a given area of the body, combined with a discrete spatial resolution, will give better information about the size and the growth of the tumor. Rather than seeing just a black spot with the resolution of 300 μm, the physician using a PET scan can now observe molecular changes (even before morphological changes occur), independent of the fuzziness caused by respiratory movement, the heart beat movement, and the 1.4 mm travel distance of the positron before encountering an electron (see Figure 7b).

As the importance of the spatial resolution was stressed in the CT catalogs of the product, now the sensitivity and efficiency in capturing the most photons in time coincidence is the parameter that the manufacturers of PET and the physicians should stress, because these features provide more useful clinical and research information.

The 3D-CBS offers improvements in both. To summarize, the unique 3D-Flow sequentially implemented parallel-processing architecture of the 3D-CBS provides higher sensitivity[5] and reduces the difference in sensitivity between PET with slow detectors and fast detectors (See Appendix C.4, C.6 and Figure 34). The signal correlation capability of the 3D-Flow with neighboring channels which provides centroid calculation (see Figure 31) with no boundary limitation, allows for building a 3D-CBS with BGO crystals that further improves the spatial resolution of current PET It can also easily reach and improve the 1.3 mm resolution of the current PET [49], [51] under the same conditions of crystal type and size of 2.1 mm x 2.1 mm.

8.7 Three-dimensional, whole-body, anatomical and functional, dynamic imaging

The capability to acquire a high data-input rate made possible by the improved electronic design of the 3D-CBS allows dynamic PET and CT imaging and real-time tracking of moving tumors[32] over most of the patient's body.

The advantage afforded by the 3D-CBS, with its large detector surrounding most of the patient's body and acquiring most of the data from photons emitted (PET) and transmitted (CT), is that it functions with lower radiation and provides better images than a smaller detector, such as the current PET or CT. Both images (anatomical and functional) produced by continuous rotation of multiple X-ray source(s) (CT) and continuous emission of the radioisotope, can be combined in a single three-dimensional image, constantly updated and displayed. All other scanners currently available or under design can only generate dynamic three-dimensional picture of the size of the multi-slice detector in CT (20 mm to 32 mm in length) and 16 cm FOV PET (although PET dynamic imaging has not yet been developed on even the short FOV PETs).

The transmission source for the CT section of the 3D-CBS can be either a radionucleide (e.g., Am-241), multiple low-power X-ray tubes, or an electron beam system such as the one shown in Figure 11 but with multiple electron beams to scan large sections of the patient's body at the same time. The detection of the CT photons can be done in counting mode (single photon), or in integrating mode. Both methods can be implemented with high accuracy of measurement through the programmability of the 3D-Flow front-end electronics, which can also account for the energy deposited in neighboring sensors. This allows for detecting very low photon transmission activity [8], which is sufficient for calculating the attenuation coefficient during PET examination. The same low-radiation activity is also sufficient to visualize the profile of the organs during a PET screening examination or when monitoring the effect of drugs. While the possibility of detecting photons at a higher rate from a higher dose x-ray source, will allow one to perform diagnostic workups of details of the anatomy of an organ when a better image in a short time is desired.

With the 3D-CBS, the physician will not have to study 30 to 200 separate slices (images), as is the case with the current imaging devices, but will be able to visualize dynamically any section of the patient's body in slow- or fast-motion in three-dimensional functional and anatomical form. Its high-sensitivity can provide the physician with the most useful information of cancer size and metabolism activity, which is related to its growth, or the reaction to a drug. Only significant pictures, which show anomalies, will be printed or transferred to film by the physician.

Typical image processing functions of rotating the objects (organs), applying some filters which highlight some phenomenon will be provided to the physician (e.g., subtracting the photon emission activity of the bladder wall to show the lower metabolic activity of the surrounding organs, etc.).

It is a unique feature of the 3D-CBS that it can acquire concurrently over the entire body, anatomical pictures of organs moved by the beating of the heart or respiration and functional images of processes which can then be associated in a single dynamic three-dimensional visualization.

Other examples where this dynamic acquisition feature is useful are those of:

a) eliminating cardiac movements which normally blur images;

b) cardiac gating procedures which use trigger signals from Electro Cardiogram (ECG) combined with data acquisition and display so that visualization of a moving organ is shown for a similar cardiac phase;

c) more precisely irradiating the patient during radiation therapy by tracking the tumor movement in real time with low dosage (in both emission and transmission); and

d) guidance in intervention procedures (tissue biopsies, spinal nerve block, drainage of fluid from lesions, etc.), etc.

[32] The capability of the 3D-CBS to track in real-time the movement of tumors in the chest or abdomen caused by respiration or/and heart beating, allows dynamic three-dimensional imaging useful in diagnosis and in precision radiotherapy (e.g., proton therapy).

9 BENEFITS OF THE 3D-CBS TO THE CURRENT DIAGNOSTIC WORKUPS

After describing the technology of the 3D-CBS and its advantages, it is important to review the benefits and cost saving on its applications. Two areas where the 3D-CBS will prove most useful, early detection and diagnostic workup, are mentioned in Section 2.2. In the second area, the 3D-CBS can be seen as a modern PET machine with over 400-fold improvement in efficiency over the traditional PET. The unique features of the 3D-CBS provide solutions to break the barriers that have limited PET performance up until now[5, 31].

Because the 3D-CBS reduces the radiation to which the patient must be exposed, it does not present any new risks, and the agencies in the U.S., such as the Food and Drugs Administration (FDA) which have approved CT and PET examinations at much higher radiation dosages, should approve 3D-CBS exams at these lower radiation dosages without argument.

9.1 The recent dramatic expansion of medical imaging market in diagnostic workups on symptomatic patients and the faster growth expected in the future

Growth in the use of combined PET/CT exams is predicted for the future by experts[9] in the medical imaging field. As an example, the U.S. market has been analyzed in detail in this document. However, the entire worldwide market is over three times the size of the market described here, and the benefits of larger diagnostic machines compared to small machines designed for scanning individual organs has been shown to be advantageous by several experts in the world[33].

Even if one makes the conservative, pessimistic assumption that there will be no growth in the market, the faster and more efficient 3D-CBS which will provide better quality exams at lower cost and with a lower radiation dose, will compete favorably with current PET designs. This document also compares operating costs of the 3D-CBS and the current PET at very high volumes of utilization and operating costs and at very low volumes of utilization and operating costs. Following, several different trends are evaluated, and justifications are provided in support of current beliefs of experts in the medical imaging field that the PET and CT market is going to grow[38] at a rate even greater than the over 60% annual growth rate of the market for PETs in past years:

1. The two major PET producers, GE and Siemens, together sold 100 PET machines during the year 2000 (at a price of over $2 million per machine) and are scheduled to sell over 150 PET machines in 2001, with back-orders extending over six months (see also CPET sold by ADAC-Philips, which is based on UGM PENN-PET 240H and Positron described in [1]). Several sources[38] indicate that the U. S. will have over 500 PETs by 2003.
2. In the United States, total health care costs [16] exceeded $1.2 trillion in 1999. Approximately 1.1% of this total has consistently been spent on medical imaging[34]. This trend will continue, because additional studies indicate that medical imaging devices save HMOs and the government billions of dollars every year[33]. Additional studies have demonstrated that PET based machines are much more likely to detect cancer[35] than CT devices [52], [53], [54]. The advantage of the 3D-CBS technology compared to others is its functioning with lower radiation to the patient, higher quality image than the current most accurate machine (the PET) at an examination price and speed comparable to a CT scan.
3. Insurance and HMO coverage of PET examinations is increasing. HCFA, the body responsible for approving Medicare and Medicaid coverage of PET applications in the U.S., has consistently expanded coverage for the PET, both with the types of cancer for which it will pay to monitor and other imaging applications of the PET.[36] The number of PET exams performed by each PET, currently averages 1,000 per year[37] [12].
4. PET technology is more advantageous compared to other imaging techniques (MRI, CT, SPECT, ultrasound, etc.) for more different types of imaging applications[33] than ever before, such as, expanding searches for cancer at different organs, cardiac monitoring, brain perfusion,

---

[33] Several studies made in Holland, Germany, and Japan show that when larger machines, such as the CT scanners were introduced into the market in the '80s, the cost of treatment and diagnosis was considerably reduced by using whole-body CT to replace many x-ray examinations (see reference [10]). The study also found that hospitals with CT showed a reduction in patient stays by 8%. Additionally, at the 1992 conference of the Radiological Society of North America (RSNA) [9], the President of RSNA showed that health care costs were reduced when devices such as CT, MR or PET were used. The study compared the relative charges for different treatments in hospitals without CT, MR, or PET to those that had such devices. A few examples are the following: (a) the cost of evaluating patients with acute head injuries prior to the advent of the CT or MR was about four times as great; (b) the cost of evaluating patients with rectal cancer prior to the use of CT or MR was about five times as great; (c) the cost of evaluating patients with a penetrating flank injury prior to using CT or MR was about five times as great; (d) the cost of evaluating patients with palpable breast masses prior to the advent of mammography was about three times as great; and (e) the cost of the evaluation for focal epilepsy prior to PET was about five times as great.

[34] The U.S. Census Bureau 1999 Electromedical and Irradiation Equipment reports a total market of $13.9 billion; $747.1 million is for CT scanners ($661.1 million of manufacturers' shipments of CT, with $86 million of CT scanners imported).

[35] Because of the higher percentage of success of the current PET with low sensitivity in identifying cancer compared to the CT (See references [52], PET 81% success compared to CT 52% for lung study; [53] PET 95% success compared to CT 68% for colon study; [54] PET 85% success compared to 67% for breast), the new 3D-CBS with higher sensitivity and the combination of the PET and CT capability in a single detector, will identify cancer and other systemic anomalies more accurately, while providing lower radiation to the patient and reducing the number of false positives and false negatives.

[36] In 1998, HCFA began reimbursement for PET detection of lung cancer; 1999, Hodgkins and non Hodgkins Lymphoma; January 2001, expanded coverage for four cancer applications and two new cancer types; and in August 2001, expended coverage to brain and coronary imaging.

[37] See the article in reference [12] reporting that in the year 2000, 250 PET units in the U.S. made over 250,000 examinations.

diabetes, efficient monitoring of hadron therapy, developing new drugs and studying their effects, etc.

5. The expansion[38] [12] of the PET is very similar to the expansion of the CT[8] market two decades ago, when the number of CT scanners expanded dramatically from 2,500 to 11,500 in 15 years (see Table IV). The CT scanner effectively replaced a series of tests. Similarly, the 3D-CBS offers for the first time, a tool to recognize many health concerns.

9.2 Projected market for the 3D-CBS as a "combined PET and CT machine" for diagnostic workups

The preliminary study of the U.S. market of the scanners related to the 3D-CBS shown in Table IV and Figure 18 and the need for PET and CT technology for diagnostic workups justifies the projected future market. (Notice the growth of 9,000 CT scanners during fifteen years, which reached 11,500 units by the year 2000 and the conservative proposed growth of only 1,000 3D-CBS units over five years). With annual growth conservatively estimated to be less than half that of the medical imaging market, the market for diagnostic workup applications will require 1,360 3D-CBS units by the year 2010, reaching an annual volume of sales of about $2.46 billion, as shown in Table V.

The 3D-CBS would be used in both the current PET market and the CT scanner market because of its superior speed, resolution and accuracy (see Section 8). Its faster scan will allow hospitals to examine about six times the number of patients per day with its PET section[42] (see Figure 3). This reduction in marginal operating costs[43], the higher revenues per day and the possibility of renting the 3D-CBS from a mobile unit one or two days per week will enable many hospitals to afford a 3D-CBS machine.

TABLE IV. NUMBER OF SCANNERS USED FOR DIAGNOSTIC WORKUPS ON SYMPTOMATIC PATIENTS IN THE U.S. FROM 1980 TO 2010. (SOURCE: NCRP[39] [55], [12]).

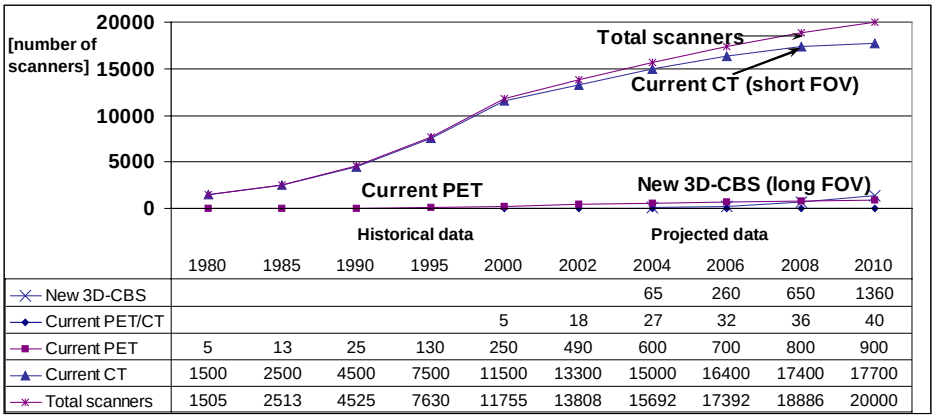

	1980	1985	1990	1995	2000	2002	2004	2006	2008	2010
New 3D-CBS							65	260	650	1360
Current PET/CT					5	18	27	32	36	40
Current PET	5	13	25	130	250	490	600	700	800	900
Current CT	1500	2500	4500	7500	11500	13300	15000	16400	17400	17700
Total scanners	1505	2513	4525	7630	11755	13808	15692	17392	18886	20000

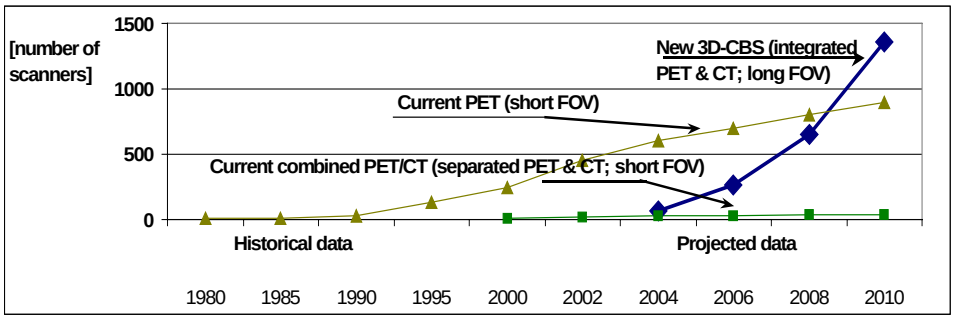

Figure 18. Magnification of the group of scanners of Table IV with volumes up to 1,500 units (historical and projected).

TABLE V PROJECTED ANNUAL REVENUES FROM THE 3D-CBS UNITS SOLD TO DIAGNOSE PEOPLE WITH SYMPTOMS.

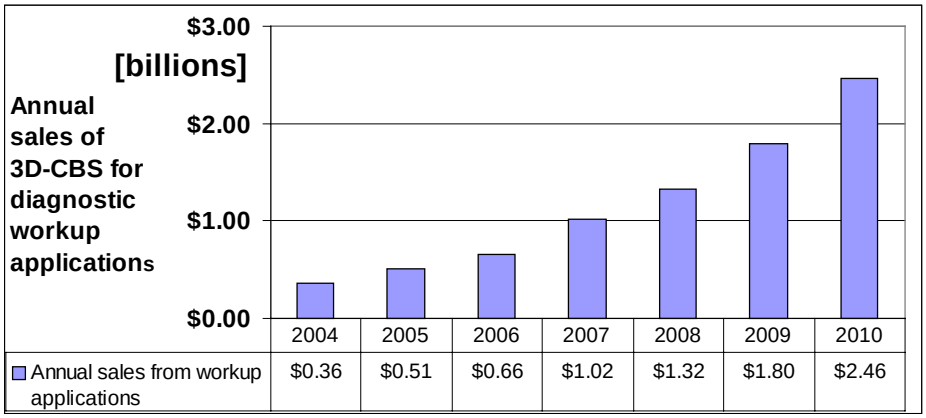

	2004	2005	2006	2007	2008	2009	2010
Annual sales from workup applications	$0.36	$0.51	$0.66	$1.02	$1.32	$1.80	$2.46

[38] Historical and projected PET data based upon the studies of Diagnostic Imaging [12] (DI predicts over 500 PET by 2003).

[39] Historical CT data are based upon studies of the National Council on Radiation Protection and Measurements (NCRP) [55], U.S. Census Bureau, Statistical Abstract of the United States: 1999, U.S. Department of health and human services Center for Disease Control (CDC), Vital and Health Statistics. Historical and projected PET data based upon the studies of Diagnostic Imaging [12]. 3D-CBS projections are estimated by the author.

10 WHAT DOORS DOES THIS NEW DISCOVERY OPEN TO BENEFIT HEALTH CARE?

The most important new uses this device makes possible are:

1. the monitoring of the effect of drugs during the staging of cancer[25] or other diseases. Because of its greatly reduced radiation requirement, the 3D-CBS allows repetitive examinations of a patient without undue risk;
2. treatment verification after surgery, chemotherapy or radiotherapy;
3. accurate measurements of the effects of new drugs;
4. three-dimensional dynamic imaging over most of the body which is unique to the 3D-CBS, because of its simultaneous acquisition of photons from a large detector; and
5. annual screening for cancer and other systemic anomalies. This will be an important contribution to the role of preventive medicine.

10.1 Projected market for the 3D-CBS for preventive health care as an annual screening device.

Besides the current market for scanners for patients who manifest symptoms of anomalies, a new market for preventive health care on asymptomatic population is now possible because of the lower radiation requirement of the 3D-CBS scanner (see Table VII).

The market for screening of the asymptomatic population can be estimated for the U.S. by calculating how many 3D-CBS units would be necessary to screen some age-groups of that population considered to be at high risk for cancer or heart disease.

At first, those over 50 years of age will be placed in the high-risk category. When a sufficient number of 3D-CBS units become available to screen most of the population over 50, screening could be extended to the population at next lower risk, i.e., those aged 45-50; and successively dropping the threshold to 40 and then 35 years of age.

Savings can be estimated, as well, by comparing the aggregate cost of current screening procedures that cover a limited number of organs of the body to that of one whole-body screening with the 3D-CBS. (See Table XI.)

This additional market of the 3D-CBS is estimated to be $2.54 billion annually by the year 2010. (See Table VI) It would require 1,464 scanners by 2010 in order to scan 15% of the U.S. population over 50 years of age. This is assuming conservatively that each 3D-CBS scanner will screen 10,500 patients/year. In the event of non-optimal utilization of the capabilities of the 3D-CBS, more scanners will be needed.

The growth projections of the 3D-CBS are conservatively based on less than half of the historical growth of the market for CT scans. Between 1985 and 2000, the number of CTs increased by over 9,000 units (see Table IV); this should be compared to the projected growth of the 3D-CBS (as shown in Table VI and Table VII) of only 1,000 units within 5 years (the high-efficiency 3D-CBS can perform the volume of work equivalent to the output of several separate PET or CT units).

Notice that the number of 3D-CBS scans for screening is not projected to exceed 16 million until the year 2010 (See Table XIV). To put these numbers in perspective, is not a large number compared to the current use of imaging devices. In 2000, in the U.S. alone, there were over 30 million CT scans, which were restricted to the diagnostic workup of patients who are showing symptoms of disease (See Table XIV and footnote[23]).

TABLE VI PROJECTED ANNUAL MARKET FOR THE 3D-CBS SCANNERS SOLD FOR CANCER SCREENING OF THE ASYMPTOMATIC POPULATION OVER 50 YEARS OLD.

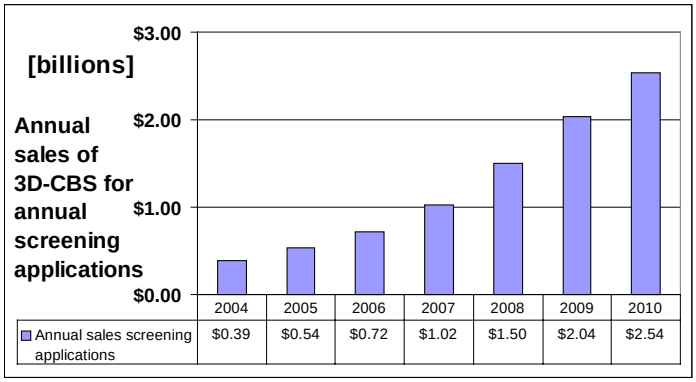

	2004	2005	2006	2007	2008	2009	2010
Annual sales screening applications	$0.39	$0.54	$0.72	$1.02	$1.50	$2.04	$2.54

TABLE VII NEW 3D-CBS SCANNER MARKET: PROJECTED GROWTH AND TOTAL NUMBER OF 3D-CBS SCANNERS NEEDED FOR THE ANNUAL SCREENING OF ONLY 15% OF THE U.S. POPULATION OVER 50 YEARS OLD BY 2010.

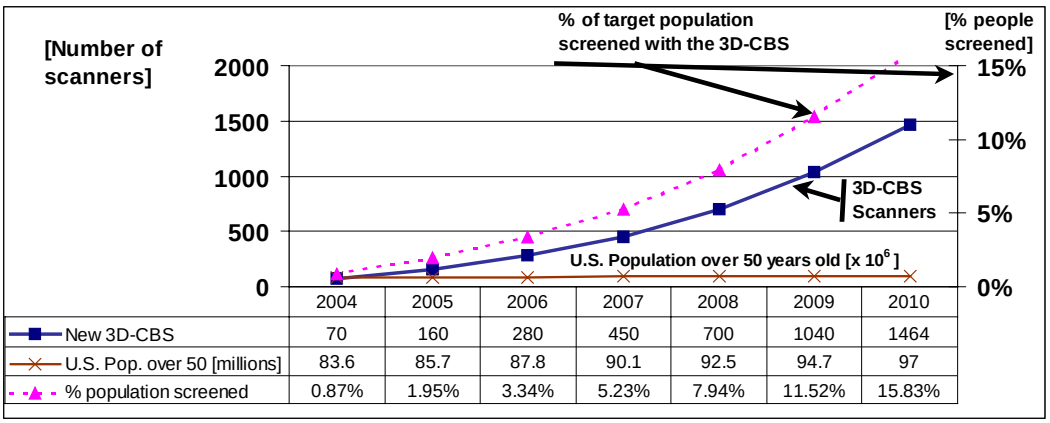

	2004	2005	2006	2007	2008	2009	2010
New 3D-CBS	70	160	280	450	700	1040	1464
U.S. Pop. over 50 [millions]	83.6	85.7	87.8	90.1	92.5	94.7	97
% population screened	0.87%	1.95%	3.34%	5.23%	7.94%	11.52%	15.83%

10.2 Saving lives through early detection.

Every year in the U.S., an estimated 1.2 million new cases of cancer are diagnosed, and each year more than 550,000 people die from various forms of cancer (for Europe this figure is 840,000). Out of a total number of 2,337,256 deaths in the US in 1998 for all ages, the most common cause of deaths for the 45-64-year-old group was cancer, accounting for one out of three deaths in that group, or 132,771 deaths (see Figure 19). The second most common cause of deaths for the same age group was heart disease; 100,124 people died from heart disease [56]. Cancer and heart disease accounted for 60% of the total 380,203 deaths in the age group 45-64 in 1998.

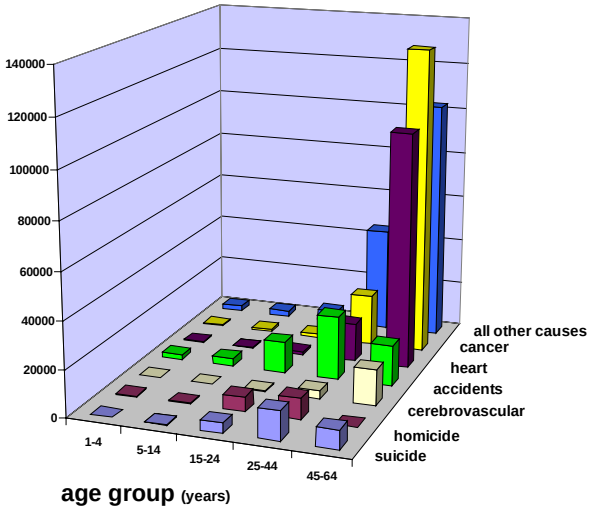

Figure 19. Deaths in United States in 1998 by cause and by age group. (Source: National Vital Statistic Reports [56]).

Figure 20 shows the impact of cancer upon the U.S. population for all races when looking at a combination of three elements: (a) the number of new cases per year per 100,000 persons (incidence rate); (b) a determination of the proportion of patients still living five years after their diagnosis (survival rate); and (c) the number of deaths per 100,000 persons per year (mortality rate).

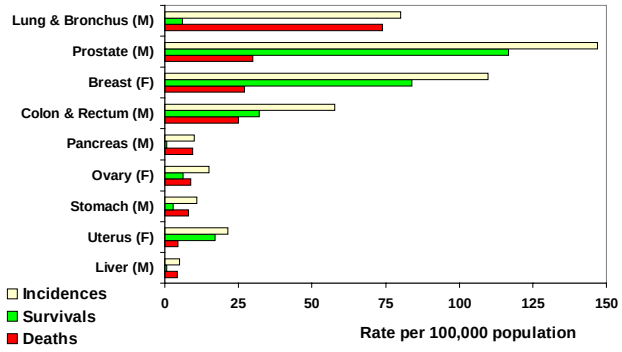

Figure 20. Cancer incidence, survival, and death rates per 100,000 people in the United States (Source: SEER,[40] NCHS,[41] and NCI).

Death rates have consistently fallen for cancer for which intense screening programs have been developed. However, Figure 20 shows that much improvement is still needed.

Although the incidence rate of diagnosed prostate and breast cancer in the U.S. is higher than that of lung cancer, the death rates for lung and bronchial cancer are higher partly because of the lack of instrumentation capable of detecting disease in these sites early enough to treat them successfully. Clearly, early detection would increase the survival rate for these types of cancer. Screening with advanced technology, such as the 3D-CBS with improved sensitivity, will also improve the survival rate for those suffering from the most common cancers, including those for which some screening devices already exist.

Although a person of any age receiving the screening could benefit from early detection of disease, for most meaningful results it is helpful to study an age group younger than the statistical life expectancy (such as 45-64) that experiences a high incidence of cancer (see Table VIII).

TABLE VIII. LIFE EXPECTANCY BY RACE IN THE UNITED STATES FROM 1980-1998 (SOURCE: NATIONAL VITAL STAT. REPORTS [57])

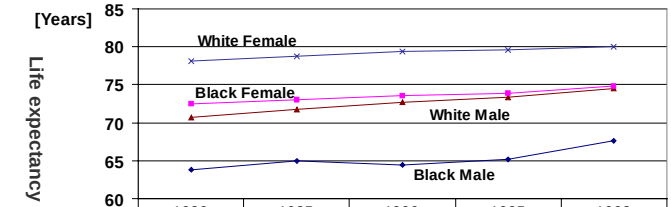

	1980	1985	1990	1995	1998
White Male	70.7	71.8	72.7	73.4	74.5
White Female	78.1	78.7	79.4	79.6	80
Black Male	63.8	65	64.5	65.2	67.6
Black Female	72.5	73	73.6	73.9	74.8

Table IX shows that during the past year there were more improvements in reducing the death rate from heart disease within the 45-64 age group, i.e., from 327 per 100,000 in 1981 to 173 in 1998, than the death rate from cancer, i.e., from 304 per 100,000 in 1981 to 229 in 1998. It doesn't appear that the high increase in drug expenditures from 1995 to 1999 provided equivalent benefits in an additional reduction of the death rate for the same period because this graph is not showing a down word slope that will compensate the up word slope of Figure 4.

TABLE IX. DEATH RATE IN 45-64 AGE GROUP IN U.S. FROM 1981 TO 1998 PER 100,000 POPULATION (SOURCE: NVSR [58], [56]). COMPARE WITH DRUG EXPENSES GROWTH (SEE FIGURE 4).

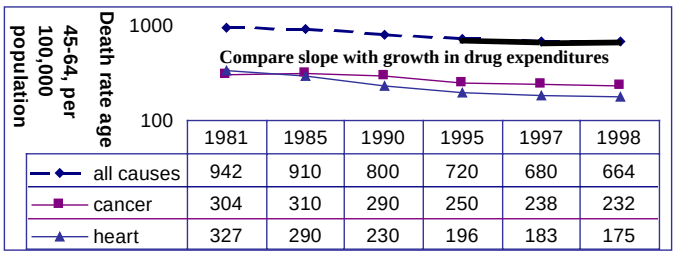

	1981	1985	1990	1995	1997	1998
all causes	942	910	800	720	680	664
cancer	304	310	290	250	238	232
heart	327	290	230	196	183	175

[40] Data for incidence rate are relative to the U.S. population during 1990-91 and are from Surveillance, Epidemiology, and End Results (SEER) program of the National Cancer Institute (NCI) and are based on data published in the SEER Statistics Review 1973-1991: Tables and Graphs (Ries, 1994). Data for survival rates for 1983-90 are from SEER, and represent approximately 10% of the U.S. population.

11 OPERATING COSTS OF THE 3D-CBS COMPARED TO CURRENT PET

The slower scanning times of the current PETs limit their patient throughput (number of PET exams that they can perform in a year). (See Table IV).

Table X shows the difference in operating costs between the same volume[42] of 1,500 exams per year for the current PETs with 25-cm FOV and the 3D-CBS used fewer hours per day.

TABLE X WORST CASE SCENARIO: EVEN IF THE 3D-CBS IS UNDERUTILIZED, IT HAS STILL LOWER OPERATING COSTS[10] THAN THE CURRENT PETS (COMPARISON OF THE 3D-CBS, WHEN IT IS USED ONLY ONCE PER WEEK[43]. WITH CURRENT PET USED DAILY).

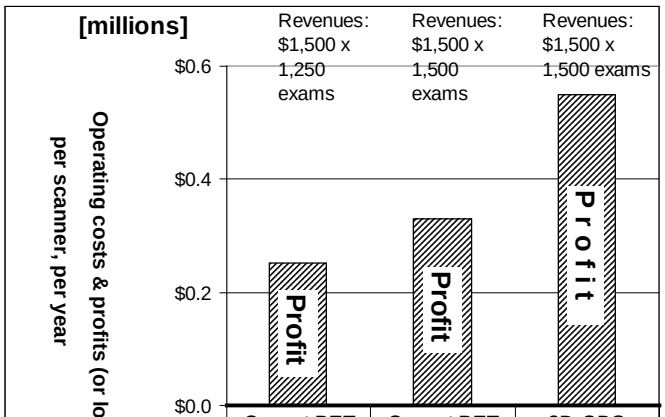

	Current PET <14 cm FOV [millions $]	Current PET ~25 cm FOV [millions $]	3D-CBS ~150 cm FOV [millions $]
Capital amortiz. (8yr)	-0.125	-0.275	-0.750
Capital cost (5%)	-0.050	-0.110	-0.300
Service contract	-0.060	-0.100	-0.200
Upgrading	-0.060	-0.100	-0.150
Building	-0.090	-0.090	-0.090
Personnel	-0.288	-0.345	-0.070
Radioisotope FDG	-0.950	-0.900	-0.140
Revenues	1.875	2.250	2.250
▨ Profit (or loss)	0.252	0.330	0.550

The significantly faster 3D-CBS could scan 1,500 patients in less than 50 days, while the current PET would require 250 days! The speed of the 3D-CBS scanner and its higher sensitivity saves costs of personnel and radioisotopes, which compensate for the higher cost of the amortization of the unit, the service contract, and the upgrades[44]. The examination price of the 3D-CBS is competitive with many of the costs for individual, organ-specific examinations used to screen people annually (as shown in Table XI[45]), and offers coverage of the whole body at once, instead of a single organ in individual exams. In addition, the current PET examinations cannot be repeated annually because of the high radiation dosage required.

Table XII shows the operational costs[46] and profits (or losses) of operating the scanners at maximum throughput when the examination price is $300/exam (cost floor of the 3D-CBS). The 3D-CBS has a profit of ~$160,000/year.[47], the PET with ~25 cm axial FOV has a loss of ~$1,503,000/year, while the PET with <14 cm axial FOV has a loss of ~$1,248,000/year.

Table XIII shows the operational costs[46] and profits (or losses) for a maximum throughput of the scanners when the examination price is $1,300/exam (cost floor of the current PET). The 3D-CBS has a profit of about $10,660,000/year[47], the PET with ~25 cm axial FOV has a profit of about $247,000/year, while the PET with <14 cm axial FOV has a profit of about $2,000/year.

Note that the slower <14 cm FOV PET cannot perform more than 1,250 full 150 cm body scans[3] within the standard 2,625 operating hours per year. The ~25 cm FOV PET cannot perform more than 1,750 exams in 2,625 hours per year, while the 3D-CBS can perform 10,500 exams.

---

41 The source of the death rate is the National Center for Health Statistics (NCHS), analyzed by NCI

42 This model allows 5 patients per day (10 hours/day) for the slower <14 cm FOV, 6 patients per day (9 hours/day) for the ~25 cm FOV PET, for 250 days/year, and 30 patients per day (7.5 hours/day) for the 3D-CBS, for 50 days/year. The cost of the ^{18}F-FDG radioisotope is estimated to be $2,800/day for the 3D-CBS, $3,600/day for the ~25 cm FOV PET, and $3,800/day for the < 14 cm FOV PET because it is slower and needs a longer scanning time. (Diabetics need to use a tracer different from fluorodeoxiglucose ^{18}F-FDG).

43 Personnel costs have been calculated from the costs in Table 5-2 on page 37 of [29]; ½ MD, 2 technologists and administrators for the >14 cm FOV for 5 days/week; ½ MD, 2 ½ technologists and administrators for the 25 cm FOV for 5 days/week; 1 MD, 2 ½ technologists and administrators 1 day/week for the 3D-CBS.

44 The operating costs involved in both the current PET and the 3D-CBS, may vary substantially in different locations. Figures conservatively use the highest costs. Source of costs for the U.S. comes from discussions with radioisotope manufacturers, users and hospital administrators, while for Europe reference [29] was used. The capital amortization for the 3D-CBS is $6,000,000/8years = $750,000/year, the PET with ~25 cm FOV is $2.2M/8years = $275,000/year, while the PET with <14 cm FOV is $1M/8years = $125,000/year. The capital cost for the 3D-CBS is calculated as 5% of $6,000,000. The cost of the building (estimated $1,000,000) where the 3D-CBS is installed is estimated to be $40,000 for capital cost, $25,000 for depreciation (40 years), and $25,000 for maintenance, including power (See also Table 5-2 of [29] for similar calculation).

45 Prices of the list of procedures of Table XI have been compiled in the Dallas area during the year 2000 and they may vary by location.

46 The comparisons between the three types of scanners fairly assume that all three are operating for the same number of hours (10.5 hours/day). This assumes 7 patients per day for the >14 cm FOV and ~25 cm FOV PET, for 250 days/year and 42 patients per day for the 3D-CBS, for 250 days/year. The cost of the ^{18}F-FDG radioisotope is estimated to be the same ($3,800/day) for the three scanners. (Diabetics need to use a tracer different from fluorodeoxiglucose ^{18}FDG). The personnel costs have been based on Table 5-2 on page 37 of [29]: ½ MD, 2 technologists/administrators for the >14 cm FOV for 5 days/week; ½ MD, 2 ½ technol./admin. for the ~25 cm FOV for 5 days/week; 1 MD, 2 ½ technologists/administrators for the 3D-CBS.

47 The capability of scanning 10,500 people per year assumes that each 3D-CBS exam last 15 to 20 minutes, with 3 to 4 minutes of scanning time (See Figure 3). Although it is commonly known that the CT scan averages only 4 minutes/patient, many times the CT scanner is used with a contrast agent. For these types of procedures, the examination may require two or more scans. A 3D-CBS with both examinations (that occur at the same time) requiring only 3-4 minutes, a throughput of 3 to 4 patients per hour is not overestimated.

A comparison of the costs and efficiencies of the 3D-CBS with other methods (see Table XI) of cancer screening reveals that a one stop, noninvasive, whole body cancer screening machine is much more cost effective.

TABLE XI LIST OF THE APPROXIMATE[45] COSTS OF SOME CURRENT PROCEDURES AND/OR EXAMINATIONS FOR CANCER SCREENING.

Breast cancer	Mammogram	$80-$200
	Sonogram	$250-400
	MRI (with contrast ag.)	$900-1400
	Biopsy	$500-700
Colon cancer	FOBT	$20-65
	Barium Enema (Fluoro)	$600-800
	Sigmoidoscopy	$300-500
	Colonoscopy	$1500-2000
Gynecological cancer	Uterine cervix: Pap smear	$40-100
	Sonogram	$450-600
	Uterus corpus (biopsy)	$500-1500
Lung cancer	Chest X-ray	$50-300
	Broncoscopy	$1200-1600
	CT chest (with contrast)	$800-1200
	Biopsy	$700-1200
Prostate cancer	Digital Rectal test	~$100
	Prostate Specific Antigen	$25-120
	Sonogram	$400-500
	Biopsy	$500-600
Lymphoma cancer	CT (with contrast ag.)	$600-1200
	MRI (with contrast ag.)	$1800-4000
	Biopsy	$1000-1600
Brain cancer	MRI (with contrast ag.)	$1000-2500
	CT (with contrast ag.)	$500-1800

Although PET technology is ideal, it was not included in Table XI because its high radiation dosage precludes FDA approval for annual examination on asymptomatic people. The 3D-CBS' requirement of only 1/30th of the radiation dosage remedies this problem. The 3D-CBS offers a cost effective, non-invasive, whole-body scan that replaces (or avoids the need for) most of the procedures in Table XI. (CT is not very efficient in detecting cancer[35], and is not recommended for whole-body annual screening because of its high radiation).

The price of the annual 3D-CBS screening examination for cancer and other anomalies will be in between the price floor of the 3D-CBS of approximately $300 per exam as shown in Table XII and the current PET price floor which reaches $1,300 per exam, as shown in Table XIII.

The 3D-CBS' examination price for greater coverage of the body is still very competitive with the cost of the current screening exams reimbursed by the government (Pap smear, mammogram, PSA, etc.) and much less than the group of the current screening examinations paid by the wealthiest (the cost of the previous exams reimbursed by the government in addition to colonoscopy, CT, Sonogram, MRI, and Biopsy can easily total over $5,000 per year).

TABLE XII COMPARISON OF OPERATING COSTS[10] WHEN SCANNERS ARE USED AT THEIR MAXIMUM THROUGHPUT, AT THE EXAMINATION PRICE FLOOR OF THE 3D-CBS ($300/EXAM). (SOURCE[46, 47] [29])

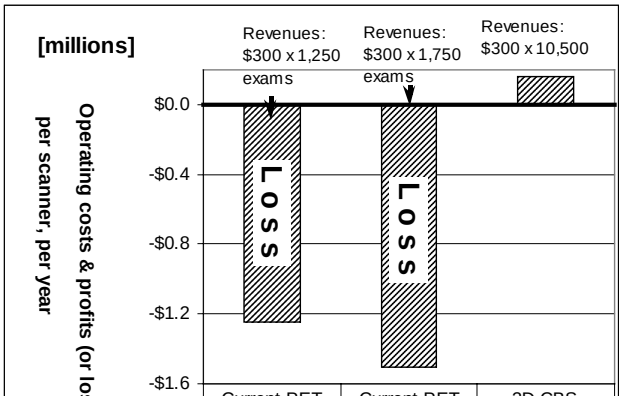

	Current PET <14 cm FOV [millions $]	Current PET ~25 cm FOV [millions $]	3D-CBS ~150 cm FOV [millions $]
Capital amortiz. (8yr)	-$0.125	-$0.275	-$0.750
Capital cost (5%)	-$0.050	-$0.110	-$0.300
Service contract	-$0.060	-$0.100	-$0.200
Upgrading	-$0.060	-$0.100	-$0.150
Building	-$0.090	-$0.090	-$0.090
Personnel	-$0.288	-$0.403	-$0.550
Radioisotope FDG	-$0.950	-$0.950	-$0.950
Revenues	$0.375	$0.525	$3.150
▨ Profit (or loss)	-$1.248	-$1.503	$0.160

TABLE XIII COMPARISON OF OPERATING COSTS[10] WHEN SCANNERS ARE USED AT THEIR MAXIMUM THROUGHPUT, AT THE EXAMINATION PRICE FLOOR OF CURRENT PET ($1,300/EXAM). (SOURCE[46, 47] [29]).

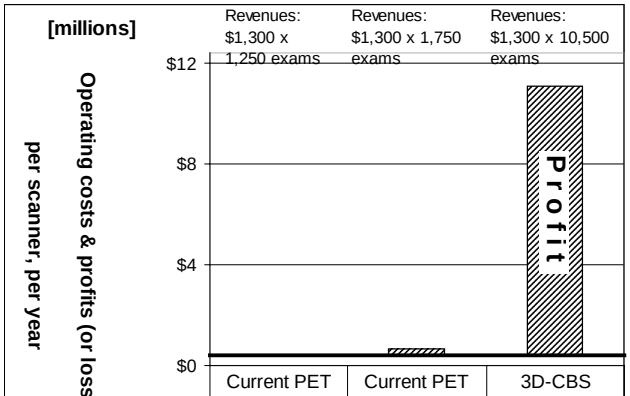

	Current PET <14 cm FOV [millions $]	Current PET ~25 cm FOV [millions $]	3D-CBS ~150 cm FOV [millions $]
Capital amortiz. (8yr)	-$0.125	-$0.275	-$0.750
Capital cost (5%)	-$0.050	-$0.110	-$0.300
Service contract	-$0.060	-$0.100	-$0.200
Upgrading	-$0.060	-$0.100	-$0.150
Building	-$0.090	-$0.090	-$0.090
Personnel	-$0.288	-$0.403	-$0.550
Radioisotope FDG	-$0.950	-$0.950	-$0.950
Revenues	$1.625	$2.275	$13.650
▨ Profit (or loss)	$0.002	$0.247	$10.660

12 AMORTIZING THE COSTS OF THE 3D-CBS COMPARED TO THE CURRENT PET

For the purpose of amortization comparison, let us assume in this section a zero profit for each scanner.

When the 3D-CBS is utilized at its full capability, the amortizing of its cost at $1,300 per exam is 1/9 the time[48] required by a current PET with ~25-cm FOV, and 1/15 the time required by a current PET with ~`4-cm FOV. (See Table XIII and Figure 21.)

A reduced scanning of the patient's body may give a different amortization time to the cost of current PET with short axial FOV, however, as mentioned before, it is not in the patient's best interest to curtail scanning, because once he has received a radiation dose, which spreads over the entire body, it is best for him to have maximum exposure by having a complete body scan.

Lowering the examination price to $300 per exam will require 6.6 years to amortize the cost of the 3D-CBS, while the current PET with ~25-cm FOV would, at that price, have a yearly operating loss of over $1.5 million.

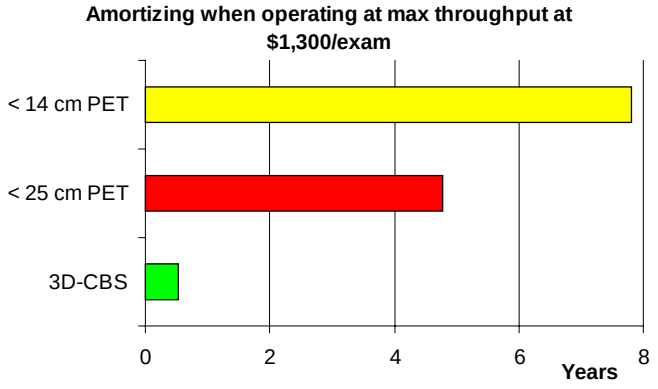

Figure 21. Amortizing the cost of different scanners when operating at their maximum throughput at $1,300 per exam. The cost of a current PET with ~ 14 cm FOV can be amortized in 7.8 years (see top bar of the graph). The cost of a current PET with ~ 25 cm FOV can be amortized in 4.7 years. (See middle bar of the graph). The cost of the 3D-CBS can be amortized in half a year (see bottom bar of the graph).

The cost of the 3D-CBS can be amortized in about the same period as the current 25-cm FOV PET when it is underutilized at 1,500 exams per year, at $1,500 per exam, performed one day per week, 7.5 hours per day. This is compared to 1,500 exams per year, at $1,500 per exam, performed on a current PET with ~25-cm FOV, when operating 5 days per week, scanning nine hour per day. (See Table X and Figure 22.)

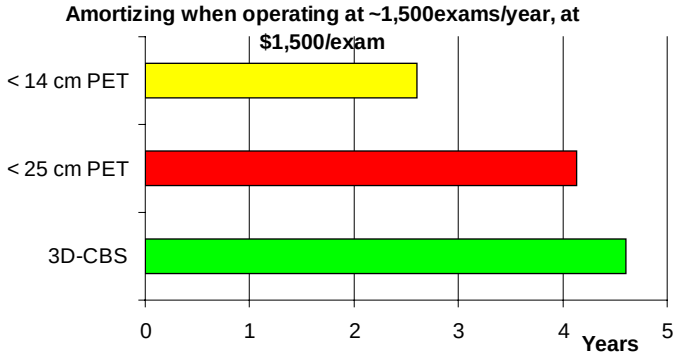

Figure 22. Amortizing the cost of different[49] scanners when operating at about 1,500 exams per year at $1,500 per exam. The cost of a current PET with ~ 14 cm FOV can be amortized in 2.6 years (see top bar of the graph). The cost of a current PET with ~ 25 cm FOV can be amortized in 4.2 years. (See middle bar of the graph). The 3D-CBS cost can be amortized in 4.6 years (see bottom bar of the graph).

To make the service available to all hospitals, including small ones with limited capital for investment in expensive instrumentation, the PET manufacturers (or other investors such as insurance companies) may sell the 3D-CBS service by the day, month, or year, as is already done by mobile PET companies.

Using this model, the hospital would be charged only by the day (e.g., one day per week), at, for example, $10,000 for the current PET with a short axial FOV (based on the PET with a retail cost of about $2.5 million), and $15,000 for the new 3D-CBS with a longer axial FOV (based on a 3D-CBS which includes PET and CT with a retail cost of about $6 million). The current PET examines about 6 patients per day at a cost of about $2,100 each. (The examination charge varies from $1,790 to $4,200. Some HMO plans in the U.S. reimburse the hospital as much as $4,200 per scan; the medicare reimbursement rate for a PET scan is $1,790). The greater number of patients examined per day at a lower cost of the FDG tracer should lower the examination cost to about $300 to $400 each.

All parties will benefit: the financial institution will have a larger business with a $6 million investment in a single unit rather than financing several smaller units, the hospital will have a better instrument, and a greater revenue because of examining more patients, and the patients and insurance companies will pay less per examination.

[48] The number of years needed to amortize the cost of the 3D-CBS (at zero profit) is calculated as: $6 million (cost of the device), divided by the sum of $0.75 million plus $10.66 million (cost of amortization during one year added to the profit). The calculation for the current PET with ~25-cm FOV is: $2.5 million (cost of the device) divided by the sum of $0.275 million plus $0.247 million. A similar calculation can be done for a ~14 cm FOV PET. See Table XIII.

[49] The number of years needed to amortize the cost of the 3D-CBS (for a zero profit) is calculated as: $6 million (cost of the device), divided by the sum of $0.75 million plus $0.55 million (cost of amortization during one year added to the profit). The calculation for the current PET with ~25-cm FOV is: $2.5 million (cost of the device) divided by the sum of $0.275 million plus $0.33 million. A similar calculation can be done for a ~14 cm FOV PET. See Table X.

13 PROJECTED NUMBER OF EXAMINATIONS BY DIFFERENT SCANNERS FROM 2004 TO 2010

Table XIV shows the projected number of examinations by different scanning machines by the year 2010, compared to the current approximately 30 million examinations per year performed with CT scan.

The combination of revenue for diagnostic workup (see Table V) and cancer screening in the U.S. (see Table VI) projects a total 3D-CBS market of about $5 billion by 2010.

In the short term, the 3D-CBS will be used primarily for diagnostic workups on symptomatic patients, because it can offer both PET and CT quality at a CT price.

For the additional new market of screening, the 3D-CBS offers the advantage of being less expensive and less invasive than other forms of screening, and with it, all the screening can be done at once instead of necessitating several separate tests. Over a period of time, the market for the 3D-CBS as a diagnostic workup tool will be small compared to the larger market for the 3D-CBS as an annual cancer screening machine.

It is important to note that even the projections for 2010 are not exagerated[9]; in 2000, there were over 30 million CT scans performed. In the graph charting for screening (see Table XIV), it is predicted that there will be only 10 million 3D-CBS scans for workups and 15 million for screening by 2010. These estimates are based on the assumption that the 3D-CBS will have less than one fourth of the U.S. CT market by 2010, and will screen annually by 2010 only 15% of the U.S. population over 50. Because the U.S. market is less than one third the entire world market and because the market in the U.S. is actually bigger than estimated in this study[9], the total, world-wide annual market could be over $50 billion for the 3D-CBS.

The average number of examinations per scanner per year is estimated at 2,600 for the CT scanner; 1,250 exams per year[42] for each current PET scanner and current CT/PET scanner; and 7,500 exams per year for each 3D-CBS scanner used for diagnostic workups and 10,500/exams per year[47] for each 3D-CBS used for annual screening[46].

14 AVAILABILITY OF THE MATERIALS FOR MASS PRODUCTION OF 3D-CBS

The use of the simpler but higher performance electronics of the 3D-CBS makes it possible to produce the 3D-CBS in large quantities using the most commonly available parts, rather than being limited, as is the case of current PET, which make use of LSO crystals. Although research continues for an ideal[6], economical, and readily available fast crystal, there is also the desire to assist patients who could benefit in the mean time from the potential of the combined technologies of the CT and PET. For this reason, one should base a design on parts which are readily available at a reasonable price at the present time, and the design should also be upgradeable to faster crystals when they become available.

An additional strength of the 3D-CBS design, therefore, is that it can use the fast LSO crystals but can also achieve improved performance now, using the cheaper, slower BGO, CsI(TI), or other slower crystals, which are currently available in abundance. The improved electronics of the 3D-CBS eliminates the great difference in performance between fast crystals and slow crystals.

Approximately 150 m^3 of scintillating crystals (calculated as ~50,000 cm^3 per 3D-CBS scanner) would be needed for the U.S. market alone during the next nine years in order to achieve the goal of 3,000 3D-CBS units. (See Figure 11 of [2], or Section 18 of [1]). This number of units will allow the scanning of about 25 million people per year by the year 2010 (which is still only about half of what the CT will be scanning during the same year. See Table XIV). If the market for medical imaging outside the U.S. advances as well, as has been the case in the past, more than 500 m^3 scintillating crystals will be needed worldwide by 2010. While the BGO and CsI(TI) crystals are available in good supply from multiple sources, LSO has had a total production capability during the past 15 years of less than 5 m^3.

TABLE XIV. PROJECTED NUMBER OF EXAMINATIONS BY DIFFERENT SCANNING MACHINES BY THE YEAR 2010.

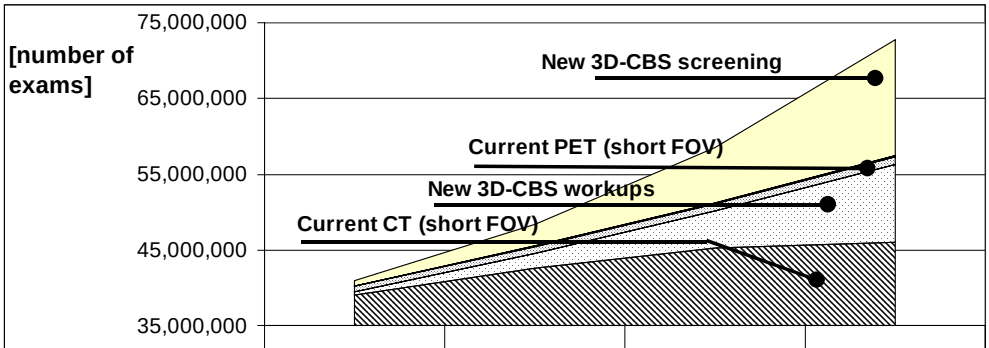

	2004	2006	2008	2010
New 3D-CBS screening	735,000	2,940,000	7,350,000	15,372,000
Current CT/PET	33,750	40,000	45,000	50,000
Current PET	750,000	875,000	1,000,000	1,125,000
New 3D-CBS workups	487,500	1,950,000	4,875,000	10,200,000
Current CT	39,000,000	42,640,000	45,240,000	46,020,000

15 WHO WILL BENEFIT FROM THE 3D-CBS?

15.1 Patients with symptoms and people with asymptomatic conditions

It is obvious that the patient will be the greatest beneficiary of this improved technology, which, in reducing the number of false positives and false negatives, produces a better image in less time and, requires only about 1/30 of radiation dosage, all at only 1/10 of the cost compared to current PET.

15.2 Hospitals and physicians

Hospitals will benefit from the 3D-CBS in many ways, some of which are:

- Lower examination cost to the hospitals (~ $300 with the 3D-CBS compared to the current PETs $1,300. See Table XII and Table XIII)
- The hospital and its physicians will be able to offer the most informed medical opinions based upon images of the highest quality depicting observable phenomena.
- The lower radiation dosage will also allow the hospital to expand its cancer research, staging, and monitoring while greatly decreasing radiation exposure to the patients.
- Hospitals will be able to utilize their staff and resources more economically. With a slight increase in medical staff (see $550,000 per year of Table XIII), the hospital could perform approximately six more scans per man-hour than with the slow scanning time of the current PET.
- The hospital will finally have a machine that has a capacity beyond its needs: the 3D-CBS can scan up to 10,000 patients per year, in contrast to the 750 to 1,750 patients-per-year capacity of current PET. This will make it possible for hospitals to absorb the operating costs and amortization costs of the 3D-CBS, even if they utilize the machine for only 1,500 PET exams per year.

15.3 Investors

Investors will have extensive lead time before competitors are able to build a product that can perform an examination at the price of $300. A prompt introduction into the market of the 3D-CBS will maximize the lead time, provide a good return on investment, and enable the investor to set the price of the machine and of the examination, as shown in Figure 1. Hospitals that have purchased the current PET cannot compete with the same low examination price during the 8 years required to amortize the capital they have spent.

The investors will benefit from the faster growth of this market with the 3D-CBS because:

1. Hospitals and Mobile PET providers will have an incentive to purchase the 3D-CBS instead of the current PET not only because of its better performance, but also because the benefits to be derived from the innovations described in this document compensate them for the increased cost of a PET with a longer FOV.
2. The combined examination time for PET and CT scan of only two to four minutes of the 3D-CBS (compared to the current PET/CT requiring 50-90 minutes for the PET because of their short FOV, which does not match the < 4 minutes for the CT), improves the cost-effectiveness by fully utilizing the capabilities of the two machines.
3. A better synergy of the two machines into a single unit will also provide the additional economic benefit that the market will share between more profit and lower examination price.
4. Lowering the examination price is beneficial for the additional reason that it makes the examination accessible to more people, increasing usage of screening, by the 3D-CBS, and in turn increasing profit again.
5. The 3D-CBS scan, even though at a lower cost per examination, will result in increased daily revenues, making financing for a unit at higher cost more easily available.

15.4 Researchers in cancer, heart disease, and new pharmaceutical products.

The possibilities of the 3D-CBS complete-body scanner with lower radiation requirements open new avenues in medical research, because annual screenings are safe. There is no longer the hazard of high radiation. Much new research will be possible: longitudinal data from annual screenings of one subject or groups of patients will show incremental change; comparative data, such as scans of all family members at different ages, will add to an understanding of the inheritance factors in the risk of cancer and heart disease; and parallel studies of various groups can be used to investigate the influences of the environment, genetics, or nutrition. These and other areas of research will help improve disease prevention.

The availability of an accurate whole-body scan device, such as the 3D-CBS, that encircles most of the radioactive area of the patient's body, allows accurate dosimetric measurements in applications such as hadron therapy, where it is necessary to monitor the destruction of cancer cells. The high sensitivity of the 3D-CBS is ideal for the research and development of new pharmaceutical components.

See also all the potential new applications listed in Section 10 of this article where PET technology could be beneficial.

15.5 Insurance companies

Insurance companies will find that the 3D-CBS will save many expensive procedures[33] (see Table XI) and that patients will have shorter hospital stays[8].

The desire of insurance companies to save money on the cost of scanning will be synergetic with the investors' desire to sell the maximum number of machines and the hospitals' need

to utilize the machine efficiently and optimize per-day patient throughput.

15.6 Government administrators

Government administrators will have a great opportunity to create a benefit for the population by reducing the radiation to patients thereby providing a powerful new tool for preventive health care. Further, the 3D-CBS helps reduce expenditures for health care, which is also an important goal.

The cost of health care last year in the U.S. was over $1.2 trillion. The National Institutes of Health, National Cancer Institute, and the American Cancer Society studies[50] reported that cancer alone cost $107 billion per year in the U.S. Scanning 15 million people per year (or 15% of the U.S. population over 50 years old) at $300/exam will cost only $4.5 billion per year and will give higher coverage at lower cost than current screening. Early detection, in addition to providing a better quality of life for people, will allow the patient to avoid expensive procedures typical when the cancer is found in its advanced development or is metastasized in the body. A practical, affordable device affording early detection would offer savings in the big picture of global health care cost reduction as well.

16 WHO MAY NOT WANT THE 3D-CBS?

Any carefully considered arguments for not promoting this project are urgently invited by the author. Timely discussion will keep the project moving forward. Avoiding a dialogue on this subject further delays benefits to the patients.

It is perfectly understandable that a hospital that has just purchased a PET with a short FOV and an efficiency of 2 photons captured out of 10,000, as well as the PET manufacturers themselves, may feel disadvantaged in having just missed out on an innovation and many hope that Table I, Table X, Table XII, and Table XIII are wrong. However, the cost of operation of the device reported in the referenced tables are conservative and are similar to those compiled by a large hospital in Zurich that has been operating PET for several years and reported in [29].

Objections to the author's claims, such as that (a) the logic (and description of the detailed implementation) of the sequentially implemented 3D-Flow parallel processing system is flawed, that (b) a DSP on each channel to improve signal-to-noise ratio is useless, or that (c) all other innovations of the 3D-CBS do not allow an increase of the FOV in a cost effective manner, cannot be sustained. Conversely, it is clear that current PET (a) do not rebuild the total energy of the photon, (b) have detector boundaries which give a lower sensitivity at the edges of the 2x2 PMT blocks with respect to the center, (c) cannot perform interpolation among all neighboring signals, thus failing to obtain good spatial resolution, and (d) have significant limitations in their electronics which prevent the cost-effective extension of the FOV. It is obvious from Figure 14 that (a) a detector with a longer FOV can capture more photons from a single organ, and (b) the 3D-CBS described in this and other documents can solve all of the above limitations.

Resistance to change occurs any time there is innovation. The worldwide market for scanners, presently about $50 billion, leaves room for many alternative designs and can provide benefits to many people, but ultimately and especially to the grass-roots consumer, the patient.

It is to be hoped that hospitals that just purchased a PET, and the companies that manufactured them will not deny or ignore the evidence but will recognize the validity of these claims and enlist in the effort to make the advancements of the 3D-CBS a reality. Mutual collaboration will advance the cause of health care and ultimately benefit all of us.

17 ACTION PLAN FOR GETTING THE WORD OUT REGARDING THE BENEFITS OF 3D-CBS

17.1 Interested in defeating cancer, heart disease, improving the quality of life and life expectancy? Then don't settle for less; contribute to the implementation of the 3D-CBS.

There is no reason to settle for two- to three-fold improvements[31] in efficiency of medical imaging instruments every five years, as has occurred in the past 25 years. (See the theoretical limits in efficiency in Figure 17, the evolution of PET during the past years in Figure 23, and the areas that need to be improved in Figure 16) This document and the references [1], [2], [3], [4], provide the blueprint for how to achieve an improvement in efficiency of several orders of magnitude, in a single giant step, with today's technology. Do not take it for granted that claims for such dramatically increased improvement cannot be achieved. The author encourages you to obtain the details, and if you have any doubts or any questions on any section of this project, please write to the address provided on the first page of this document.

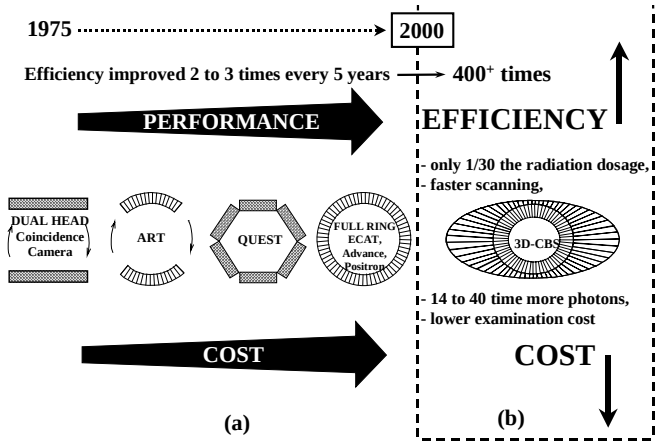

Figure 23. The evolution of positron imaging systems (original source of the figure [5], on the left). Section (a) shows the evolution of the PET using the past and current approach, while Section (b) shows the improvements achievable with the new 3D-CBS described in this document.

[50] See web site of the American Cancer Society or call 1-800-ACS-2345.

Given the potential health benefits of significantly improving the methods of detecting cancer at an early stage, the worst thing that could happen to this project is that it should be stalled due to inaction. Claims as weighty as those in this document (see summary on Table XV) ought to be reviewed and discussed. Even a small response of support, further inquiry, or a critical analysis of a claim significantly aids this project. It is essential to continue the dialogue in order to facilitate a common understanding of this project. Your request for more details is most welcome.

TABLE XV. SUMMARY OF THE ADVANTAGES AND DIFFERENCES OF THE 3D-CBS COMPARED TO THE CURRENT PET.

Current PET	New 3D-CBS	Advantages/ differences
Efficiency: 0.007% to 0.025%	**Efficiency: > 10%**	**Improved 400⁺ times**
Image Quality: POOR	**Image Quality: VERY GOOD**	**Improved 14 to 40 times**
Radiation to the patient: 1100 mrem to 1600 mrem	**Radiation to the patient: 25 to 45 mrem**	**Reduced to 1/30**
Cost of Equipment $2 to $3 million	**Cost of Equipment ~ $6 million**	**Increased from 2 to 3 times**
Examination Cost: $2,000 to $3,000 (10 mCi of FDG tracer = $600 55 minutes scan time)	**Examination Cost: $300 to $400** (0.4 mCi of FDG tracer = $60 4 minutes scan time)	**Reduced to 1/10**
Annual Screening? NO (because exposure to high radiation prohibits annual scan)	**Annual Screening? YES** (because exposure to low radiation permits annual scan)	

17.2 Request for comments

This is a complex project that requires the interest and involvement of knowledgeable, experienced individuals. The interested reader could contribute much to the advancement of the science of medical imaging by critiquing this document and questioning any material that appears to him as inaccessible, unrealistic or unclear.

For those readers who would like to participate actively in this project but are unable to do so on a regular basis, their one-time (or sporadic) input is urgently requested. They could also ask to be included in the list of the people who would like to be kept informed on the progress of this project. All comments, questions, or technical criticisms will be gratefully received. They will help the author to ascertain those areas that need further development or to clarify the proposed technology. The claims of the author so far have not been shown to have significant flaws; if they exist, they should be identified and discussed as soon as possible.

The role of readers is essential to help change the direction[52] of the design of future PET toward the 3D-CBS design (from short FOV to whole body, from high radiation to much lower radiation with improved image quality and time resolution). Many people whose lives in the future could be saved by early detection will be grateful to those who spent the time in addressing the issues and expressing their opinions on this project.

Up to this point, the work in developing the concepts and providing the feasibility and justifying the benefits of the 3D-CBS has been carried on and supported wholly by the author with no use of funding from the National Institute of Health (NIH) or from the National Science Foundation (NSF). If you agree that it is worthwhile to pursue the development of this revolutionary approach to the electronics and the unique 3D-CBS design, the author would like to request a statement of support from you, urging funding for this project from NIH or from NSF, as soon as possible. If, however, you believe that funding this project is not a high priority, please communicate the reasons to the author. Participating now in the simple act of voicing your opinion may help to make life better for someone else tomorrow.

The author would especially welcome the substantive assistance of qualified persons and organizations. Many talents and abilities are needed in this multifaceted project, and contributions of materials and workmanship are crucial. Replies should specify the nature of the contribution and the time commitment being offered. Special thanks go in advance to all those who would consider spending some time on this document and project.

Please send comments and replies to:

info@3d-computing.com

The web site, www.3D-Computing.com, will post questions, answers and different opinions regarding this project in the hope that public dialogue will hasten the development of the highly efficient 3D-CBS.

If you are interested in additional technical information on this project, please find the article [2] presented at the IEEE conference in Lyon, France in October 2000, at www.3d-computing.com/pb/ieee2000-563.pdf.

Additional details on the PET section of the 3D-CBS can be found in the book [1] at amazon.com.

Additional information on the technology of the unique architecture which breaks through the efficiency barrier of current medical imaging instrumentation in capturing more photons [4] has been reviewed by scientists and accepted for publication by Elsevier in the scientific journal "Nuclear Instruments and Methods in Physics Research" and is available at the technical libraries of universities.

Spontaneous comment (possibly with the references that substantiate them) is especially desirable. Consideration of the following statements may help to focus your response:

1 A safe and efficient tool for diagnostic workups, with lower radiation requirements and improved image quality compared to the current PET, is desirable.

2 A safe and efficient annual full-body screening for disease with low radiation and low cost is a desirable goal.

3 There is no reason to pursue only two- to three-fold improvement[31] in the efficiency of medical imaging instruments every five years, as has occurred in the past 25 years, when the technology exists today that makes it possible to approach the theoretical limit of efficiency in one giant step (see the inclined arrow of Figure 17).

4 A judicious investment in the development of this project, which offers an improvement in efficiency of over 400 times (See Section 8.5) over the current design, will pay off in the long run, both in monetary return and in improved public health.

5 The unique 3D-Flow sequentially implemented parallel-processing architectural approach of the 3D-CBS permits not only the cost-effective extension of the FOV, but also the complete extraction of information concerning the interaction of the photon with the crystals. This allows for a considerable reduction in the radiation dose for the patient, not only on PET examinations, but on CT examinations as well.

6 The long field of view of over 1000 mm allows for a dynamic anatomical imaging (CT), which could be extended to most of the body in a single rotation when using several x-ray generators (or multiple electron beams as shown in Figure 11). This would be a far more advanced solution compared to the current trend of the large companies toward increasing the (CT) dynamic[51] imaging to 20 mm and 32 mm FOV.

7 The 3D-CBS is designated to use materials such as BGO and CsI(TI) crystals, which have been available for many years, and can achieve good performance with an electronics using only 80 MHz processor and 20 MHz DAQ. This device could have been built several years ago using the approach described in this document. (In the event you can see any major technological problem that could have presented obstacles during the past years or that in your opinion may still present obstacles, please describe them as specifically as possible. Objections to the described technology or to the claims of efficiency and economy should be aired and discussed)

8 Prompt verification and funding of this project is critical. This must be done as soon as possible in order to prevent further unnecessary loss of lives.

9 The unique approach of the 3D-CBS electronics provides a solution to efficiently handle a high data input rate and extract the characteristic of the interaction between the photon and the detector. Because of this, it is beneficial to all parties (patients, hospitals, investors, etc.) to increase[52] the FOV instead of decreasing it, as in the latest PET and PET/CT devices introduced to the market this year by the two major companies in this field, GE and CTI/Siemens.

10 Pharmaceutical companies need a more efficient and economical tool, such as the 3D-CBS, for researching the development of new drugs. The long FOV, high sensitivity, good spatial resolution, whole-body dynamic, anatomical and functional three-dimensional imaging are crucial for such companies.

11 Prescribed drugs and their dosages should be carefully monitored and tailored to optimize their effects on each individual patient

12 With the 3D-CBS, the physician will not have to study 30 to 200 separate slices (images), as is the case with the current imaging devices, but will be able to visualize dynamically any section of the patient's body in slow- or fast-motion in three-dimensional functional and anatomical form. This feature of creating a three-dimensional image of the patient's entire body is not possible with current PET and CT scanners, because the data on different sections of the body (~32 mm for CT and ~16 cm for PET) are acquired at different times.

13 The image quality of the 3D-CBS will be superior because of the high processing capability at the front-end electronics with a set of DSP on each electronic channel. This provides less "bad" information (noise, randoms, scatter, etc.) to the workstation that rebuilds the entire image. For the same amount of data, the physician will have less time to wait and will receive a higher quality image.

14 This project will create healthy competition in the medical imaging field now dominated by two large manufacturers, General Electric and CTI/Siemens, while opening a new direction toward the design of PET with a unique approach in the electronics that permits a cost-effective increase in the FOV[52].

15 Providing the ability to continue this project and the building of a prototype based on this design might also influence companies currently producing PET, to offer a better machine to the patients but are now limited by inefficient electronics compared to the 3D-CBS.

---

[51] The industry is going in the direction of dynamic imaging for CT, according to the latest announcements of GE, Siemens and Marconi. They will have 8 slices and even 16 simultaneous slices in 2002 with an overall time resolution of a few tens of a second. In comparison, the 3D-CBS offers an essentially infinite time resolution in PET, sampling every 50 ns with a resolution of 500 ps but having the detector covering most of the patient's body simultaneously. In CT mode, the time resolution is similar to the most recent announcement of CT dynamic imaging, but with the advantage, again that most of the patient's body is observed simultaneously instead of only a 32-mm slice.

[52] The main players in this field are CTI/Siemens and General Electric, which together share more than 90% of the market. The CTI/Siemens PET 1996 model 966/EXACT3D had a FOV of 23.4 cm, while the two new devices introduced in the spring 2001, the PET EXACT ACCEL with LSO crystals and the PET/CT, model "biograph," have taken a step backward, decreasing the FOV to only 16.2 cm. The new PET model Advance Nxi from General Electric which was introduced during the spring 2001 is still using the same short FOV of 15.2 cm and the same materials such as 12,096 BGO crystals (8 x 4 x 30 mm) assembled in 18 rings of 672 crystals per ring as was the PET manufactured by the same company over 8 years ago. The analysis made in this document concludes that the operating costs of a 25 cm FOV PET are higher than a PET with a ~ 14-cm FOV (see Table I). However, in contrast, a PET applying the new 3D-CBS technology has lower operating costs when using a FOV over one meter in length. Although the cost of a ~ 150 cm FOV machine is higher, the improvement of the quality of the image and the examination speed that can be provided by using the 3D-CBS technology result in a compensating reduction in operating costs. The 3D-CBS technology puts the patient's interest first by lowering the risk of radiation and giving maximum body coverage. The new products from General Electric and Siemens show that their intention is to keep on producting the 15 cm FOV PET without pursuing radical improvements, such as using a set of DSP on each electronic channel that fully extracts the characteristics of the interactions between most of the photons and the detector. Their conservatism implies a much higher radiation dose for the patient and lower efficiency in detecting tumors.

This project needs serious consideration and support by the government, because it will produce a life-saving improvement in medical imaging that large private companies are apparently unwilling to pursue.

APPENDIX A. VERIFICATION THAT INVESTMENT IN THE 3D-CBS IS JUSTIFIED

Appendix A.1. World-wide health care expenses

The expense for health care as a percentage of the gross domestic product (GDP) of a few countries of the world is reported in Table XVI.

TABLE XVI. HEALTH CARE EXPENDITURES AS A SHARE OF THE GROSS DOMESTIC PRODUCT IN DIFFERENT COUNTRIES FROM 1980 TO 1997 (SOURCES[53]).

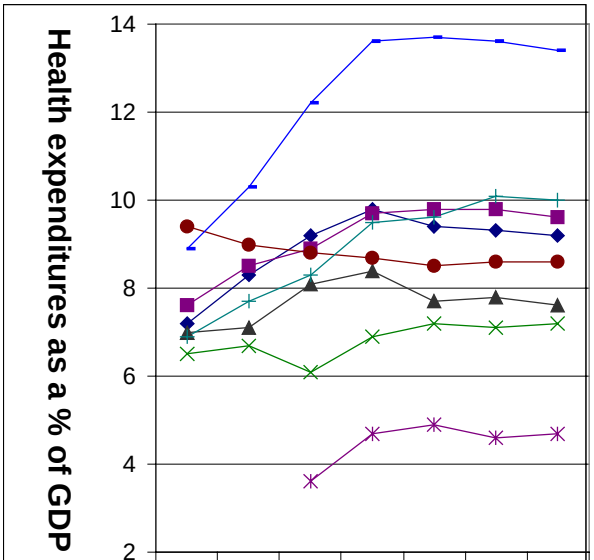

	1980	1985	1990	1994	1995	1996	1997
Canada	7.2	8.3	9.2	9.8	9.4	9.3	9.2
France	7.6	8.5	8.9	9.7	9.8	9.8	9.6
Italy	7	7.1	8.1	8.4	7.7	7.8	7.6
Japan	6.5	6.7	6.1	6.9	7.2	7.1	7.2
Mexico			3.6	4.7	4.9	4.6	4.7
Sweden	9.4	9	8.8	8.7	8.5	8.6	8.6
Switzerland	6.9	7.7	8.3	9.5	9.6	10.1	10
USA	8.9	10.3	12.2	13.6	13.7	13.6	13.4

During 1980 Sweden dedicated a higher percentage of its GDP to health than any other country in the world, although, the United State has always had the highest per capita expenditures. During the following years, Sweden lowered the percentage of the GDP for health care and has been almost stable at 8.6% until 1997. After 1980, the United States had the largest health expenditure expressed as a percentage of the GDP, with a rapid growth to 13.6% reached in 1994. Since 1995, this figure has been decreasing slightly.

Japan had a decrease from 1985 to 1990, but increased after that date to reach a stable value around 7.2%. On the other hand, Italy had a sharp increase in the health care expenditures in 1990 and sharply declining one in 1995 and then stabilized around 7.7%. Canada showed a reduction after 1994. Switzerland's expenditures grew constantly to reach 10.1% of their GDP in 1996. Expenditures by the other countries listed in Table XVI also grew constantly in percentage of the GDP. The United States, however, has a much higher health care expenditure per capita (see Table XVII) than any other country (e.g., $3,912 compared to the average of $2,300 for other industrialized countries in 1997).

The following is the total health care expenditures as a percentage of GDP for some selected countries for the year 1996: U.S., 13.6%, Germany, 10.8%, Switzerland, 10.1%, France, 9.8%, Canada, 9.3%, Netherlands, 8.7%, Sweden and Australia, 8.6%, Greece, 8.4%, Iceland, 8.2%, Denmark, 8.1%, Austria, 8%, Portugal, 7.9%, Italy, Norway, and Finland, 7.8%, Spain, 7.4%, New Zealand, 7.3%, Japan, 7.1%, United Kingdom, 6.9%, Luxembourg, 6.8%, Hungary, 6.6%, Ireland, 6.4%, Korea, 5.9%, Poland, 4.9%, Mexico, 4.6, Turkey, 3.8%.

The detailed study of health care expenditures in United States is similar to the ones carried out for other countries in the past. In fact, several studies were made in the Netherlands, England, Germany, and Japan two decades ago when the CT[8] was first introduced. A few years later the advantages of larger, more technologically advanced imaging devices such as CT and MRI devices contributed to improvement in health care and also a reduction in health care costs[33], even though the CT and MRI units were more expensive than the older technology in use at that time. For example, Japan, which has more CT scanners per million inhabitants[8], has lower per-capita expenses and lower health care expenditure as a percentage of GDP than the U.S.

TABLE XVII. PER CAPITA HEALTH CARE EXPENDITURES IN DIFFERENT COUNTRIES FROM 1980 TO 1997 (SOURCES[53]).

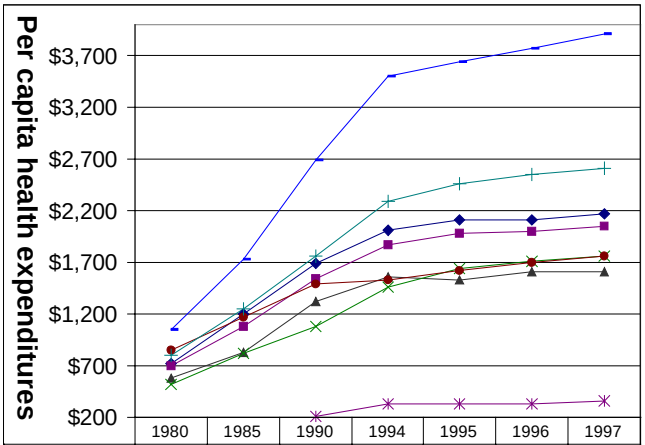

	1980	1985	1990	1994	1995	1996	1997
Canada	$716	$1,201	$1,695	$2,006	$2,106	$2,112	$2,175
France	$701	$1,082	$1,539	$1,869	$1,984	$2,005	$2,047
Italy	$579	$830	$1,321	$1,562	$1,534	$1,615	$1,613
Japan	$524	$820	$1,082	$1,463	$1,637	$1,713	$1,760
Mexico			$210	$328	$335	$330	$363
Sweden	$850	$1,172	$1,492	$1,533	$1,623	$1,701	$1,762
Switzerland	$801	$1,250	$1,760	$2,294	$2,464	$2,548	$2,611
USA	$1,052	$1,735	$2,689	$3,501	$3,637	$3,772	$3,912

53 Sources: Schieber GJ, Poullier JP, and Greenwaid LG. U.S. health expenditures performance: An international comparison and data update. Health Care Financing Review vol 13 no 4. Washington: Health Care Financing Administration, September 1992; Anderson GF and Poullier GP. Health spending, access, and outcomes: Trends in industrialized countries. Health Affairs vol. 18 no 3, May/June 1999; Office of National Health Statistics, Office of the Actuary. National health expenditures, 1997. Health Care Financing Review vol. 20 no 1. HCFA pub no 03412. Washington: Health Care Financing Administration, March 1999; Organization for Economic Cooperation and Development Health Data File. Organization for Economic Cooperation and Development.

Appendix A.2. Health care expenses in the U.S.

Table XVIII shows the historical and projected data of the percentage distribution of personal health care expenditures in U.S. by type of service during the years 1980-2010 [16]. The historical data from 1990 to 2000 of Table XVIII must be compared with the projected data reported by HCFA in [17], [18], [19], [20], [21], [22], [23] during the previous years. During the previous years, HCFA overestimated the increase in overall health care cost for future years but grossly underestimated spending on pharmaceuticals.

The percentage of distribution for type of service is different for different countries. For example, in the United States many hospitals have closed during the past years and Table XVIII shows that this trend is expected to continue. However, in other countries the percentage of health care expenditures for hospitals is much higher than in the U.S., and it is well known that for a similar procedure, the patient's stay in the hospital is much shorter in the U.S. than in hospitals of European countries. With the exception of the categories "construction" and "research" which are considered investment, all other categories [13] are expenses (e.g., what the hospital intends to receive, rather what it charged). The figures showing sales of medical and irradiation equipment were taken from statistics from the U.S. Census Bureau [15].

It is important to note that the sharp increase in drug expenditures from 1995 to 2000 does not correspond to a greater decrease in the death rate for the same period in Table IX. This might raise the question whether the increase in drug expenditures would be more cost-effective if the possibility existed to optimize their use by verifying their effect with a technologically advanced medical imaging instrument such as the 3D-CBS.

TABLE XVIII. HISTORICAL DATA AND PROJECTED DATA OF THE PERCENT DISTRIBUTION OF PERSONAL HEALTH CARE EXPENDITURES IN U.S. DURING THE YEARS 1980-2010, BY TYPE OF SERVICE. (SOURCE: HCFA[19] [16]). SEE ALSO THE TOTAL HEALTH CARE EXPENSES IN TABLE II.

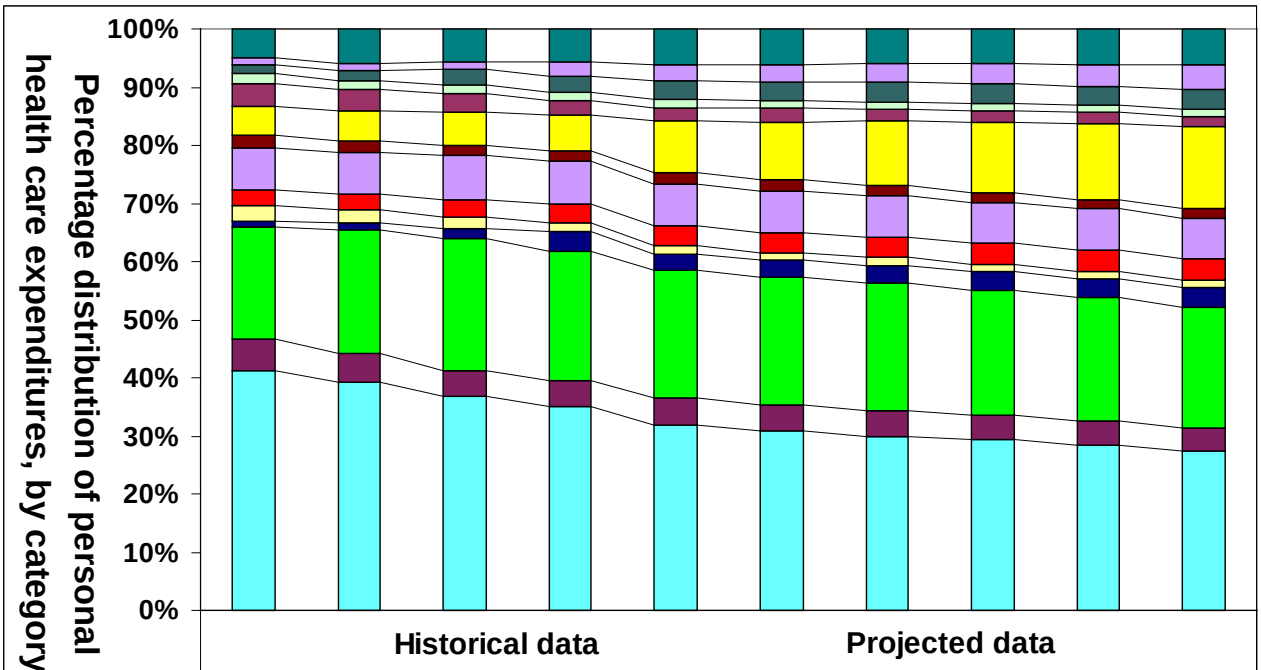

	1980	1985	1990	1995	2000	2002	2004	2006	2008	2010
Admin.	4.94	5.8	5.6	5.7	6.1	6.1	6	6	6.1	6.22
Other pers.	1.33	1.2	1.3	2.3	2.8	2.9	3.1	3.4	3.7	4.17
Other Profess.	1.46	1.9	2.6	2.8	3.1	3.2	3.3	3.3	3.3	3.38
Vision	1.61	1.5	1.6	1.5	1.4	1.4	1.3	1.3	1.2	1.26
Other Med. Prod.	3.94	3.6	3.1	2.4	2.3	2.3	2.1	2	1.9	1.86
Drugs	4.9	5.1	5.7	6.1	8.9	10	11	11.9	12.9	13.87
Research	2.22	1.9	1.8	1.7	1.8	1.8	1.7	1.7	1.7	1.74
Nursing care	7.19	7.1	7.5	7.5	7.3	7.2	7.1	7	7	6.95
Public	2.74	2.7	2.9	3.1	3.3	3.4	3.5	3.6	3.7	3.8
Construction	2.77	2.2	1.9	1.5	1.4	1.3	1.3	1.3	1.3	1.25
Home Hlth care	0.96	1.3	1.8	3.3	2.7	3	3.1	3.2	3.2	3.29
Physician	19.15	21	22.6	22.2	22	21.8	21.7	21.3	21	20.69
Dental	5.42	5	4.5	4.4	4.5	4.5	4.4	4.3	4.2	4.12
Hospital	41.32	39	36.5	34.7	31.7	30.6	29.8	29.1	28.2	27.31

Figure 24 shows the percentage distribution for the selected years 1980, 1999, and 2010 of U.S National Expenditures (NHE) by type of service as defined by HCFA on http://www.hcfa.gov/stats/nhe-oact/lessons/ (The group "drugs" is limited to spending for prescription drugs purchased from retail outlets. The value of drugs and other products provided to the patient by hospitals (on inpatient or outpatient basis) and nursing homes and by health care practitioners as part of a provider contact are included in estimates of spending for those providers' services. (Source: [16]).

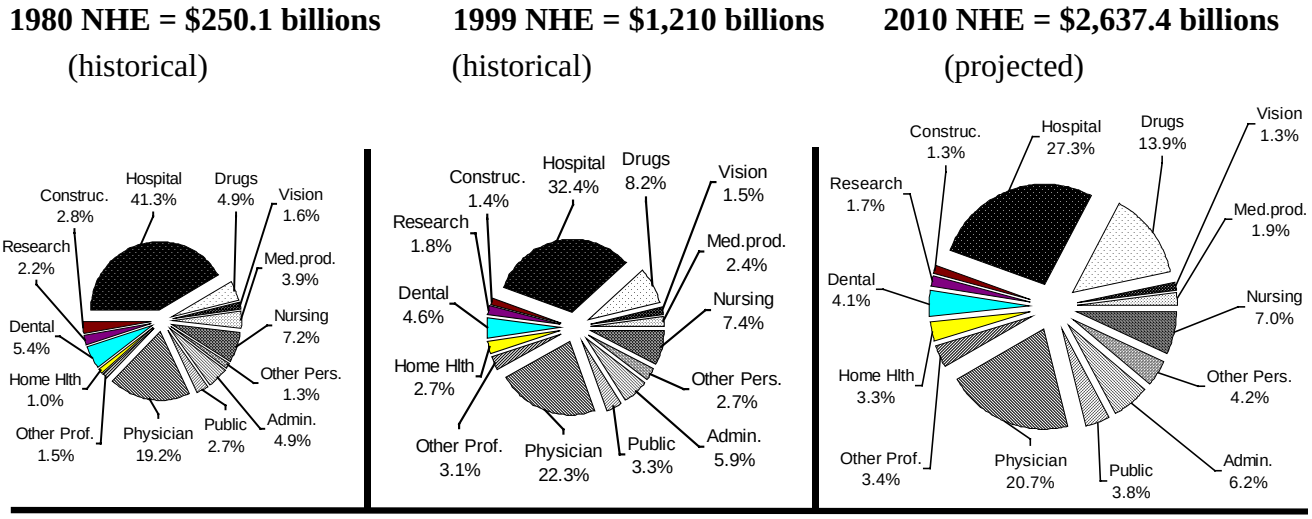

Figure 24. Percent distribution of health care expenditures, by type of service: United States, selected years 1980, 1999, and 2010. (Source: [16], [17])

Figure 25 shows the percentage distribution of health care expenditures by type of service in the U.S. during the selected years 1980, 1999, and 2010 when all expenses of the category "prescription drugs" in the U.S. are consolidated in one single category. (Source: IMS health [14]). Historical data for electromedical and irradiation instrumentation were obtained from the U.S. Census Bureau; projected data for 2000 to 2010 were based on the growth of the previous decade in the same category.).

It is clear from Figure 25 that the electromedical and irradiation instrumentation, with a percentage of around 1% of total health care costs, cannot be the cause of the overall increase in these total costs. It is also clear that drug expenses are increasing more than all other expenses.

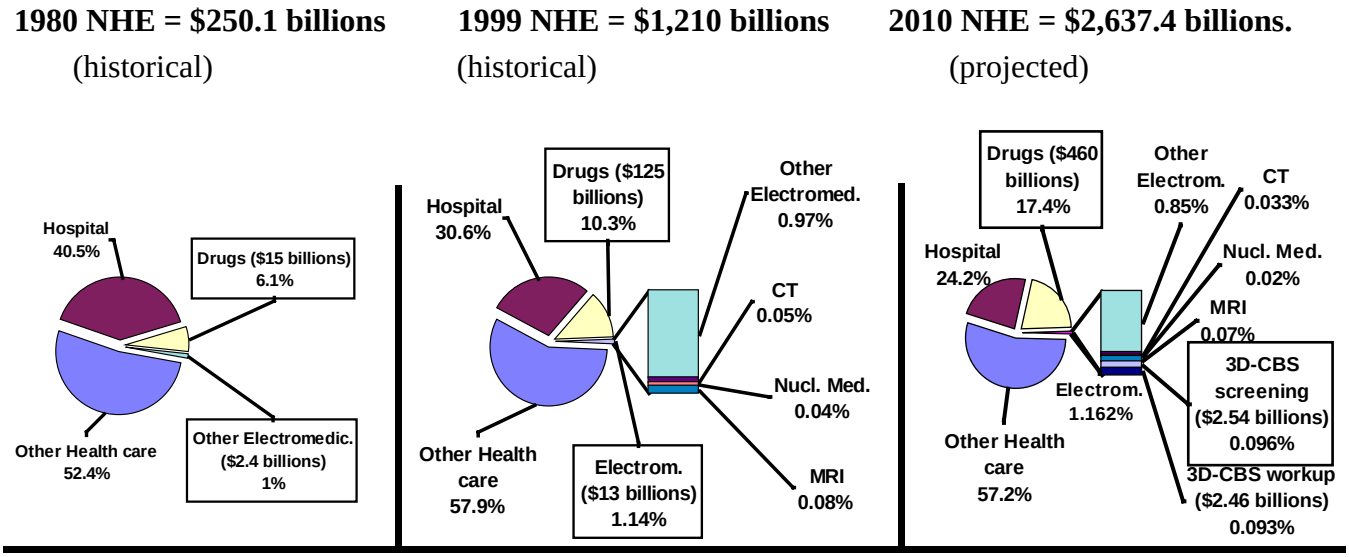

Figure 25. Consolidation of all "drugs" expenditures in one single category (Source: IMS Health [14], [15].

(Notice how the expense for hospitals is reduced while the expense for drugs, projected in 1992 by HCFA [17] to be 5.8% by 2000 and 5.5% by 2010, increased instead to 10% in 1999 and is now projected to increase to 17.4% by 2010.)

APPENDIX B. ADDITIONAL INFORMATION ON VERIFICATION OF THE TECHNOLOGY

Design Real-Time is an integrated high-level design environment for the development, verification, and implementation of scalable high-speed real-time applications for which commercially available processors fail because of throughput requirements.

The Design Real-Time software tools allow the user to design fast programmable real-time 3D-Flow systems [4], [24] with different sizes, topologies, and performance (8-bit, or 16-bit wide internal buses). The steps are: a) to create a system and simulate it in software, b) using the Electronic Design Automation (EDA) tools, to create a component in hardware, simulate, and verify each feature against the requirements of each section of the software system (e.g. stack, pyramid, real-time monitoring).

Design Real-Time:

- Interfaces with third-party EDA tools;
- Is based on a single type of replicated component, the 3D-Flow Processing Element (PE in the form of an IP block);
- Is technology independent because the PE-IP block can be targeted to the latest technology;
- Takes the user to a higher level of abstraction and productivity gain during the design phase because of the simplicity of the 3D-Flow architecture, and the powerful tools, the set of predefined macros and the real-time algorithms available to the user;
- Allows for implementation of the user's conceptual idea into the fastest programmable system at the gate level.

Appendix B.1. 3D-Flow Design Real-Time tools

1. Create a new 3D-Flow application (called project) by varying system size, throughput, filtering and routing algorithm, and by selecting the processor speed, lookup tables, number of input and output bits for each set of data received for each algorithm execution;
2. Simulate a specified parallel-processing system for a given algorithm on different sets of data. The flow of the data can be easily monitored and traced in any single processor of the system and in any stage of the process (see Appendix C.6 and Figure 34);
3. Monitor a 3D-Flow system in real-time via the RS232 interface, whether the system at the other end of the RS232 cable is real or virtual; and
4. Create a 3D-Flow chip accommodating several 3D-Flow processors by means of interfacing to the EDA tools.

A flow diagram guides the user through the above four phases. A system summary displays the information for a 3D-Flow system created by the Design Real-Time tools.

Appendix B.2. Interrelation between the entities in the Real-Time Design Process

Figure 26 is separated into three sections. On the left is shown the flow of the software design and simulation process to create and simulate a 3D-Flow system, on the right is shown the System-On-a-Chip for High-speed Real-time Applications and TESting (SOC-HRATES) hardware design process. The center of the figure shows the common entities of the system:

1. The IP 3D-Flow processing element is the basic circuit to which the functionality required by different applications has been constrained;
2. A set of 3D-Flow real-time algorithms and macros organized into a library;
3. The System Monitor software package that allows the user to monitor each 3D-Flow processor of the 3D-Flow system (hardware or VPS –Virtual Processing System--), via RS-232 lines. The System Monitor (SM):
   a) Performs the function of a system-supervising host that loads different real-time algorithms into each processor during the initialization phase;
   b) Detects malfunctioning components during run-time. (A sample of data, containing the status of each processor, is captured at the processor speed of 80 MHz at a preset trigger time for 8 consecutive cycles (called snap-shot), and is transferred at low speed (at the RS-232 speed of 230 KBaud) to the System Monitor for debugging and/or monitoring);
   c) Excludes malfunctioning processors with software repair by downloading into all neighbors a modified version of the standard algorithm, instructing them to ignore the offending processor.

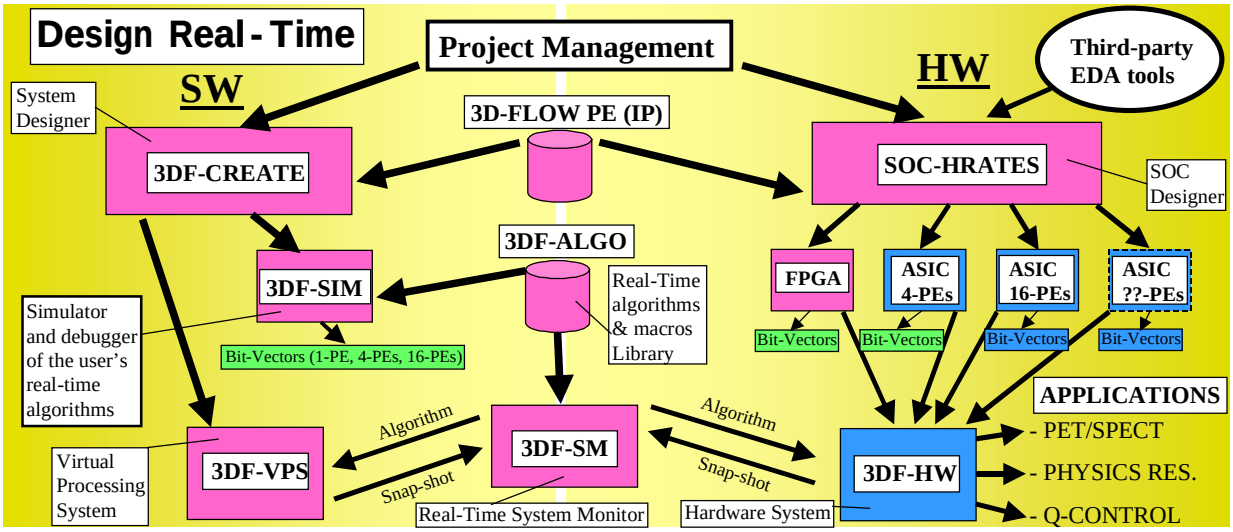

Figure 26. Interrelation between entities in the Real-Time Design Process.

The "3DF-CREATE" software module allows the user to:

1. Define a 3D-Flow system of any size;
2. Interconnect processors for building a specific topology with or without the channel reduction stage ("pyramid");
3. Modify an existing real-time algorithm or create a new one. The complexity of the real-time algorithms for identifying particles arriving from multiple channels at a high rate at the input of the 3D-Flow system, such as the ones reported in [26], [4], [59], [60], have been examined and fewer than 10 layers (corresponding to 20 steps, each executing up to 26 operations) of 3D-Flow processors are required;
4. Create input data files to be used to test the system during the debugging and verification phase.

The "3DF-SIM" module allows for simulation and debugging of the user's system real-time algorithm and generates the "Bit-Vectors" to be compared later with the ones generated by third-party silicon foundry tools.

The "3DF-VPS" module is the Virtual Processing System that emulates a 3D-Flow hardware system.

The right side of Figure 26 shows the flow of the hardware implementation of the 3D-Flow system in a System-On-a-Chip (SOC). The same common entity, the IP 3D-Flow processing element (PE), shown in the center of the figure and previously used as the behavioral model in the simulation, is now synthesized in a specific technology by using the same code.

The number of chips required for an application can be reduced by fitting several PE's into a single die. Each PE requires about 100K gates and the gate density increases continually. Small 3D-Flow systems may fit into a chip. For this reason, it is also called SOC 3D-Flow. However, when an application requires the building of a 3D-Flow system that cannot be accommodated into a single chip, several chips each accommodating several 3D-Flow PEs can be interfaced with glueless logic to build a system of any size to be accommodated on a board, on a crate, or on several crates [4].

Appendix B.3. Design Real-Time verification process

The verification process of an entire 3D-Flow system can be performed down to the gate-level in the following steps:

- The 3DF-SIM: a) extracts from the system the input data for the selected 3D-Flow processor(s) for which an equivalent hardware chip (which was targeted to a specific technology) has been created, and b) generates the Bit-Vectors for the selected processor(s);
- The same input data and the same real-time algorithm are applied to the hardware 3D-Flow model, and the simulation is performed using the third-party tools;
- Bit-Vectors generated by third-party tools using the hardware model are compared with the Bit-Vectors obtained by the previous software simulation (3DF-SIM);
- Discrepancies are eliminated.

Appendix B.4. Results from the use of Design Real-Time

The use of the Design Real-Time tools has made it possible to determine the parameters that led to design the data acquisition and processing system for pattern-recognition (particles in HEP experiments) described in [4] and [25], providing:

1. Simulation and implementation results of a real-time system for the Level-0 trigger of LHCb [4], [2] experiment at the Large Hadron Collider at CERN [61] (which are described in the following sections of this publication); and
2. The simulation and verification of the LHCb HEP Level-0 system trigger algorithm simulated using 3DF-SIM vs. the results (test pattern in the form of bit-vectors) obtained from the EDA tools from the design of
   a) a single 8-bit wide internal bus 3D-Flow PE version synthesized for different FPGAs,
   b) a 3D-Flow ASIC chip containing four PEs with 16-bit wide buses synthesized into a 0.5 μm technology, and
   c) the same four PEs into a 0.35 μm ASIC technology.

   Simulation has been performed, and Bit-Vectors have been compared between the system simulator (3DF-SIM) and a 3D-Flow chip implemented with 0.35 μm Cell Based Array (CBA) technology at 3.3 Volts. The CBA ASIC EDA design tools show dissipation of 884 mW @ 60 MHz and a die size of 63.75 mm^2 for a chip with 4 3D-Flow processors.

Implementation with the current technology of 0.18 μm which has a gate count of ~65K gates per mm^2 requires about 1.5 mm^2 of silicon per PE. A chip accommodating 16 PEs dissipates 23 nW Gate/MHz, and requires a silicon area of about 25 mm^2 in 0.18 μm technology (leading to a chip @ 1.8 Volts, 676-pin EBGA, 2.7 cm x 2.7 cm).

Appendix B.5 Implementation merits of the 3D-Flow design

The execution of complex real-time algorithms for capturing most of the interactions between the photons and the crystals and accurately measuring their characteristics was not possible earlier without using electronics that were too costly and complex. The merit of the 3D-Flow architecture is not only in the special "fusion" between pipelining and parallel processing, but is also in its simple hardware implementation.

The hardware implementation of this parallel processing system, described below, can achieve high-speed data throughput with a relatively low-speed 3D-Flow processor (of the order of 100 MHz) allowing the implementation of a system at low power consumption, which minimizes the problems of ground bounce and crosstalk.

One of the key features of the 3D-Flow architecture is the way the processor chips are interconnected on the PCB board, which is the result of (a) a special sequential/parallel architecture, (b) the assignment of the signals of the 3D-Flow processor to the pins of the chip with a particular criterion, and (c) the special data moving instructions of the processor.

During the pin assignment phase of the ASIC design, each pin carrying a 3D-Flow bottom port output is placed adjacent to a pin carrying the input of the related top port bit.

This allows for uniform trace length when connecting processors of adjacent, cascaded 3D-Flow chips and also allows traces that do not cross each other.

This regular pattern of the PCB traces eliminates crosstalk and signal skew and easily allows impedance matching and a simple low-cost PCB construction.

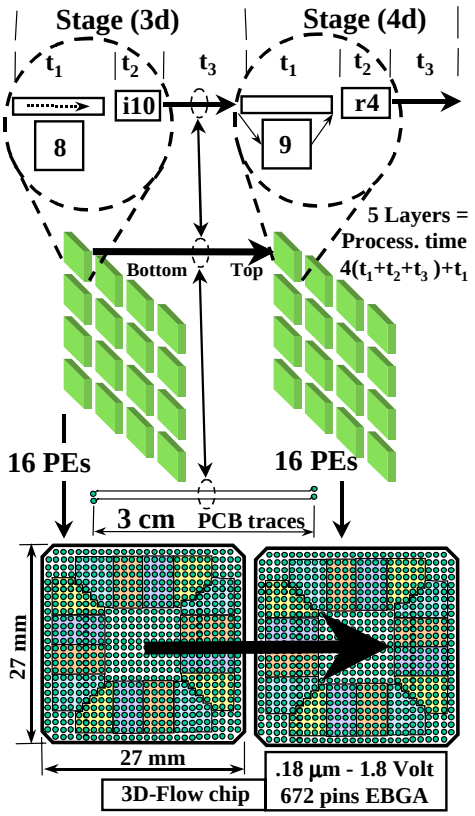

Figure 27. Implementation merit of the 3D-Flow system. The connection of the signals of the bottom port of one processor of the 3D-Flow architecture shown within the dashed line of Figure 10 can be connected to the top port of the next processor (see solid horizontal arrow) with very short and equidistant traces of 3 cm. (See also bottom right of Figure 30 and top left of Figure 12 for the complete layout of 64 channels on an IBM PC board). All traces can be easily kept to the same length because during ASIC pin assignment design phase, for each pin carrying an input for the top port, a signal of its equivalent bottom port has been assigned to its adjacent pin. The top section of the figure shows the detail of two stages of Figure 10. (Note that one 3D-Flow processor consists of three units which are incorporated into the chip: a bypass switch, a register, and a processor). The middle section of the figure represents the logical layout of the 16 processors, which are accommodated in a single chip. The lower section of the figure shows how the connection is made between the bottom port of the processor in one chip and the top port of the processor on the adjacent chip via 3-cm PCB traces. Such component layout and connection allows for (a) a low-power dissipation driver for a single load unit, (b) reduced ground bouncing and noise, (c) easy implementation of matched impedance PCB traces, (d) reduced crosstalk and signal skew, (e) easy construction of the PCB with no crossing traces, and (f) modularity. These features provide the advantage of using the same chip (by cascading them) for other configurations and/or applications with more complex algorithms requiring more layers of processors.

One simple way to implement the communication between the 3D-Flow chips is as follows (see Figure 28):

- Four CMOS signals at 160 MHz carrying the information from the bottom port of one processor on one chip to the top port of the adjacent chip through a matched impedance line 3 cm in length. Each of such lines dissipates only 2 mW. It is not a problem to achieve this speed easily because RamBus [62] technology runs at over 500 MHz, and this implementation is facilitated by the traces having equal length, which eliminates signal skew. Sixteen bottom ports per chip, for a total of 64 (16 x 4) CMOS lines, dissipates only about 128 mW per chip.
- One 1.28 Gbps, low voltage differential signaling (LVDS) transmitter and one receiver for each North, East, West, and South port at the periphery of the 3D-Flow processor chip can reach the longer distance to other boards and consumes, with newest technology, less than 20 mW for the transmitter and 6 mW for the receiver, for a total of 416 mW per chip. The speed of 1.28 Gbps over LVDS distances of less than one meter is not an issue because there are LVDS links over 2.5 Gbps commercially available.

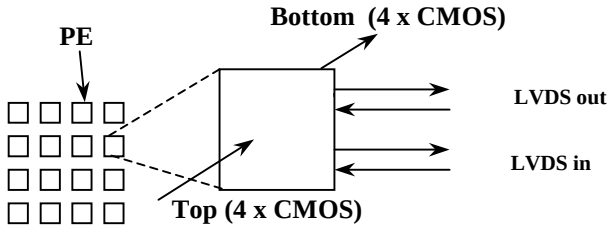

Figure 28. Input output signals for Top, Bottom, North, East, West, and South (NEWS) ports of the 3D-Flow chip.

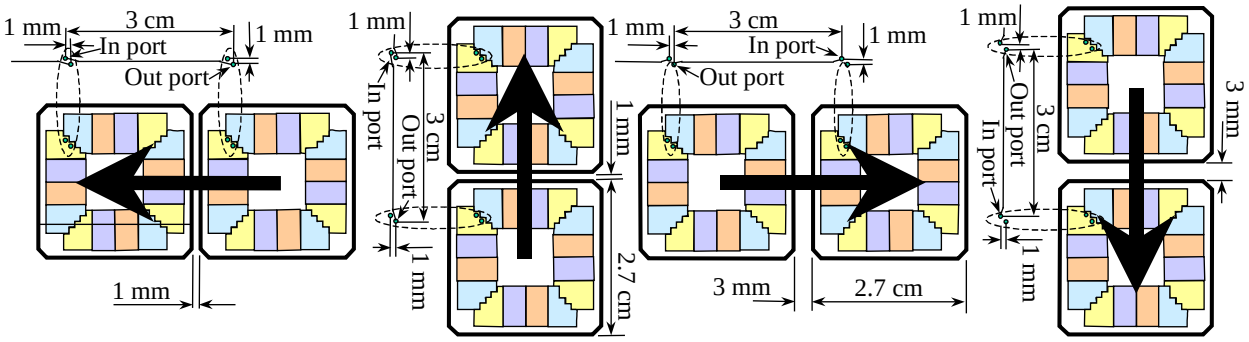

Figure 29. Equal-length connections between bottom and top ports of two 3D-Flow processors located on adjacent chips. When input and output of a given port bit are assigned to adjacent pins, it is possible to obtain connections in any direction with uniform trace length as shown in the figure. (See the 3D-Flow components layout on the bottom right of Figure 30). The 16 groups of input and output pins for each of the 16 processors in the chip are shown in the figure. The NEWS connections between "on-chip processors" remain inside the chip and are not carried to the pins.

The core of the 3D-Flow processor implemented in about 100,000 gates consists of the standard instruction set of a DSP with some special instructions for data movement to/from I/O ports and internal units, and special instructions for the photon identification.

The 3D-Flow instruction set includes operations such as multiply-accumulate, arithmetic and logic operations, and in addition has operations to move data to/from the 10 input output ports and operations comparing the received data with the 8 or 24 neighbors in a single cycle (to check for local maxima). Up to 26 operations in different units (2 ALUs, 1 MAC/Divide, 64 registers, 5 input FIFOs, 32 comparators, 1 timer, 4 data memories, all connected via four internal busses) can be executed in a single cycle.

This balance of operations of moving and computing data allow for the execution of the real-time algorithms for the identification of most of the particles, including photons at different energies. These real-time algorithms require a program of ten to twenty lines of code, which is loaded into the processor program memory through a RS-232 port. The same port monitors the system during real-time algorithm execution; and when it finds a faulty processor or connection, it loads a different program in the neighboring processors in order to isolate the problem.

Photon-identification algorithms and fault-tolerant programs that isolate faulty processors or connections have been simulated from system to gate level.

Even if one would use an array of 1.5 GHz Pentiums, the global performance in identifying photons at a high rate could not be achieved because of (a) the different architecture of a Pentium, (b) its different I/O, (c) prohibitive power dissipation, and (d) its high cost.

Appendix B.6 Example of the use of the 3D-Flow design in a cost-effective system for capturing photons in medical imaging

Figure 30 (bottom left) shows the logical and physical layout of the complete 3D-CBS system consisting of an elliptical gantry for the torso and a circular gantry for the head. Any shape of the gantry, from the simplest circular gantry for head and torso to the elliptical or to the shape closest to the human body can be used.

Tradeoffs should be made between (a) cost savings in crystals and the Time of Flight gained by the photon reaching the detector and (b) the higher complexity in the image reconstruction software (when shapes other than circular designs are used).

The right side of the figure shows a crystal detector block coupled to a PMT. The use of several layers of crystals with different decay times (light pulse duration) allows the measurement of the depth-of-interaction (DOI). The crystals can be cut into small elements assembled with short, equal-length reflecting slits to allow light sharing between PMTs or it can be implemented in large blocks to save cost (See Appendix C.4, and Section 11.2.4 of [1]).

The signal of the phototube is sent to the first layer of a 3D-Flow system [4]. A total of 1,792 phototubes are required (256 for the head and 1,536 for the torso). The top right of the figure shows the relationship of one phototube to the first layer[55] of the 3D-Flow system (six layers, plus one 3D-Flow chip for the pyramid for each board; see at the bottom right of the figure how the chips shown on the top right of the figure are positioned on the PCB board, one next to the other, with the arrow as shown also in detail in Figure 27).

The processing of the signals from the entire 3D-CBS detector is done by 700 3D-flow chips, which are accommodated on 28 IBM PC DAQ-DSP boards. (See the relation between the detectors, photomultipliers, signals, and the 28 3D-Flow DAQ-DSP boards in the center left of the figure). The real-time algorithm is described in Figure 34 and the functionality of the 3D-Flow DAQ-DSP board is described in Section 13 and in Section 15.1.1. of [1].

The bottom right of Figure 30 shows the estimated component layout of the 3D-Flow DAQ-DSP board implemented in an IBM PC platform for all 3D-CBS functions. Each 64-channel 3D-Flow DAQ-DSP board consists of 32 ADC AD9281 (or equivalent, 28-pin SSOP); 2 x 32-channel preamplifiers (256-pin FineLine BGA); 2 x 32-channel TDC (225-pin BGA MO-151); 25 x 3D-Flow (672 FineLine BGA); and 3 x FPGA (484-pin FineLine BGA). A SO-DIMM memory and an FPGA on the back of the board can be installed if a larger buffer of CT events is desired.

The connections carrying the information between neighboring 3D-Flow processors are described in detail in Section 15.3 and shown in Figure 15-7 of [1].

See Figure 12 for the layout of the hardware of the entire system.

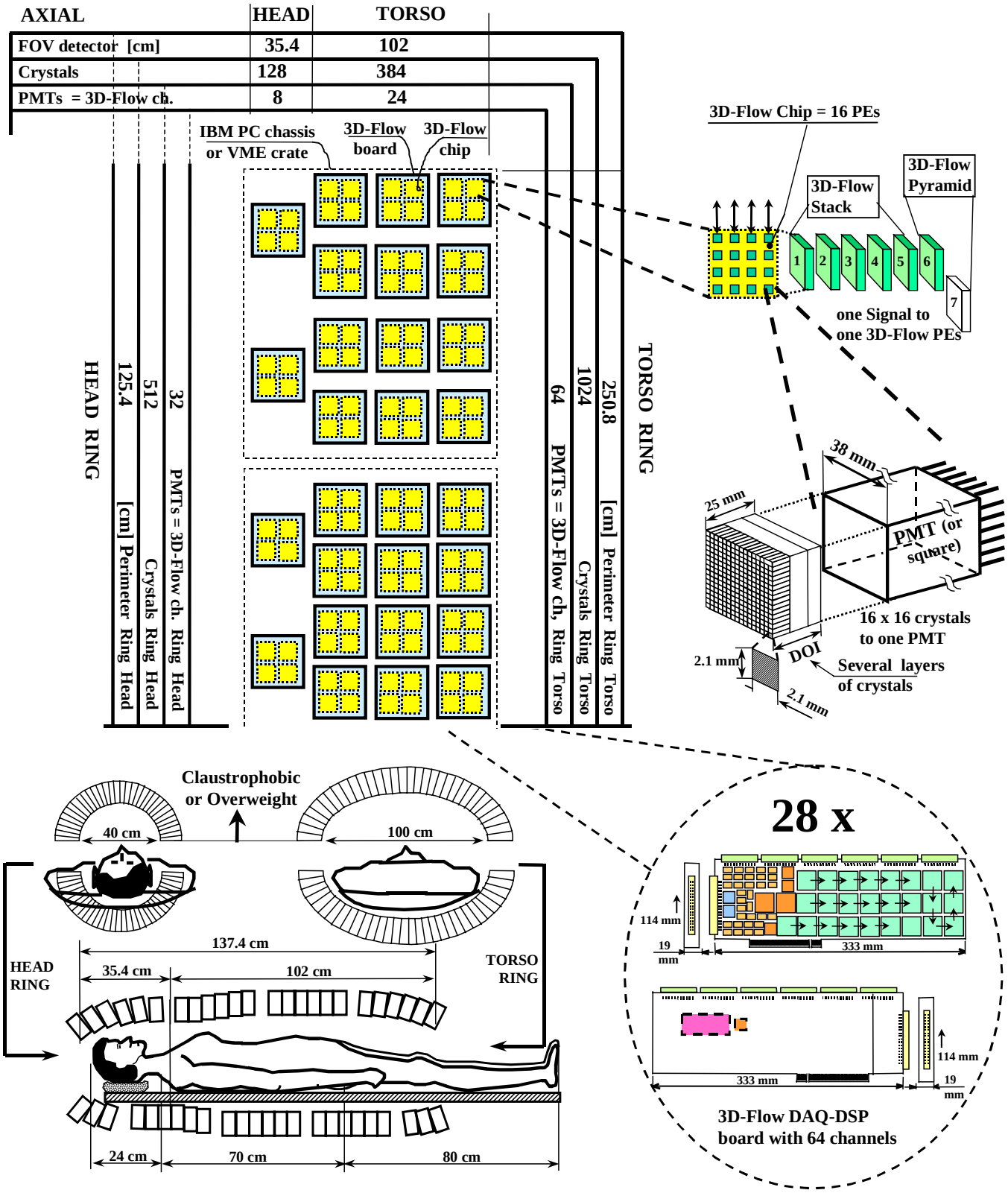

Figure 30. Logical and physical layout for a 3D-CBS device with long FOV. (See harware assembly on Figure 12.)

APPENDIX C. DEFICIENCIES OF CURRENT PET MACHINES AND THEIR REMEDIES

Although the current CT images are of good quality at the expenses of a relatively high x-ray beam (which should be lowered in order to lower the risk to the patient), the current PET images are of poor quality because only a few emitted photons from the patient's body are captured by the PET detector. Other deficiencies of the current PET machines are: low coverage of the entire body, high radiation dose, slow scanning time, high examination costs. The increased efficiency of the 3D-CBS in capturing photons will provide improvements in both: lowering the radiation dosage for CT scans and improving the PET image quality (in addition to lowering the PET radiation dosage).

Appendix C.1. Limiting factors of current PET.

A list of the main areas of inefficiencies in the current PET which prevents maximum exploitation of positron emission technology follows:

1. The image quality of the current PET is poor because it has:
   a) a short FOV, limited by a non efficient electronics that does not offset the cost of the detector if the FOV were increased (see also next section about false positives and false negatives);
   b) no accurate time-stamp assigned to each photon (a) limiting the detection of neighboring photons emitted within a short time interval, (b) causing long dead-time of the electronics and (c) increasing randoms[54] (most PETs do not have any photon time-stamp assignment);
   c) analog signal processing on the front-end electronics limiting photon identification because of poor extraction of the characteristics of the incident photon and absence of the capability to improve the signal-to-noise (S/N) ratio;
   d) detector boundary limitations to 2x2 PMT blocks, no correlation between signals from neighboring detector blocks, no full energy reconstruction of the photons that hit the detector, (most of current PET do not attempt to make any energy reconstruction of the event, but make decisions in accepting or rejecting a photon first and later an event based on the threshold of a single signal).
   e) dead-time of the electronics. Dead-time of the electronics is due to any bottleneck (e.g., multiplexing of data from many lines to a single line, saturation on input, processing, saturation on output) present at any stage of the electronics;
   f) saturation of the electronics at the input stage due to its inability to detect and process two nearby photons that hit the detector within a short time interval;
   g) costly and inefficient coincidence detection circuit (most current PET [34], [32] have a coincidence detection circuits that tests all possible combinations for coincidence of the Lines of Response (LOR) passing through the patient's body even if no photon hit the detector elements at the extremity of the LOR). Although current PETs have made a compromise in coincidence detection efficiency versus circuit complexity, by using a coarse segmentation of the detector in order to reduce the number of LOR to be tested for coincidence, that approach is however an impediment to increasing the FOV (See more details in Section 14.7.2 of [1] and Section 6.3 of [26]). This approach adds unnecessary complexity to the electronics of the current PET and makes it unreasonably costly to build a circuit with an acceptable efficiency when more detector elements are added to the detector (which is required in extending the FOV);
   h) saturation of the electronics at the output stage due to the limiting architecture of the coincidence detection circuit (See Section 14.7.2.4 of [1]);
   i) a high number of "Randoms" due to the non accurate measurement of the photon arrival time and to the long (about 12 ns) time window used when determining if two photons belong to the same event;
   j) poor measurement of the attenuation of different tissues at different locations in a patient's body. These measurements are necessary for calculating the attenuation correction coefficients for PET scans;
2. The false positives and false negatives shown in images from current PET, are a consequence of all of the above not having: (a) a DSP on each electronic channel, with neighboring signal correlation capabilities, which extracts with zero dead time, the full characteristics of the incident photon and improves the S/N ratio of each signal before adding it to other signals, (b) good attenuation correction coefficients, (c) a good, efficient, and simple coincidence detection circuit, and (d) a sufficiently long FOV (short FOV prevents capturing most photons as shown on the left side of Figure 1 and Figure 16) that are the impediments in obtaining good quality images;
3. The high radiation dose delivered to the patient is required by the current PET because each examination needs to capture the amount of photons which provide a sufficient statistic to yield a good image. The short FOV and the inefficient electronics allows accumulation of fewer than 2 photons in coincidence for every 10,000 emitted. This inefficiency requires one to administer a necessarily high radiation dosage to the patient in order to keep the examination time within an hour.
4. The slow scanning time is caused by the short FOV of the current PET and the low efficiency of the electronics. The limited efficiency mentioned above of 2 out of 10,000 requires a long acquisition time. Examinations longer than one hour are unacceptable because (a) the biological process desired to be observe and the radioisotope decay activity would be over, (b) the patient would be

[54] Randoms are photons in time coincidence belonging to two different events.

uncomfortable, and (c) the cost would be even higher that what it already is.

5. The current high cost of the examination is due to:
   a) the high cost of the huge dose of radioisotope required;
   b) the slow scanning time that allows only six to seven patients per day to be examined; and
   c) the cost of highly paid personnel who must operate the slow machine.

Appendix C.2. Distinctive innovative features of the 3D-CBS

The technological innovations of the 3D-CBS design are the following:

1. ***Accurate time determination of the arrival of the incident photon to the detector and a "time-stamp" assignment to the detected photon (500 ps resolution).*** The front-end circuit of the 3D-CBS accurately determines the photon arrival time, by means of a Constant Fraction Discriminator (CFD) and a Time-to-Digital converter (TDC). This arrival time is further improved with the DSP real-time algorithm which assigns the time-stamp to each event. (See also Sections 13.4.4 and 13.4.10 of [1])

2. ***Digital processing of the front-end electronics versus analog processing.*** (See Figure 33). With the advent of fast analog-to-digital converters and new processors oriented toward digital signal processing (DSP), there arose the tendency to treat analog signals in digital form, thus using discrete algorithms instead of analog functions [63]. The advantages of the digital versus analog processing are principally perfect stability (no drift due to temperature or aging), repeatability (not dependent on component tolerance) easy design (programming an algorithm), lower cost of programming the same devices for different functions, absence of the need for component calibration while system calibration can be performed easily by reading parameters acquired during a calibration procedure, accuracy limited only by converter resolutions and processor arithmetic precision, low power consumption, testability, and high circuit density. **In contrast, upper speed limits of DSP using the standard DSP architecture are inferior to those of analog processing. This is the reason why many applications are still using analog processing.** The manufacturers of current PET are among those still using analog processing as is described in detail in Section 14.7.1.1 of [1], or as can be found directly from the manufacturers documentation in [33]. However, this barrier has been overcome with the 3D-Flow sequentially-implemented parallel architecture described in Section 4. With the 3D-Flow architecture using a clock of only 80 MHz (or at a speed that can be implemented with a low cost CMOS technology), it is now possible to have all the DSP advantages listed above in addition to special instructions for particle identification, while sustaining a high data input rate.

3. ***Elimination of the saturation at the input stage for any detector type and speed and for any simple or complex real-time algorithm***. The implementation that satisfies the requirements of eliminating saturation at the input stage is the use, for each electronic channel, of a number of cascaded 3D-Flow processors as shown in Figure 10 which are proportional to the processor speed, the number of steps of the algorithm to be executed, and the data input rate. For example: sampling a PET detector at 20 MHz (see details in reference [4], and Section 13.4.3 of [1]) with a 3D-Flow processor running at 80 MHz that requires the execution of a real-time algorithm of less than 20 steps, needs a 3D-Flow system of 5 layers[55]. Although the entire PET electronic system can receive a data packet every 50 ns, each layer can execute an algorithm lasting up to 20 x 12.5 ns = 250 ns, thus each layer takes one data packet from the detector and skips 4 sets of data packets that will be forwarded to the other processors, **via the bypass switches**, (or multiplexers) that are located in the other four layers (see Figure 10). If the sampling rate of the detector increases or if the algorithm becomes more complex, one or more layers of 3D-Flow processors are added in order to reach a situation where the system will never saturate.

4. ***The implementation of a new concept where all signals within a defined view angle of the detector from the emitting source at the center of the detector are processed and correlated digitally***. A programmable algorithm (see next section and references [1], [4], [26]) is executed in real-time on all signals received from a defined view angle, together with the signals of the neighboring detector elements in order to extract, directly from the raw data, all information of the interaction between the photon and the detector (see Appendix C.6 and Figure 34). In current PET, the approach is to extract from a few signals one type of information, from other sets of signals other information, and so on. The next level of their electronics combines the results of the first level of the processing of partial data. The reason for using this approach, which provides less accuracy in the calculation of the parameters characterizing the incident photons, is because **the electronics of current PET can only handle a few operations on a few data at a high rate.** The 3D-Flow architecture, on the other hand, can handle more data, perform complex real-time algorithms on them while receiving them at a high data input rate because of the sequentially-implemented parallel architecture described in the next section. The combination of the raw data received from the detector within a defined view angle is performed in a FPGA circuit (from PMT, photodiodes, time-to-digital converter, etc.) [25]. These data are then sent to the 3D-Flow processor in a formatted 32- or 64-bit word (See reference [4], and Section 13.4.3 of [1]).

[55] A layer is an array of 3D-Flow processors (e.g., it can be the same number of processors as the number of channels of the PET/CT detector), where each processor is interconnected to its four neighbors through North, East, West and South ports. Several layers make a 3D-Flow stack.

5. ***The 3D-Flow sequentially-implemented parallel architecture (see*** Table III ***and*** Figure 10***) allows execution of complex, programmable real-time algorithms*** which include correlation with neighboring signals, and fully reconstruct the energy, extract the information of the type of interaction between the photons and the crystal, improves the signal–to-noise ratio, measures accurately the depth of interaction, resolves photon pileup, and capture most of them (See example of the real-time algorithm for photon identification on Appendix C.6 and Figure 34 of this document and Sections 13.4.11.2, and 13.4.11.3 of [1]). **Thus this architecture improves image quality, and leads to lower radiation dosage and to shorter scanning time.** The concept of the 3D-Flow architecture is described in simple terms in [64], while a more complete description of the concepts, implementation and application can be found in [1], [2], [3], [4], [24], [25], [26], and [27]. **One of the differences is that in the standard pipeline a data packet moves, at each clock, from one stage to the next, while in the 3D-Flow system a data packet remains in the same stage for several clocks, until the entire algorithm is completed**. The basic 3D-Flow component has been implemented in a technology-independent form and has been synthesized in 0.5 μm, 0.35 μm technology, and in FPGA's Xilinx, Altera and ORCA (Lucent Technologies). (See Appendix B.5). Among the features of the 3D-Flow architecture, the following are listed as pertinent advantages which suit this project:
   - Eliminates saturation on the input data, no deadtime, no bandwidth limitation (see Appendix C.1 item 1.e and Appendix C.2 item 3)
   - Allows execution of programmable, simple or complex real-time algorithms with an execution time of an uninterruptable sequence of operations which is longer than the time interval between two consecutive input data. The same 3D-Flow system can be used for different crystal detectors (slow and fast) and can be adapted for an optimal extraction of the information of the interaction of the incident photon with the crystal detector by simply loading a different real-time pattern recognition algorithm in the 3D-Flow program memory (see Appendix C.6 and Figure 34).
   - Eliminates the boundaries by using a convenient way to communicate with the neighbors (3x3, 4x4, 5x5, etc.) through North East, West, and South ports.
   - The balance of the operations of the 3D-Flow processor between moving and computing data (see Appendix B.5), allows for the execution of all typical DSP filtering techniques, for signal-to-noise ratio improvement and algorithms for photon identification: all essential to improving PET efficiency. Among the operations performed are also those of digital signal-processing operations on the incoming bit string such as: (a) variable digital integration time, pile-up identification/correction, which allows for maximum count rate capabilities while preserving spatial resolution; (b) depth of interaction, which reduces the parallax error by performing calculations based on pulse shape discrimination (PSD), and/or pulse height discrimination (PHD); (c) local maxima, to avoid double counting, (d) centroid calculations to improve spatial resolution and/or techniques of the most likely position given the statistical nature of the signals; (e) correlation with neighboring signals; and (f) improving the timing resolution from the information received from the time-to-digital converter (TDC) and the pulse shape analysis.
6. ***A simplified coincidence detection circuit***. In the new design described in [1], only the detector elements (coupled to a PMT or APD), that are hit by a photon which has been validated by a thorough real-time, front-end pattern recognition algorithm, are then checked for coincidence. **This method is much simpler than the one used in the current PET, which compares all of the possible LOR** (see references [34], [32] or Section 14.7.2.1 of [1] for more details). The number of comparisons for finding the coincidences in the 3D-CBS is proportional to the radiation activity and not to the number of detector elements in the current PET (e.g., for about 80 million hits per second into the detector, corresponding to a limit of the radiation dose to the patient, only 120 million comparisons per second are necessary. See Section 4.2 of this document and Section 13.4.14 of [1] for the implementation of the coincidence circuit with the 3D-Flow and the flow chart of the programs). In the new design, the coincidence detection problem is solved with a simple electronic circuit that funnels all hits detected to a single electronic channel, sorts the events in the original sequence, as shown in Figure 13-22 of [1], and compares all hits within a given time interval, for validation of time-stamp and location situated along an LOR passing through the patient's body.
7. ***Elimination of the saturation at the output***. The elimination of the saturation at the output stage is easily achievable by implementing a circuit that performs the number of comparisons corresponding to the highest radiation activity that a detector should ever receive. Assuming at most four hits at the detector during one sampling of 50 ns, (corresponding to a rate of 80 million single photons per second hitting the detectors), then because we can have at most 6 comparisons out of four data, the total number of comparison to avoid saturation will be 120 x 10^6 comparisons per second. (See section 13.4.14 of [1] for more details).
8. ***The new electronic design now makes the extension of the PET FOV cost-effective***. One of the most important benefits of the use of the innovations set forth in this document is that of efficiently capturing more photons. This moves beyond the point where the current PET manufacturers erroneously thought that **the benefits of capturing more photons and decreasing the examination time could not offset the significant increases in the costs associated with PETs with a longer FOV.** In addition, these innovations permit a reduction of the radiation dose to the patient permitting

annual examinations on asymptomatic people. The use of the 3D-Flow architecture described in Section 4.1 and the funneling circuit of the coincidence detection section described previously, allows one to extend the FOV of the PET to any length and to any number of detector elements.

9. ***The incorporation of the Electron Beam Computed Tomograph (EBCT) and Positron Emission Tomograph (PET) into a single apparatus with a single detector,*** eliminating completely the motion artifact in the image, is facilitated by the use of the 3D-Flow DSP that can efficiently execute the calculations for identifying and separating from the same crystal detector the two types of incident photons (CT X-rays and PET γ rays).
10. ***The accurate measurement of the attenuation during a CT x-ray transmission*** scanning will be used to calculate a more accurate attenuation correction coefficient for the PET examination.

Furthermore, the 3D-CBS incorporates innovations in the following other fields: hardware, software, cabling, system architecture, component architecture, detector element layout, data acquisition and processing, and detection of coincidences.

Appendix C.3. Limitations of current PET remedied by 3D-CBS

In order to reconstruct an image of the metabolism of the cells of the patient's body, it is necessary to capture the amount of photons in coincidence which provide a sufficient statistic to yield a good image. If the electronics is not rigorous in selecting the "good[24]" photons, the image quality will be poor and the machine will require additional scanning time. This presents the disadvantages that (a) a particular biological process might be finished by the time the scan has accumulated the necessary amount of photons; and (b) the "bad" photons acquired along with the "good" ones cannot be subtracted during off-line filtering algorithms without subtracting many good photons along with them.

The current PET imaging machines do not thoroughly analyze in real-time the data received from the detector which contains the information of the characteristics of the interaction between the incident photon and the crystal. The result is that many "good[24]" photons are missed and photons are captured that later in the process must be disregarded as "bad" photons. This fails to provide a clear image to help the physician recognize subtle differences in normal anatomies. The innovations set forth in this document have remedied the above in the following manner:

The remedies offered by the 3D-CBS to the above deficiencies

1. The image quality of current PET is improved with the following (see the same items listed as a problem in Appendix C.1):
   a) ***a FOV longer than one meter***, covering almost the entire size of the patient's body. The simpler, lower cost, more efficient electronics described in this article and in references [1], [2], [3], [4], [24], [25], [26], [27] allows for the capturing more "good" photons providing the benefit of improving the image quality, decreasing the radiation dose to the patient and shortening the examination time which compensates for higher cost of the detector of a PET with a longer FOV;
   b) ***accurate photon arrival time determination*** and assignment to the input data packet using the circuit described in Appendix C.2, item 1, Section (b) of Figure 33, of this document and in Sections 13.4.4 and 13.4.10 of [1]. The determination of the accurate arrival time of the photon at the detector allows for better identify of "good" events by the coincidence detection circuit;
   c) ***digital signal processing on the front-end electronics at each electronic channel with neighboring signal correlation*** as described in Appendix C.2, item 2 of this document and in reference [2]. Using digital signal processing techniques, one can most efficiently extract the characteristics of the interaction between the incident photon and the crystal detector and improve the signal-to-noise ratio on each signal before adding them with other signals (see Figure 34);
   d) ***elimination of detector boundaries by means of the North, East, West, and South communication ports*** of the 3D-Flow architecture as described in Appendix C.2, item 5, Appendix B.5 of this article and in Section 13.4.8 of [1]. The possibility of exchanging the information, to/from neighboring detectors, in real-time during acquisition, allows for the complete reconstruction of the energy of the emitted photon, which permits a better selection and classification of them;
   e) ***elimination of dead-time in the electronics***. The analysis of bottlenecks in the electronics of current PET and the design of a dead-time free system with the 3D-Flow architecture is described in detail in Section 13 and 14 of [1];
   f) ***elimination of the saturation of the electronics at the input stage***. The bypass switches of the 3D-Flow architecture (see Table III and references [2], [4]) allow the electronics of the 3D-CBS to sustain, with zero dead time, a data input rate of 20 million events per second in each channel. (This is equivalent to a total system input bandwidth for 1,792 channels of about 35 billion events per second compared to the 10 million events per second offered by the current PET.) This capability **eliminates electronic saturation when any type of (fast or slow) detector is used.** Electronics saturation, which is a cause of inefficiency of the current PET, should not be confused with detector saturation of the slow crystals. For example, considering a BGO crystal with a decay time of about 300 ns and an over all recovery time of about 700 ns, one could conservatively consider that the crystal will saturate at about 1 MHz. Because detectors are made of many crystals cut in 2 mm x 2 mm, or 4 mm x 4 mm, only a small portion where the photon hits the detector and a few surrounding detector elements, could be affected by crystal saturation if another photon should arrive during

the same time interval of 1 μsec. However, the 3D-CBS electronics has the capability of detecting any other photon arriving in any other part of the detector during the same time, up to one every 50 ns (in order to cope with fast crystals) at the same location, with a time difference resolution between two different detected photons of 500 ps. (The 500 ps resolution of the electronics which is provided by the resolution of the Time-to-Digital converter, in some cases may be higher than the time resolution of slow crystals. See Section 13.4.10 of [1]);

g) ***a simplified coincidence detection circuit whose complexity depends on the total radiation activity (which is limited by the maximum radiation to the patient) and is independent from the number of detector elements*** (see Appendix C.2, item 6) captures more photons in coincidence more efficiently at a lower cost, improves image quality, allows lower radiation dosage, and leads to shorter scanning time. The coincidence circuit of the 3D-CBS is comparing only the signals of the detector elements that received a photon instead of comparing signals from all possible connections (LOR) of detector elements with an LOR passing through the patient's body, as is implemented in current PET [34];

h) ***elimination of the saturation at the output***. Using the 3D-Flow coincidence detection approach, the elimination of the saturation at the output stage is relatively simple because after having set the maximum radiation dose that will ever hit the detector, it is sufficient to implement the circuit(s) that performs the number of comparisons necessary to detect the maximum number of expected photons in coincidence (See Appendix C.2, item 7 of this document and Section 14.7.2.4 of [1]). This number will always be lower and simpler than the coincidence detection circuit used in the current PET, which performs about 3 billion comparisons per second in seven ASICs [34]. This circuit would be simpler because 3 billion comparisons per second corresponds to an isotope dose to the patient higher than 100 mCi, which will not be administered because it is too dangerous for the patient;

i) ***reduction of the number of "randoms[54]"*** by means of the accurate determination of the arrival time of the incident photon hitting the detector. The accurate calculation (by means of a CFD, TDC and/or further improved with a DSP real-time algorithm. See Section (b) of Figure 33 of this article and Section 13.4.10 of [1]). The assignment of the time-stamp to each event allows for the use of a shorter time interval between two detected photons when determining if they belong to the same event. Reducing randoms improves image quality, lowers radiation dosage and shortens scanning time;

j) ***a very accurate calculation of the attenuation correction coefficients*** is needed for PET image enhancement, using the information acquired during CT transmission scan. (See Section III of [2]);

2. Reduction of false positives and false negatives because of the improvements described above and in Section 8.1 in capturing more "good" photons and eliminating the "bad" photons at the front-end electronics during real-time processing. The main reasons that will allow for acquiring better images, which will allow the physician to recognize subtle differences in normal anatomies are: (a) the presence of a 3D-Flow DSP on each electronic channel, with neighboring signal correlation capabilities (see Figure 13 and Figure 14), which extract with zero dead time, the full characteristics of the incident photon and improves the S/N ratio on each signal before adding it to other signals, (b) good attenuation correction coefficients, (c) a good, efficient, and simple coincidence detection circuit (see Appendix C.2 item 6), and (d) having a sufficiently long FOV which allow for capturing most photons as shown in Figure 1 and Figure 16.

3. Reduction of the radiation dose delivered to the patient to a negligible level (1/30 the radiation administered during a current PET examination) that will permit annual screening and even several examination during the treatment of the disease with no hazard to the patient, allowing better monitoring. This is possible because the 3D-Flow sequentially-implemented parallel architecture described in Appendix C.2 item 5 of this document and in Section 13, 14 and 15 of [1] and in references [2], [3], [4] allows for the detection at a high data input rate, about 1,000 photons out of every 10,000 emitted, and capturing the amount of "good" photons in time coincidence in a shorter time which provides a sufficient statistic to yield a good image. Figure 16 shows the factors contributing to the increase in the delivery of a higher radiation dose to the patient when current PET are used.

4. The fast scanning time of the 3D-CBS is possible because of the long FOV of its detector and of the highly efficient electronics. The high efficiency mentioned before of 1,000 out of 10,000 photons reduces acquisition to a short time. This permits examinations to be performed in 15 to 20 minutes with 3 to 4 minutes of scan time (a) facilitating the capture of a specific biological process one desires to observe, (b) without making the patient uncomfortable, and (c) at a cost that would be greatly reduced from the current one;

5. The factors that will reduce the cost are:

   a) the lower cost of the negligible dose of radioisotope required;

   b) the fast scanning time that allows for the examination of about 40 patients per day; and

   c) the cost of highly paid personnel who can now perform a larger number of examinations per day instead of only 6 to 7 patients/day when using a slow machine.

Figure 3 shows how the 3D-CBS can acquire photons in coincidence per examination in a shorter time compared to the current PET. Thus one can scan more patients per hour, which it lowers the examination cost.

List of the innovations which provide additional improvements to medical imaging technology

1. ***A single detector assembly for PET and CT, covering most of the patient's body (current PET/CT use two detectors, one for each modality with a moving table on which the patient goes sequentially through both).*** In addition to completely eliminating picture blurring, this feature improves the imaging capabilities allowing the superimposition of anatomical pictures with functional imaging. It also provides very accurate attenuation correction coefficients, and utilizes the synergy of the other innovations to decrease the cost per examination.
2. ***The use of a detector shape as close as possible to the size and shape of the human body*** (e.g. elliptical for the torso and a detector ring with a smaller diameter for the head), saves costs in the detector and improves photon detection capabilities which have to travel a shorter distance from the body to the detector, thus randoms can be reduced because a shorter time interval between two photons hits can be set. The 3D-Flow DSP capabilities can perform a good DOI measurement providing higher resolution at a lower cost than what would have been achieved by using a detector with a wider diameter ring and no DOI measurements.

Appendix C.4. The unique assembly of the 3D-CBS, with no detector boundaries, compared to the current PET detector assembly

The assembly of the detector of current PET (see left side of Figure 31) can be compared to the assembly of many individual (2x2 PMT) cameras, each having a diminished sensitivity at the borders. The longer slits at the edges of the 2x2 PMT block provide relatively poor light collection, and therefore, poorer energy resolution.

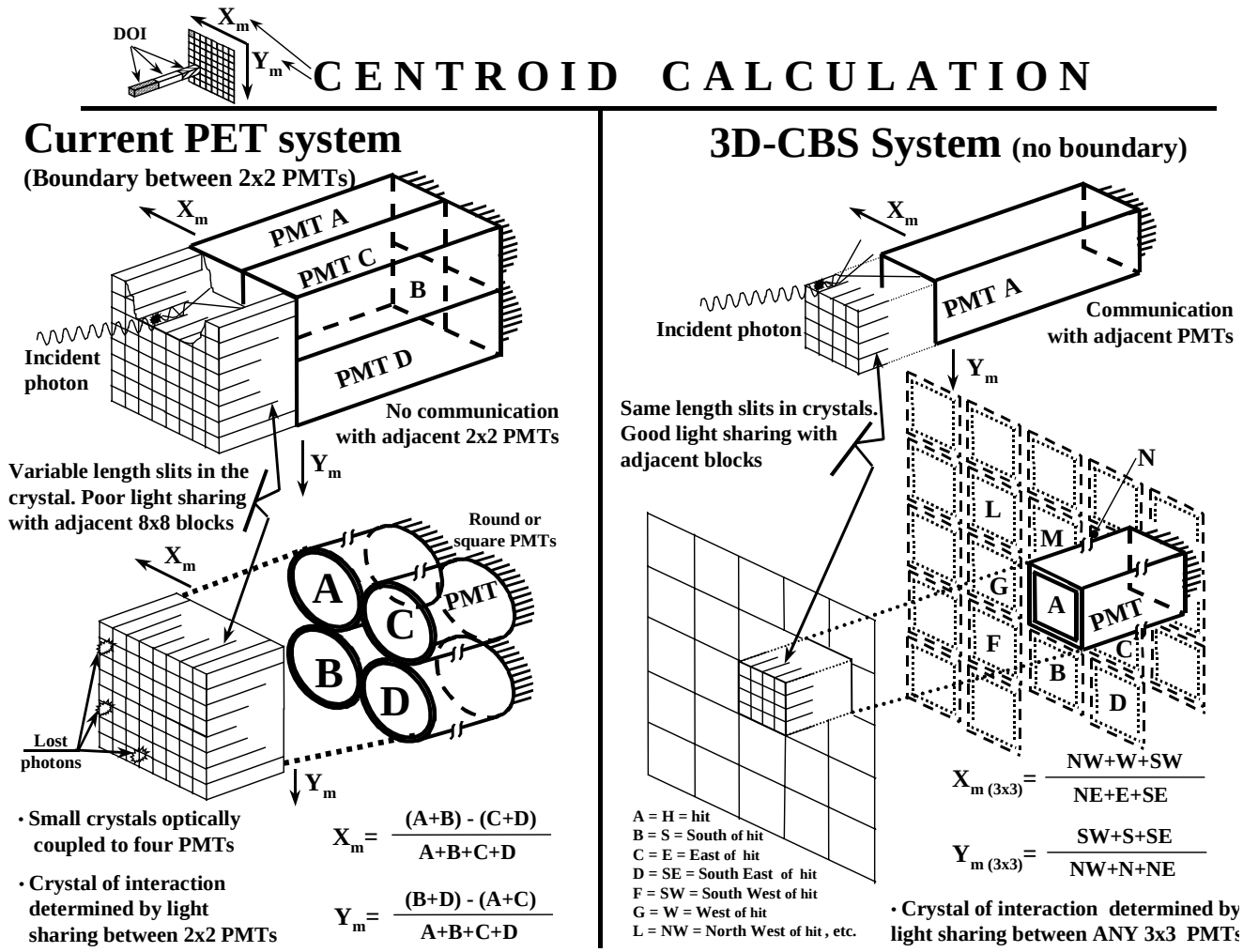

Figure 31. Comparison of the assembly of the 3D-CBS crystals coupled to the PMT (or APD) sensors allowing centroid calculation with no detector boundary limitation vs. the detector assembly of current PET which has a 2x2 PMTs (or module) detector boundary limitation. The block detector of current PET (figure at left) consists of four 4 PMT tubes coupled to a set of crystals (64 in the example of the figure). The variable lengths of the slits (made of reflecting material) in the crystal act like a light guide that allows more or less light sharing between the four PMTs. The long slits of reflecting material at the edges of the 8x8 crystal block allow minimal or no light sharing between adjacent 8x8 crystal blocks (or 2x2 PMT blocks). The identification of the crystal of interaction in the 2x2 PMT block is made through the Anger logic shown at the bottom right of the figure. The crystals at the edges and corners of the 8x8 crystal block contributes a smaller signal compared to the inner crystals, making their identification more difficult (see

measurements on Figure 3 of [65]). The 3D-CBS assembly (figure at right) solves these problems by permitting all crystals to have the same degree of light sharing with adjacent crystals with slits of equal length. This allows for sharing the light with adjacent PMTs in the four directions with no boundaries. The interconnections in the North, East, West, and South directions of the electronic channels of the 3D-Flow system allow any PMT receiving the highest signal to be identified as the center of a 3x3 (or a 5x5) cluster which then rebuilds the total energy of the incident photon by summing all the adjacent signals and by calculating the centroid as show at the bottom of the figure (figure at right).

The disadvantages of the 2x2 PMT block detector assembly are well known and are reported in several articles (e.g., in [66], the following is stated: "…edge crystals have relatively poor light collection, and therefore, poorer energy resolution, while the central crystals are more likely to accept events that have undergone inter-detector scatter, which yields higher sensitivity but poorer spatial resolution …. the modifications of the LUT's were designed to trade resolution for sensitivity and vice versa with the goal of achieving uniform resolution and uniform sensitivity within individual detector modules and an improved signal-to-noise ratio in the final image…" In another article [65], this statement appears: "…there are also some disadvantages to the block design such as poorer count-rate performance and pile-up…"). The designers who have been trying to solve the limitation of the detector block design with boundaries and short and long slits by making compromises between sensitivity and resolution will find the 3D-Flow architecture design useful, because it effectively eliminates the detector boundaries and allows any group of crystals coupled to a PMT to share the light with all adjacent PMTs.

The 3D-CBS detector assembly with short slits of reflecting material of equal length between the crystals (over the entire detector array as shown on the right side of Figure 31) allows light sharing between PMTs and improves the detection uniformity over the entire detector eliminating boundaries between 2x2 PMTs (or between modules when no slits are used).

The 3D-CBS implemented with the 3D-Flow system, has a geometry of the PET/CT sensors mapped to the 3D-Flow processor array in a manner that allows for the exchange of information among the adjacent PET/CT sensors through short signal delays. Every 50 ns all signals from the entire detector array of 1,792 channels are sent to the first array of 1,792 3D-Flow processors connected to the detector. To assure the processing of a complex algorithm such as the example of Figure 34, a set of 3D-Flow DSP processors are used at each of the 1,792 channels as shown in Figure 9, or Figure 10 in order to handle data arriving at the input of the system with a time interval shorter than the time required to execute the real-time algorithm. This arrangement and the processing in parallel of the 1,792 signals using the 3D-Flow architecture provides the advantage of (a) zero dead-time due to electronics, (b) a detector dead-time of only 1/1792 of the entire detector size for the light-pulse duration of the crystal, and (c) the advantage of also detecting hits occurring within a short distance (2 to 4 cm, depending on the size of the PMT used) between detector elements.

The authors of [67] will find in the 3D-Flow architecture a solution to the problems encountered in trying to achieve "…high sensitivity, high and uniform spatial resolution across the field-of-view…". The detector described in [67] and shown in Figure 32 makes use of large modules with only nine analog signals, which cannot separate the information of events occurring at the same time. The same article also states that "…recent theoretical studies have suggested that the sensitivity of small-animal PET scanners should be very high if tracer-specific activity problems are to be avoided in animals whose body masses are hundreds to thousands of times smaller than human subjects…" The 3D-Flow architecture of the 3D-CBS with a set of DSP processors on each channel allows maximum sensitivity which can solve this problem.

Conversely, the electronics of current PET which does not have a DSP (or a set of DPSs) on each individual channel, and which performs the summation of several signals in analog (such as in the case of four signals relative to 64 crystals as shown in the left side of Figure 31, or several signals relative to a group of 486 crystals as shown in Figure 32), has the limitation of (a) dead-time of the electronics, (b) detector dead-time of 1/6 the entire detector size for the light-pulse duration of the crystal (in the case of Figure 32), (c) the loss of hits occurring within a short distance, and (d) the loss of hits occurring at the edges and corners of a 2x2 PMT block (or module).

Figure 32 shows the limitation in efficiency when larger detector blocks are used and signals are added to form a few analog signals that contain the information of several crystals (486 in the example) as reported in reference [67].

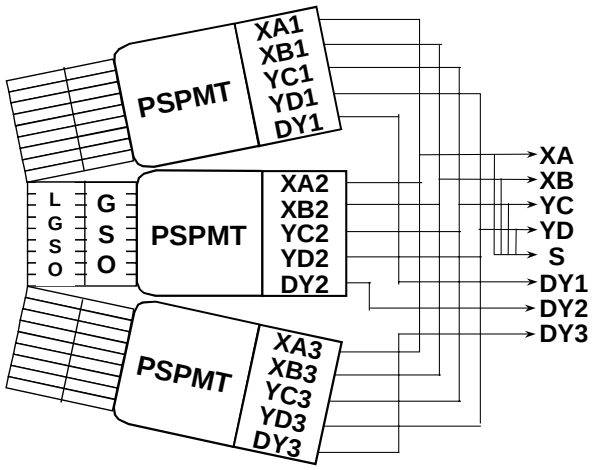

Figure 32. Inefficiency of a large detector block without a DSP on each channel. Example of the assembly of three modules of a sector of a six-sector small-animal detector [67]. The detector in the example consists of an array of crystals coupled to a position-sensitive PMT (PSPMT). The eight X and Y anode signals of each of the three PSPMTs are combined into four position signals, XA, XB, YC, and YD. Three additional signals, DY1, DY2, and DY3, identify the PMT of interaction. Although only eight signals are used to locate the interaction between the photon and the crystal, this approch introduces several limitations such as electronics dead-time, large detector dead-time (1/6 of the entire detector for the light pulse duration of the crystal compared to 1/1792 of the 3D-CBS), boundary limitations, the

impossibility of improving the signal-to-noise ratio on each signal before their summation and the impossibility of separating the analog signal (which is the sum of several signals) for better processing of an event occurring in a specific Region of Interest (ROI), etc. All the above limitations would be solved with the use of an architecture such as the 3D-Flow with a set of DSPs on each channel (before their analogue summation) and the possibity of correlating signals between neighboring channels.

Appendix C.5. Front-end electronics (FE) of the 3D-Flow system compared to FE of current PET devices

The characteristics of the interaction between the photons and the crystal can be extracted from (a) the shape of the signal generated by the transducer (photomultiplier, APD, or photodiode, etc.); (b) the area contained below the curve of the signal (which is proportional to the energy of the incident photon); (c) the correlation of each signal with its eight (or twenty-four) neighbors in all four directions; and (d) the signal timing information telling when the event occurred.

The approach used in the electronics of the current PET of adding to each signal three neighboring signals from only one direction (see Figure 33a), prevents the characteristics[56] of the interaction between the photons and crystals from being fully and accurately extracted. The shape of the resulting sum of the four signals has lost the information of each individual signal, and from that point on it will be impossible to separate the sum of four signals back into the four individual signals. Furthermore, in the current PET, the sum of those four signals are not correlated with their neighboring sum of four.

Figure 33b displays a schematic of the Digital Signal Processing of the 3D-Flow system with digital signal integration functionality as opposed to the analog signal processing implemented in the current PET systems in Figure 33a.

The specific circuit shown in Figure 33a (see also left side of Figure 31) is used in several models of PET devices manufactured by CTI/Siemens [33]. Although it has the merit of remote control of eight parameters to fine-tune each channel (the gain of the four preamplifiers, the constant fraction discriminator threshold, the x and y offset, and the time alignment of the system clock), those variables still place a limit on the processing of the analog signal when compared to the flexibility of digital signal processing.

In the same circuit used in the current PET, the signals received from four photomultipliers (PMTs) are then combined and integrated over a period of the order of 1 μs to form an energy signal and two position signals (axial and transaxial).

Any attempt at processing the above signals and extracting information on one channel fails, because the signals carry the information of four PMT channels and cannot be reconstituted as the original four PMT signals for further enhancement of energy, spatial resolution, or timing resolution and combinations with other signals. The attempts made in the current PET, with its mix of look-up tables and analog processing to decode the position and energy information absorbed, by the crystal that was hit [33], will never achieve good performance, because the neighboring information to the four PMTs (2x2 array) is missing.

The sum of four analog signals used in current PET may be critical because it adds in the noise as well, while the 3D-Flow converts the ADC counts of each individual channel through the internal look-up tables and subtracts the noise of each channel individually by means of its DSP functionality, before summing them.

Using a look-up table immediately after receiving data from each channel (instead of receiving data from each group of four as it is shown in Figure 33a), the new proposal of Figure 33b provides the possibility of including all specific corrections for each channel (gain, non-linear response of the channel, pedestal subtraction, etc.).

The 3D-Flow can extract much more information (area, decay time, etc.) from the signal received by performing digital signal processing on the last four or five signals received from the direct PMT channel and from the three, eight, fifteen, or twentyfour signals from the neighboring PMTs via the North, East, West and South ports of the 3D-Flow.

The tuning of each channel with a digital look-up table is also convenient because the calibrating parameters can be generated automatically from calibration measurements.

Appendix C.6. Photon identification: The PET/CT real-time algorithm for extracting the characteristics of the interaction between the photon and the detector using the 3D-Flow system.

The real-time algorithm for extracting the characteristics of the interaction between the photon and the detector consist of a sequence of the order of ten to twenty instructions executed by each 3D-Flow processor in the system.

The real-time algorithm can be created and simulated by the 3D-Flow design real-time tools (see Appendix B).

The entire 3D-Flow system is a single array with no boundary limitations (see right side of Figure 31). The neighboring sensors in the PET/CT detector array are reflected with an identical neighboring scheme in the 3D-Flow, processor array. Each channel (defined as all signals, from all subdetectors within a given view angle) in the 3D-Flow processor array, sends its information to, and receives their information from, its neighbors. This is equivalent to the exchange of information among adjacent channels (or sensors) in the 3D-CBS detector array. The practical implementation of the data exchange between neighbors is shown in detail in Figure 15-7 of [1].

[56] If the properties of the particles are not fully extracted, the photons of the "good" events cannot be recognized with respect to the "bad" events. Consequently, the numerous bad events (noise) that were not subtracted at the very front-end electronics and that could not be subtracted with filtering algorithms at the back-end (unless several good events are subtracted along with them), will fail to provide a clear image necessary to assist the physician in recognizing subtle differences in normal anatomies (misleading "false positive" and "false negative" readings, which is attributing cancer when is not present and missing cancer when is present).

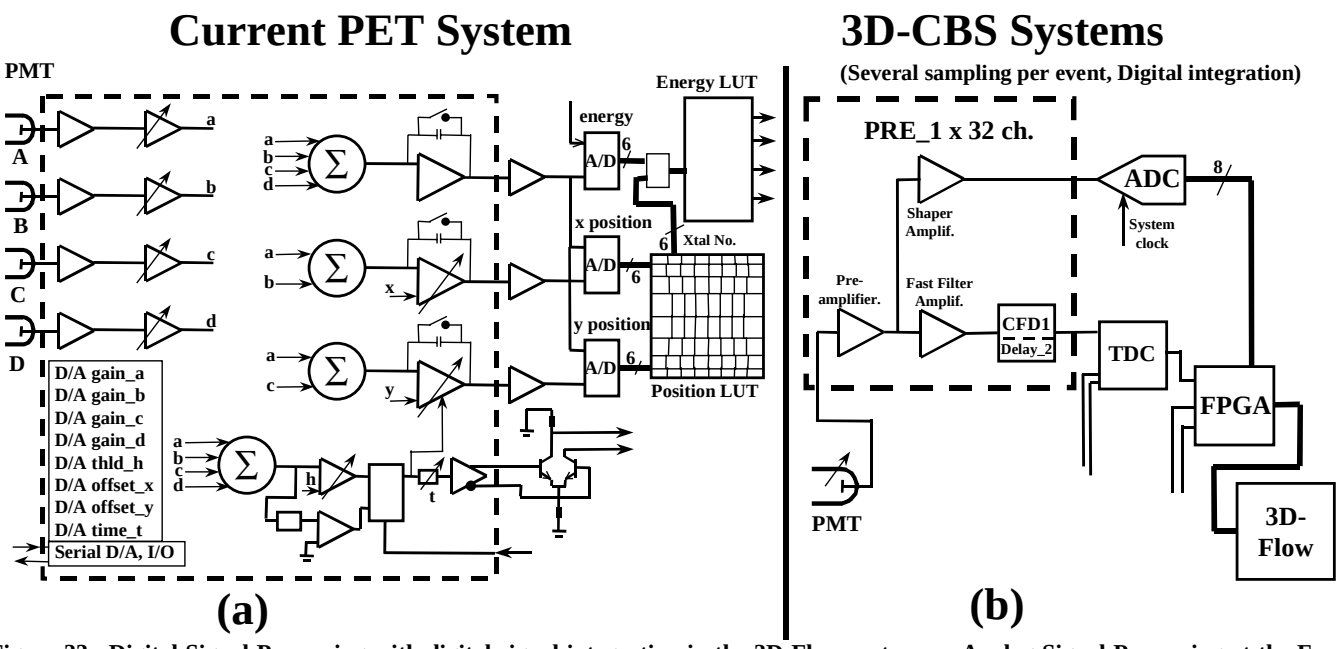

Figure 33. Digital Signal Processing with digital signal integration in the 3D-Flow system vs. Analog Signal Processing at the Front-End electronics for PET.

Once all data from each channel and its neighbors are moved into a single processing element, any pattern recognition-algorithm, and/or signal-to-noise filtering algorithm, well known in the literature, can be applied by using the DSP functions of the 3D-Flow processor. This is achieved with instructions of arithmetic and logic operation including multiply-accumulate and divide

These operations are accomplished in parallel on each electronic channel. In the example of the application of Section XII of [2], for instance, each of the 1,792 processors of one layer[55] of the 3D-Flow stack[57] executes in parallel the real-real time algorithm, from beginning to end, on data received from the PET detector, while processors at different layers of the 3D-Flow stack operate from beginning to end on different sets of data –or events— received from the PET detector.

The centroid calculation when the 3D-Flow is used is straightforward after having gathered the information form 3, 8, 15, or 24 neighbors in a single processor, as shown in Figure 34 for a 3x3 centroid calculation and in Section 13.4.11.3 of [1] for a 5x5 centroid calculation.

One example of a more accurate centroid calculation compared to the 2x2 PMT example of current PET is the one shown on the right side of Figure 31. The calculation of Δ_x is the ratio of the sum of the energies of all sensors west of the central element, divided by the sum of all sensors east of the central element ($\Delta_x = \Sigma E_W / \Sigma E_E$). Similarly for the calculation of Δ_y the ratio of the sum of the energies of all sensors north of the central element is divided by the sum of all sensors south of the central element ($\Delta_y = \Sigma E_S / \Sigma E_N$.).

The complete energy of the incident photon can be rebuilt by adding to the channel with the highest energy (head of a cluster which has been detected by the "local maxima" operation), with the energy values of the 3x3, or 4x4 surrounding channels. Alternatively, when larger areas of 5x5 or 6x6 are added, the complete energy of photons which went through crystal scatter can be rebuilt.

Increasing energy accuracy will improve spatial resolution, scatter rejection/acceptance, and attenuation correction.

Figure 34 shows an example of the execution on the 3D-Flow processor of a real-time algorithm which extracts the properties of the incident photon.

In the synchronous 3D-Flow system, every 50 ns, upon reception of the 64-bit word from the FPGA, all processors of one layer of the 3D-Flow stack execute the following steps in parallel (see Figure 34):

- Get data from detectors, convert ADC counts into energy value through Lookup Table.
- Fetch four signals from fast crystals, time of flight (TOF) TOF/decay time information, calculate DOI, or integrate signals from slow crystals, check for pileup and calculate DOI (by computing the signal decay time).
- Calculate attenuation; calculate Time Stamp.

[57] The system architecture consists of several processors arranged in two-orthogonal axes: One called layer is an array of 3D-Flow processors, where each processor is interconnected to its four neighbors through North, East, West and South ports. Several layers, assembled one adjacent to another to make a system is called "stack." The first layer is connected to the input sensors, while the last layer provides the results processed by all layers in the stack. Data and results flow through the stack from the sensors to the last layer. An electronic channel (see also Figure 9 and Figure 10) consist of one set of 3D-Flow processors connected from bottom port of one chip to the top port of an adjacent chip (with the top port of the first chip connected to the signal received from the detector and the bottom port of the last chip connected to the pyramid) see its hardware implementation on the top left of Figure 12, and more in details on Figure 5 and 6 of [2] and on Section 13 and 15 of [1].

- Send data to North, East, West and South neighbors. Increment Time stamp.
- Save first 3x3 data into Sum1, route 3x3 corner values.
- Get energies from four NEWS neighbors, add and save them for local maxima calculation.
- Get energies from four corner neighbors, add and save them for local maxima calculation.
- Compare 9 energy values for "Local Maxima" tests whether the energy of the central cell is larger than any of its neighbors. (This operation is executed in one CPU cycle). Compute the total energy sum of a 3x3 array by adding the partial sums, Sum1 and Sum2. Check for "photopeak" and "scatter." Calculate 3x3 "centroid" compute the energy asymmetries, for subsequent determination of the point of impact ($\Delta_x = E_W/E_E$ and $\Delta_y = E_S/E_N$.) Format output-word, or reject event.

At this stage of the real-time algorithm there is much information computed that allows conclusions to be drawn: whether the photon is a 60-120 keV (CT x-ray), or 511 keV (PET γ-ray), and if attenuation, DOI, timing, and spatial information are available. Any further operation can be executed upon 9 data (the one received from the detector and its 8 neighbors) by the CPU of the 3D-Flow processor, which can, in a single cycle, execute up to 26 operations of a standard computer.

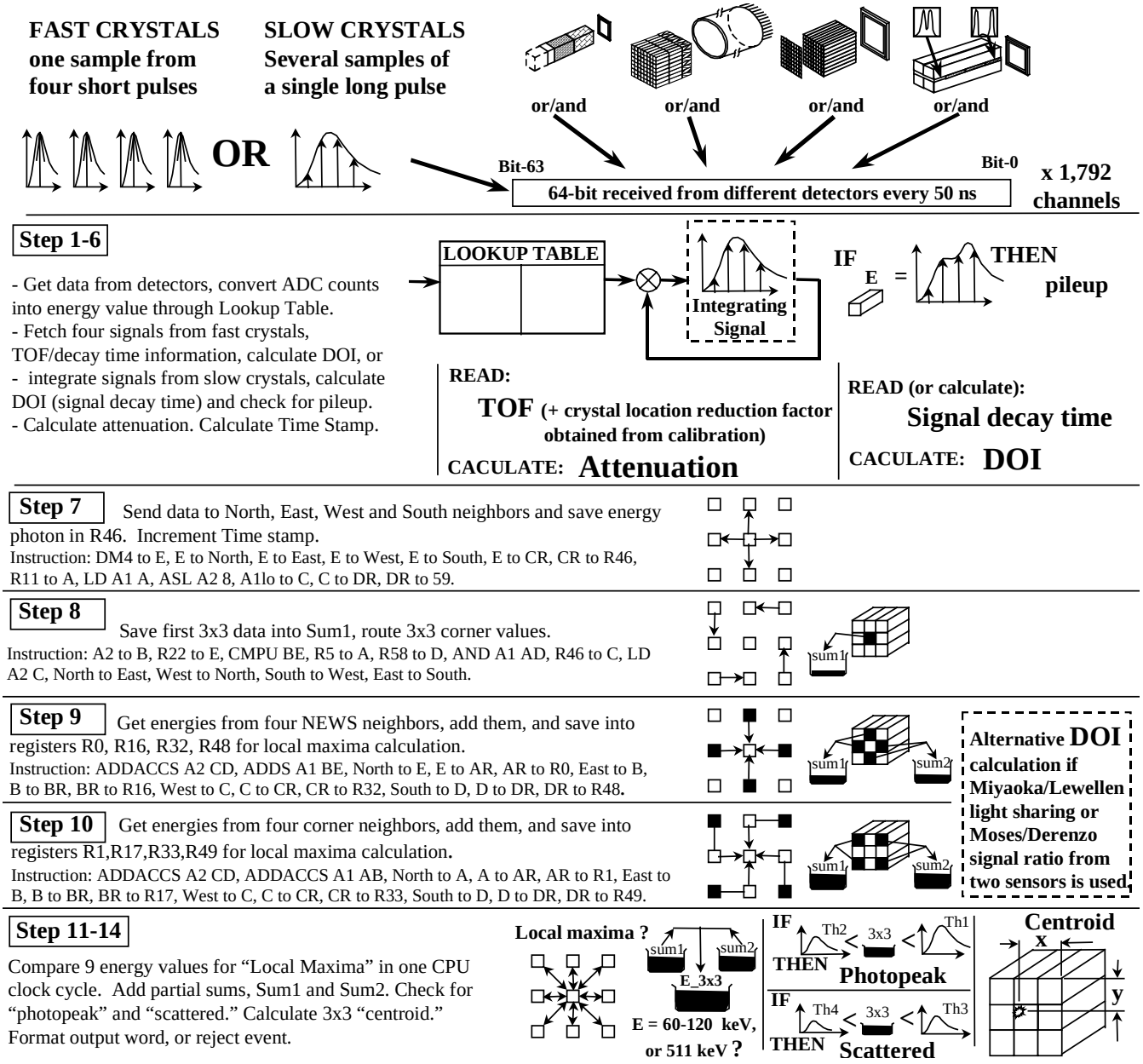

Figure 34. Simulation of the photon detection algorithm with the 3D-Flow for PET/CT.

Acronyms:

3-D Complete Body Scan (**3D-CBS**); Arithmetic Logic Unit (**ALU**); Avalanche Photo Diode (**APD**); Bismuth Germanium Orthosilicate (**BGO**); European Center for Nuclear Research (**CERN**); Constant Fraction Discriminator (**CFD**); Central Processing Unit (**CPU**); Cesium Iodide activated by

Thallium (**CsI(TI)**); Computed Tomography (**CT**); Depth of Interaction (**DOI**); Digital Rectal Examination (**DRE**); Digital Signal Processing (**DSP**); Electronic Design Automation (**EDA**); Food Drug Administration (**FDA**); Field Programmable Gate Array (**FPGA**); Fluorodeoxyglucose (**FDG**); First-In-First-Out (**FIFO**); Field Of View (**FOV**); Gallium Arsenic (**GaAs**); General Electric (**GE**); Gross Domestic Product (**GDP**); Health Care Financing Administration (**HCFA**); Health Maintenance Organization (**HMO**); Intellectual Property (**IP**); Line of Response (**LOR**); Lutetium orthosilicate (**LSO**); Multiply Accumulation Unit (**MAC**); Magnetic Resonance Imaging (**MRI**); Thallium-activated Sodium Iodide (**NaI(TI)**); National Center for Health Statistics (**NCHS**); National Cancer Institute (**NCI**); National Health care Expenditures (**NHE**); Positron Emission Tomography (**PET**); Printed Circuit Board (**PCB**); Pulse Height Discrimination (**PHD**); Prostate Specific Antigen (**PSA**); Pulse Shape Discriminator (**PSD**); Surveillance, Epidemiology, and End Results (**SEER**); System-On-a-Chip (**SOC**); Superconducting Super Collider (**SSC**); Time-to-Digital converter (**TDC**); United States (**U.S.**); Yttrium Orthosilicate (**YSO**).

Trademarks:

The following trademarks are the property of the following organizations:

ECAT, EXACT HR, ECAT, ACCEL, and Biograph are trademarks of CTI/Siemens.

GE Advance, Advance Nxi, Discovery LS are a trademark of General Electric Corporation.

CPET is a trademark of ADAC, a Philips Medical System Company

IBM PC is a trademark of International Business Machines Corporation.

Windows NT is a trademark of Microsoft Corporation.

About the author:

Dario Crosetto has collaborated for the past twenty years in extensive physics experiments at the European Center for Particle Physics (CERN) in Geneva and at the Superconducting Super Collider Laboratory (SSCL) in Texas, U.S. He has designed the critical part of the electronics (recognizing particles arriving at million events per second) for experiments costing up to half a billion dollars (see the Gammas Electrons and Muons Technical Design Report –GEM TDR- at www.3d-computing.com/pb/gem-tdr.pdf and [68], [69]). He was designated principal investigator of government grants, the largest of which was $750,000. He was responsible for the implementation of an Application Specific Integrated Circuit (ASIC) for a physics experiment (thousands of those ASICs are now in use). He has designed a DSP parallel processing system for the trigger of a physics experiment. This same design was implemented in VME and subsequently entered into the commercial market, where it was used by a German company in applications for quality control in lamination processes. He improved the electronics of PET and other applications for medical imaging devices during the past ten years.

18 REFERENCES

[1] Crosetto, D. “400+ times improved PET efficiency for lower-dose radiation, lower-cost cancer screening.” ISBN 0-9702897-0-7. Available at Amazon.com

[2] Crosetto, D.: A modular VME or IBM PC based data acquisition system for multi-modality PET/CT scanners of different sizes and detector types. Presented at the IEEE Nuclear Science Symposium and Medical Imaging Conference, Lyon, France, 2000, IEEE-2000-563, http://www.3d-computing.com/pb/ieee2000-563.pdf.

[3] Crosetto, D.: Real-time, programmable, digital signal-processing electronics for extracting the information from a detector module for multi-modality PET/SPECT/CT scanners. Presented at the IEEE Nuclear Science Symposium and Medical Imaging Conference, Lyon, France, 2000, IEEE-2000-567, submitted to IEEE, Trans. Nucl. Science. http://3d-computing.com/pb/ieee2000-567.pdf.

[4] Crosetto, D.: LHCb base-line level-0 trigger 3D-Flow implementation. Nuclear Instruments and Methods in Physics Research, Section A, vol. 436 (Nov. 1999) pp. 341-385

[5] Phelps, M.E., et al., The Changing of Positron Imaging System. Clinical Positron Imaging, vol. 1(1):31045, 1998

[6] Ordonnance sur la radioprotection (OraP) Le conseil federal suisse. 19 decembre 2000.

[7] Anderson I., Jansson, L.: Reduced breast cancer mortality in women under age 50: updated results from Malmo Mammographic Screening program. J. Nat. Cancer Inst. Monogr. (22):63-67, 1997.

[8] Kimiaei, S. and Larsson, S.A. Simultaneous SPECT and CT with an Opposed Dual Head Gamma Camera System and Conventional Parallel Hole Collimators. IEEE Trans. Nucl. Sci., vol. 43(4), pp. 2239-2243. August 1996.

[9] Parker, R.G.: The “Cost-Effectiveness” of Radiology and Radiologists. Radiology, November 1993, vol. 189(2):363-369.

[10] Moore, A.T., Dixon, A.K. et al. Cost benefit evaluation of body computed tomography. Health Trends, August 1997, vol19(3):8-12.

[11] Barnet, R.M. et al.: Review of particle physics. American Institute of Physics (AIP). Physical review D54, 1 (1996).

[12] Rollo, F.D.: It’s here, and it’s for real. Diagnostic Imaging. ISSN 0194-2514. January 2001, pp. 36-43 and 63.

[13] HCFA, National Health Accounts: Lessons from the U.S. Experience. Definitions, Source and Methods in the U.S. National Health Accounts. http://www.hcfa.gov/stats/nhe-oact/lessons/

[14] Friedman, K. Kulp, K. and Berryann, M. Business Watch. 1999 in review. The industry hits new heights at the close of the millennium. IMS Health, May 2000.

[15] U.S. Department of Commerce Economics and Statistics Administration, U.S. Census Bureau. Electromedical and Irradiation Equipment.

[16] Hefler, S. et al.: Health Spending Growth Up In 1999; Faster Growth Expected In The Future. Health Affair, March/April 2001, pp. 193-203

[17] Burner, S.T., Waldo, D.R., and McKusick, D.R.: National health expenditures through 2030. Health Care Financing Review. Fall 1992, Vol. 14, Number 1.

[18] Levit, K.R. et al. National Health Expenditures, 1994, Health Care Financing Review / Spring 1996/Vol.17, Number 3.

[19] Levit, K.R. et al. National Health Expenditures, 1995, Health Care Financing Review / Fall 1996/Vol.18, Number 1.

[20] Burner, S.T., et al. National Health Expenditures Projections, 1994-2005, Health care Financing Review / Spring 1995/Vol.16, Number 4

[21] Levit, K.R. et al. National Health Spending Trends in 1996 Health Affairs. January/February 1998.

[22] Braden, B.R., et al. National Health Expenditures, 1997, Health Care Financing Review / Fall 1998/Vol.20, Number 1

[23] Smith, S., et al. National Health Projections Through 2008, Health care Financing Review / Winter 1999/Vol.21, Number 2.

[24] Crosetto, D., "System Design and Verification Process for LHC Programmable Trigger Electronics" IEEE NSS-MIC Seattle (WA) Oct. 24-30, 1999.

[25] Crosetto, D.: Detailed design of the digital electronics interfacing detectors… LHCb 99-006, 5 May, 1999 CERN – Geneva

[26] Crosetto, D. "High-Speed, Parallel, Pipelined, Processor Architecture for front-end Electronics, and Method of Use Thereof." LHCb 96-2, TRIG 96-1. CERN, Geneva.

[27] Crosetto, D., "Real-Time system design environment for multi-channel high-speed data acquisition system and pattern-recognition" IEEE Real Time Conference, Santa Fe, (NM) June 14-18, 1999.

[28] Zaidi, H. Scatter correction in 3D PET European Journal of Nuclear Medicine (2000) 47:2722-2735.

[29] Von Schulthess, Gustav K.: Clinical Positron Emission Tomography (PET) Correlation with Morphological Cross-Sectional Imaging. University hospital, Zurich, Switzerland. Published by Lippincott Williams & Wilkins. 2000

[30] Bar-Shalom, R., Valdivia, A.Y., and Blaufox, M.D.: PET Imaging in Oncology. Seminars in Nuclear Medicine, Vol. XXX, No. 3 (July), 2000: pp 150-185.

[31] Jones, W.F. et al.: Next generation PET data acquisition architectures," IEEE TNS, vol NS-44, pp. 1202, (1997).

[32] Dent, H.M., et al.: A real time digital coincidence processor for positron emission tomography. IEEE Trans. Nucl. Sci., vol. 33(1):556-559, 1986

[33] Binkley, D.M. et al.: A custom CMOS Integrated Circuit for PET tomograph front-end applications. IEEE, conf. rec. pp. 867-871, 1993.

[34] Mertens, J.D., et al.: US Patent No. 5,241,181. "Coincidence detector for a PET scanner." Assignee: General Electric Company, August 31, 1993.

[35] Saoudi, A., and Lecomte, R.: A Novel APD-based detector module for multi-modality PET/SPECT/CT scanners. IEEE Conf. Rec. Nucl. Sci. Symp. and Med. Imag., pp. 1089-1093, 1998.

[36] Miyaoka, R.S., et al.: Effect of Detector Scatter on Decoding Accuracy of a DOI Detector. IEEE Conf. rec. of the Nucl. Sci. Symp. and Med. Imag. M3-34, Seattle, October 24-30, 1999

[37] Huber, J., et al.: Development of a 64-channel PET detector module with depth of interaction measurement. IEEE presentation at the Nucl. Sci. Symp. and Med. Imag., M4-6, Seattle, October 24-30, 1999.

[38] Binkley, D.M. et al.: A custom CMOS Integrated Circuit for PET tomograph front-end applications. IEEE, conf. rec. pp. 867-871, 1993.

[39] Boyd, D.P., et al.: A proposed dynamic cardiac 3D densitometer for early detection and evaluation of heart disease. IEEE TNS, 2724-2727, (1979).

[40] Boyd, D.P., and Lipton, M.J.: Cardiac computed tomography, Proceedings IEEE, 198-307, (1983).

[41] Rumberger et al.: Electron Beam Computed Tomographic Coronary Calcium Scanning: A review and guidelines for use in asymptomatic persons. Mayo foundation for Medical Education and Research, vol. 74, pp. 243-252, (1999).

[42] Lehmann, et al.: First results of Computerized Tomographic Angiograph using EBT. Journal of Radiology, vol. 9, pp.525-529, (1999).

[43] Teigen, et. al.: Pulmonary Rmbolism: Diagnosis with Electron Beam CT. Journal of Radiology, vol. 188, pp. 839-845.

[44] Karp, J.S., et al.: Performance Standard in Positron Emission Tomography. J Nucl. Med. 1991; 12:2342-2350.

[45] Wienhard, K. et al.: The ECAT EXACT HR: Performance of a New High Resolution Positron Scanner. IEEE TNS., 1997, pp. 1186-1190.

[46] DeGrado, T.R. et al.: Performance Characteristics of the Whole-Body PET Scanner. Journal of Nuclear Medicine, vol. 35(8):1398-1406, August 1994.

[47] Meier, D., et al.: Silicon Detector for a Compton Camera in Nuclear Medical Imaging. CERN-EP/2001-009 January 29,2001, presented at the Nucl. Sci. Symp. And Medical Imaging on October 2000, Lyon, France.

[48] Schmand, M., et al.: Performance results of a new DOI detector block for high resolution PET-LSO research tomograph HRRT. IEEE Trans. Nucl. Sci., vol. 45(6):3000-3006, December 1998.

[49] Schmand, M., et al.: Performance Evaluation of a new LSO high resolution research tomograph –HRRT. IEEE Nucl. Sci. Symp. and Medical Imaging conference, Seattle (WA), M4-2, October 24-30, 1999.

[50] ECAT ACCEL Positron Emission Tomograph from CTI/Siemens

[51] Cherry, S.R., et al.: MicroPET: A High Resolution PET Scanner for Imaging Small Animals. IEEE. Trans. Nucl. Sci., vol. 44(3):1161-1166, June 1997.

[52] Wahl RH, Quint LE, Greenough RL, et al. Staging of mediastinal non small lung cancer with FDG-PET, CT and fusion images: preliminary prospective evaluation. Radiology 1994;191:371-377.

[53] Shiepers C, Penninckx F, Devandder N, et al. Contribution of PET in the diagnosis of recurrent colorectal cancer; comparison with conventional imaging. EUR J Surg Oncol 1995;21:217-522.

[54] Hoh C.K, et al.: Whole-body PET with FDG: a potential complementary imaging technique to mammography for detection of primary recurrent and metatic breast cancer. Radiology 1993:A38-A44.

[55] NCRP Report No. 100. Exposure of the U.S. Population from Diagnostic Medical Radiation, National Council on Radiation Protection and Measurement, 7910 Woodmont Ave / Bethesda, MD 20814.

[56] National Vital Statistics Reports NCHS, Centers for disease control and prevention, National center for health statistics, vol. 48, number 11, page 26, July 24, 2000.

[57] National Vital Statistics Reports NCHS, Centers for disease control and prevention, National center for health statistics, vol. 48, n. 18, page 2, February 7, 2001.

[58] National Vital Statistics Reports NCHS, Centers for disease control and prevention, National center for health statistics, vol. 33, number 3, supplement page 18, June 22, 1984.

[59] S. Conetti and D. Crosetto, "Implementing the Level-0 Trigger," IEEE Trans. Nucl. Sc. 43 170 (1996).

[60] G. Corti, B. Cox, and D. Crosetto, "An Implementation of the L0 Muon Trigger Using the 3D-Flow system." LHCb 98-13.

[61] http://wwwlhc01.cern.ch (Large Hadron Collider Project at CERN, Geneva, Switzerland).

[62] http://www.rambus.com/developer/downloads/RAC.d.0064.01.111.pdf. See t_{CYCLE} = 1,875 ns at pages 56, and timing diagram on Figures 40, 41

[63] Crosetto, D.: Digital Signal Processing in high energy physics. Lecture before the CERN School of Computing at Yesermonde, Belgium 2-15 September 1990. Publ. by CERN 91-05. 14 May 1991.

[64] Crosetto, D.: Understanding a new idea for cancer screening. ISBN 0-9702897-1-5, Available at Amazon.com.

[65] Cherry, S.R., et al..: A comparison of PET detector modules employing rectangular and round photomultiplier tubes. IEEE Trans. Nucl. Sci, vol. 42(4):1064-1068 (August 1995).

[66] Cutler, D., et al.: Use of a digital front-end electronics for optimization of a modular PET detector. IEEE Trans. Nucl. Sci. vol. 13, No. 2, June 1994, pp. 408-418.

[67] Seidel, J., et al.: Experimental Estimates of the Absolute Sensitivity of a Small Animal PET Scanner with Depth-of-Interaction Capability. IEEE Transaction Nulc. Sci. and Med. Imag., Conf. record, Lyon, France, October 2000. Article 777.

[68] LHC-B Letter of Intent. A dedicated LHC Collider Beauty Experiment for Precision Measurements of CP-Violation. CERN.LHCC 95-5 LHCC/I8 25 August, 1995, pp. 83-84.

[69] LHCb Technical Proposal. A Large Hadron Collider Beauty Experiment for Precision Measurements of Cp-Violation and rare decay. CERN.LHCC 98-4 LHCC/P4 20 February 1998. pp. 102-104.